Notch Signalling Pathway

A brief history

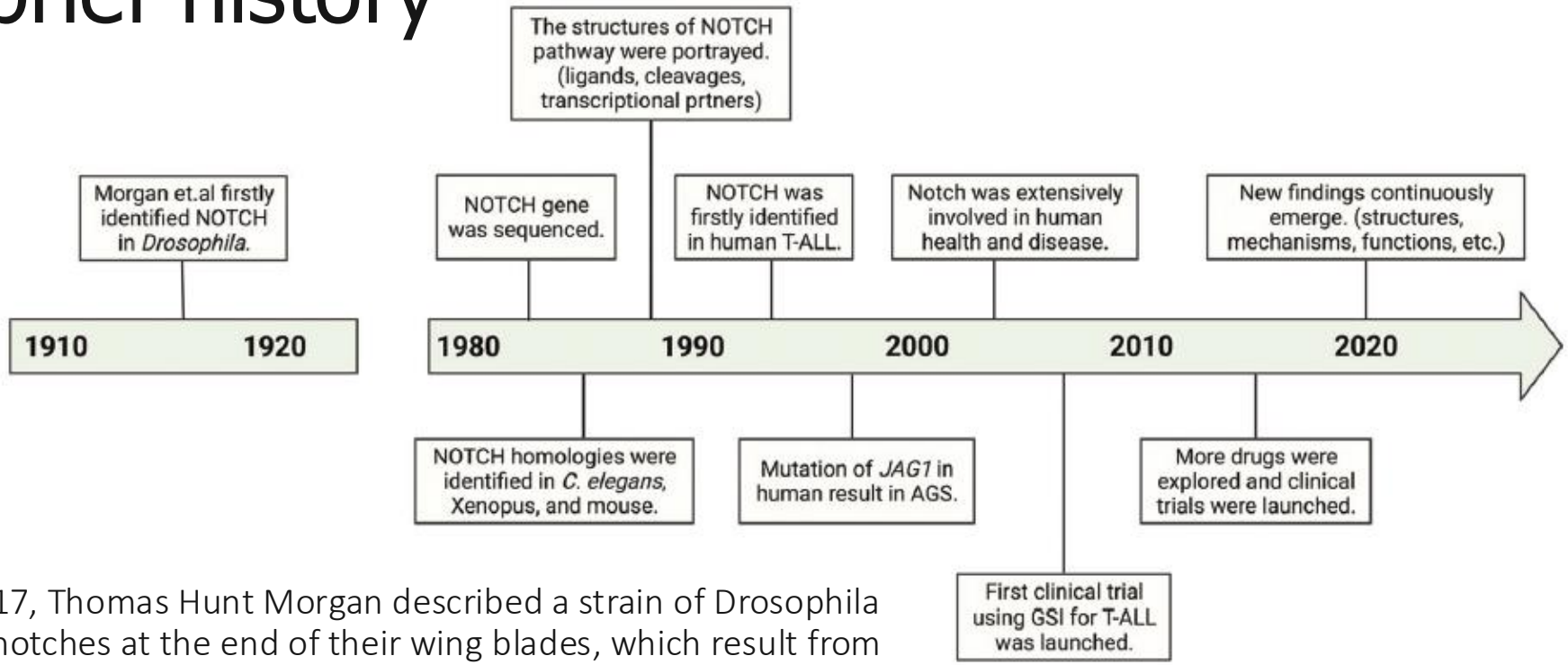

- In 1917, Thomas Hunt Morgan described a strain of Drosophila with notches at the end of their wing blades, which result from haploinsufficiency
- Notch gene was cloned in the mid-1980s
- In 1988 and 1989, LIN-12 and GLP-1 were identified as NOTCH homologs in C. eleganS.
- In 1990, XOTCH was identified in Xenopus, and the cDNA of the mammalian NOTCH gene was cloned.
- In 1991, the NOTCH gene was first linked to human T cell acute lymphoblastic leukemia (T-ALL).
- In 1997, Alagille syndrome (AGS) was found to be caused by the mutation of JAG1, which encodes a ligand of NOTCH1.

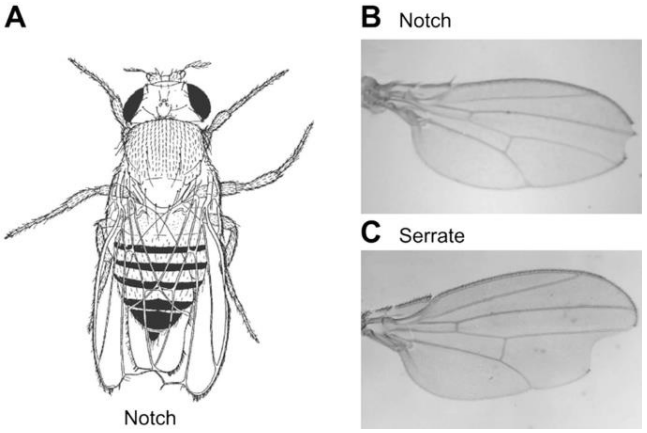

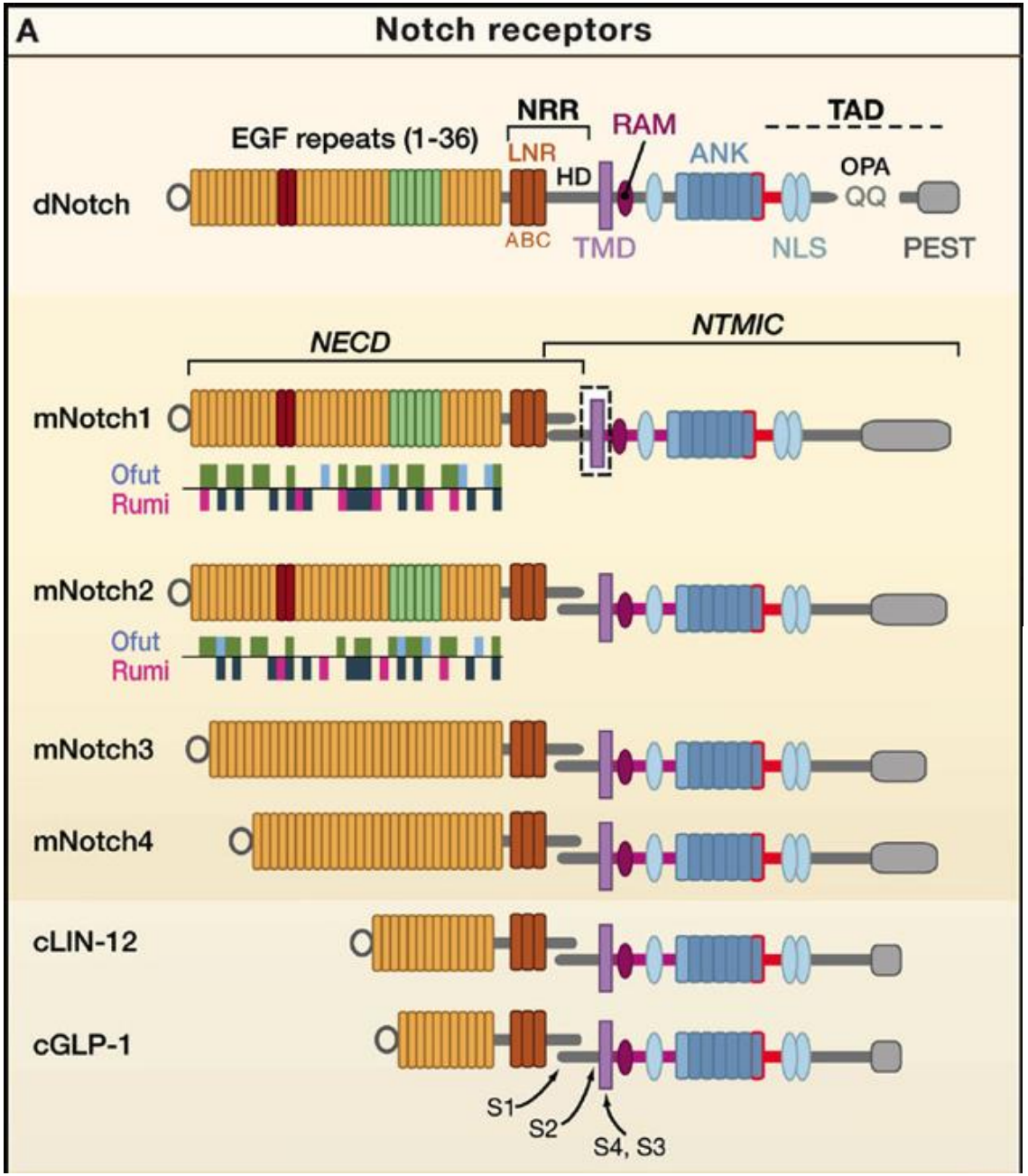

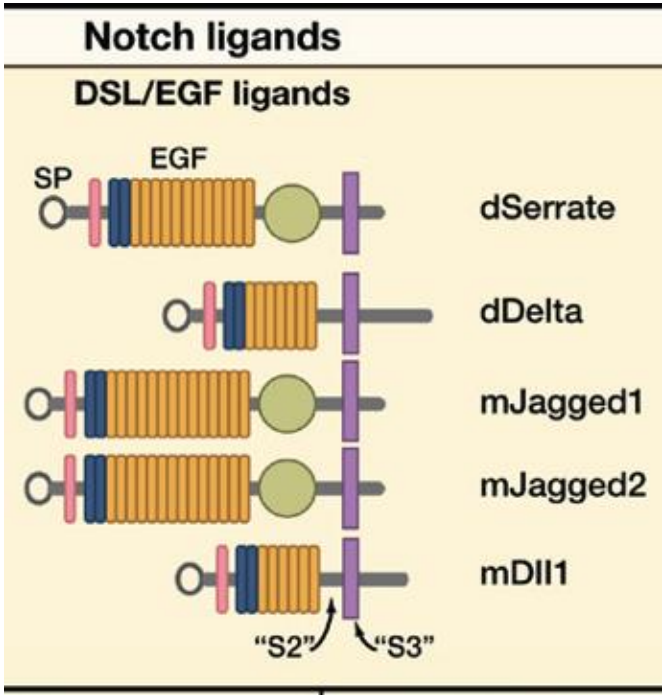

Notch receptors are transmembrane proteins that contain multiple EGF-like repeats, involved in ligand interactions, fucosylation and glucosylation, a transmembrane domain (TMD), a RAM (RBPjκ association module) domain, nuclear localization sequences (NLSs), seven ankyrin repeats (ANK) domain, and a transactivation domain (TAD) that habors a PEST domain.

Notch ligands can be divided into several groups on the basis of their domain composition.

The Notch signalling pathway

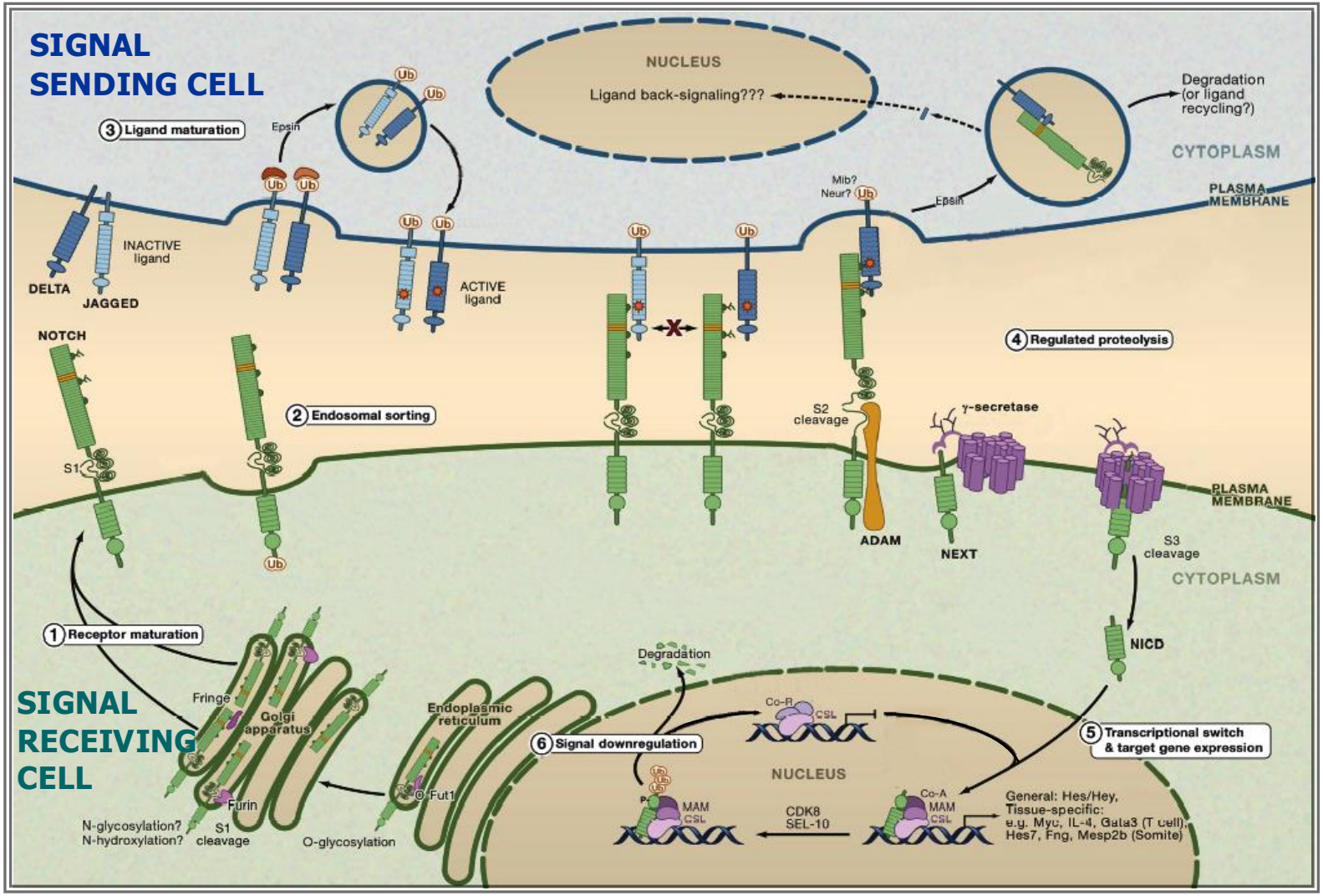

UNIQUE FEATURES

- each Notch molecule is irreversibly activated by proteolysis
- signals only once without amplification by secondary messenger cascades

Notch biosynthesis

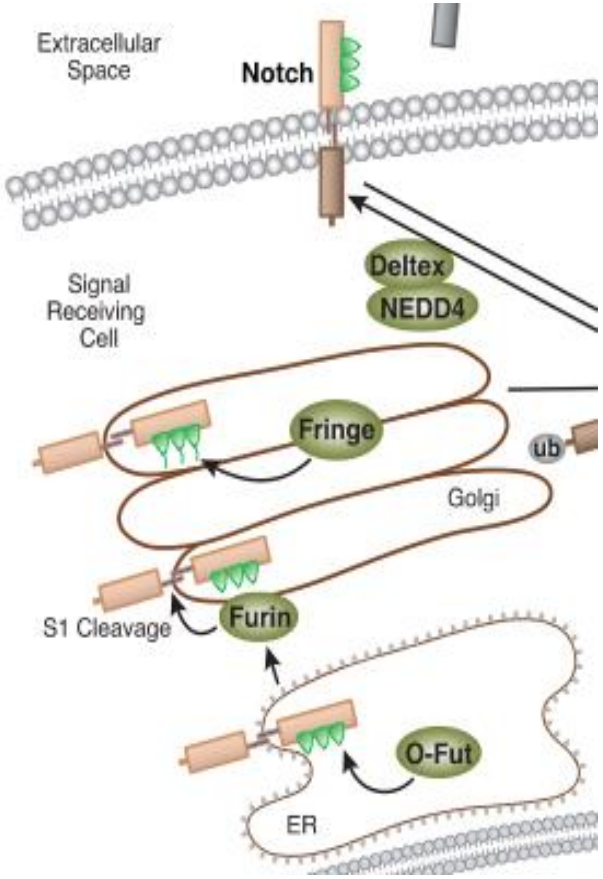

NOTCH precursors are generated in the endoplasmic reticulum (O-fucosylation, O-glucosylation, and O GlcNAcylation) and then translocated into the Golgi apparatus, where the O-fucose is extended by the Fringe family of GlcNAc transferases, while O-glucose is extended by xylosyltransferases.

The glycosylation of NOTCH is vital to its stability and function.

The glycosylated NOTCH precursors undergo S1 cleavage in the Golgi apparatus at a conserved site (heterodimerization domain) by a furin-like protease, before being transported to the cell membrane.

The canonical Notch signalling pathway:

Notch activation

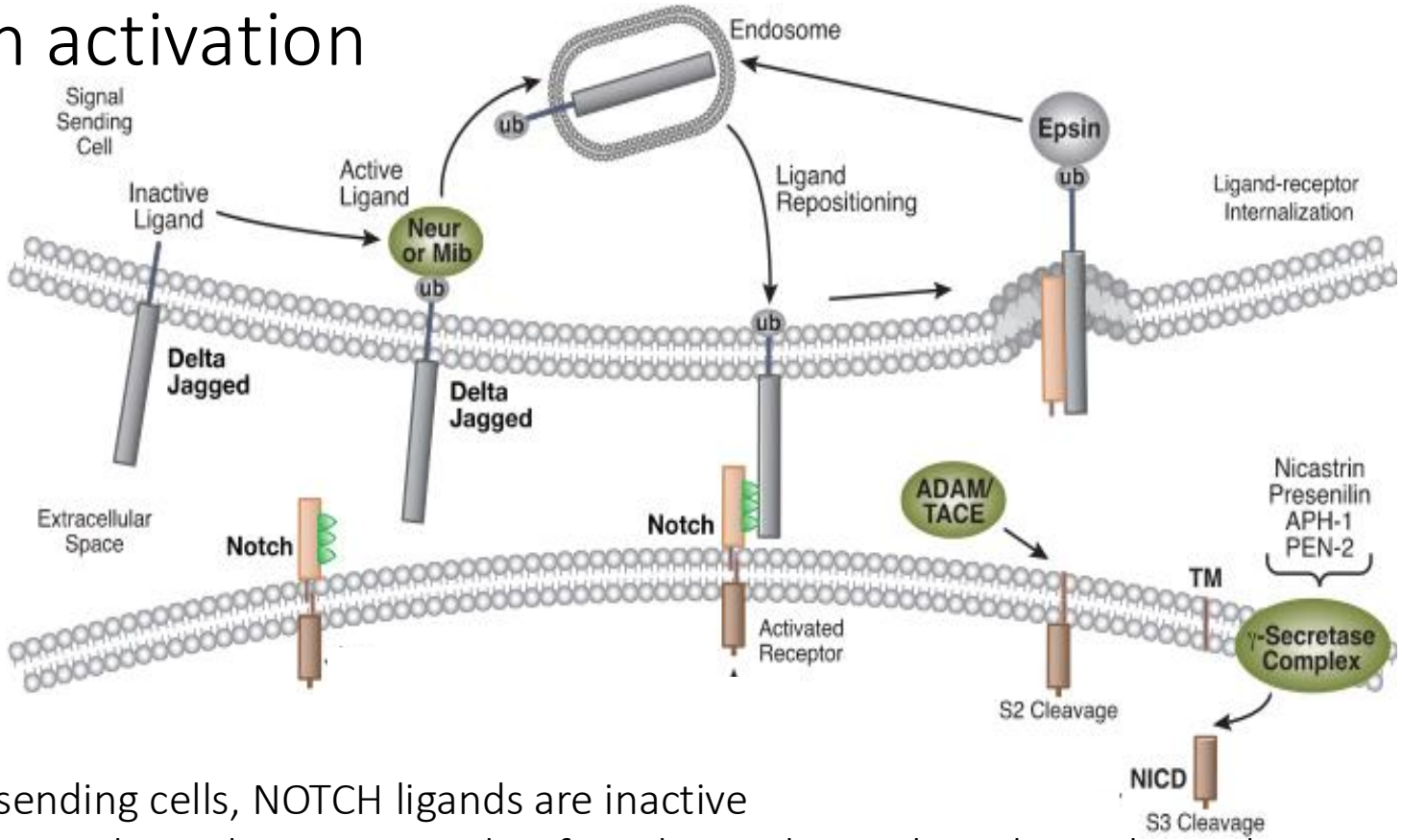

In signal-sending cells, NOTCH ligands are inactive before ubiquitylation by Neur or Mib. After ubiquitylation, ligands can be endocytosed, thus producing a pulling force for the binding receptors. Without the pulling force, the S2 site is hidden and thus, the NOTCH receptors are resistant to cleavage by ADAMs. With the pulling force, the S2 site is exposed for cleavage. ADAMs and the pulling force are both necessary for S2 cleavage. Juxtamembrane Notch cleavage at site 2 generates the NEXT fragment, which is cleaved by the γ-secretase complex to release the Notch intracellular domain (NICD) and Nβ peptide. NICD is translocated into the nucleus via the nuclear localization sequences and importins alpha 3, 4, and 7.

Notch trafficking

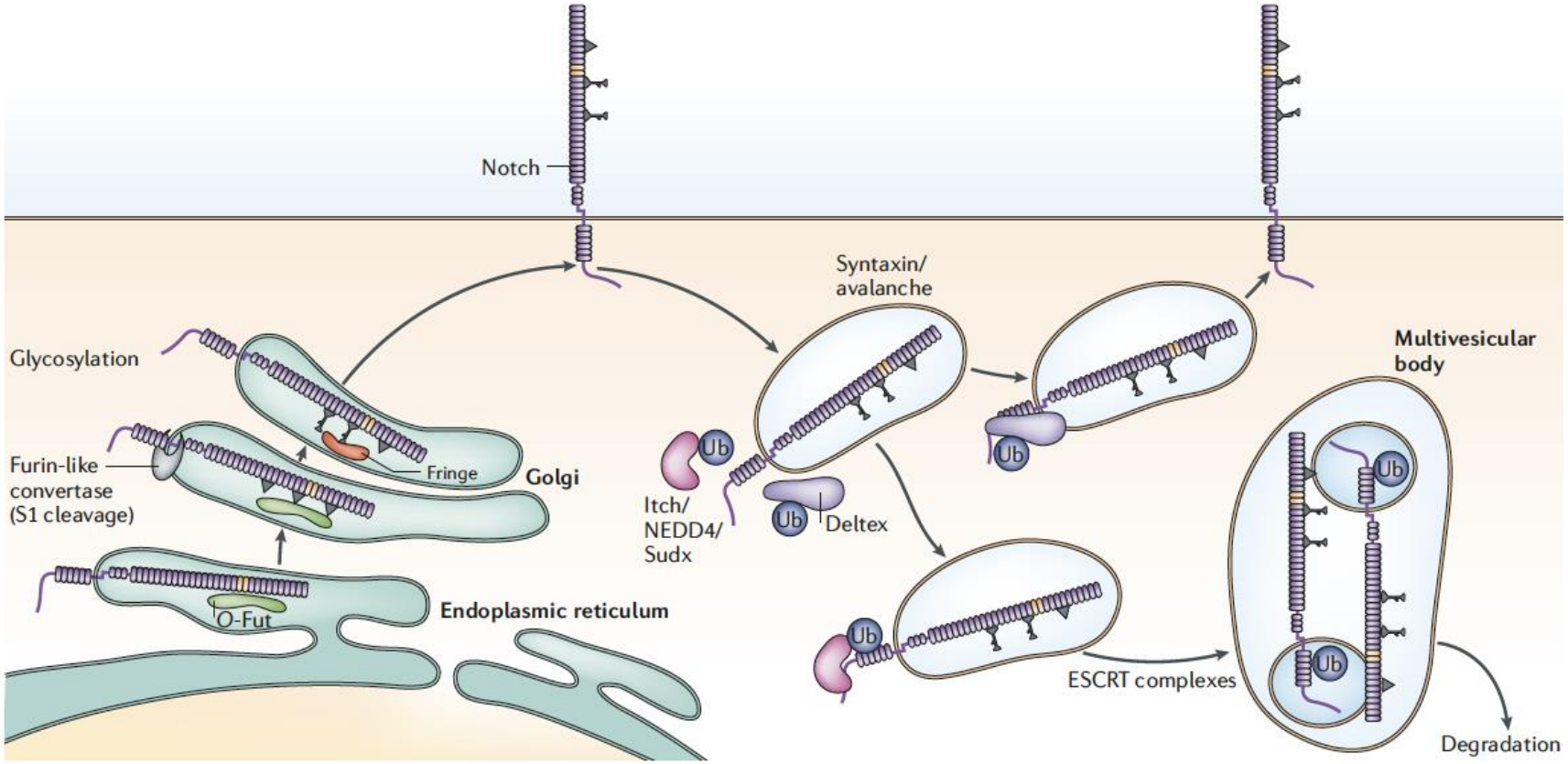

Figure 3 | **Processing and trafficking regulate Notch-receptor activity.** Notch (purple) is produced in the endoplasmic reticulum where it interacts with the *O*-fucosyl transferase (*O*-Fut; green) and is transported to the Golgi. In the Golgi, it is processed by Furin-like convertase (grey, S1 cleavage) and glycosylated (shown as dark grey protrusion from Notch) by *O*-Fut and other glycosyltransferases (for example, Fringe; red) before export to the cell surface. Notch that is endocytosed from the cell surface can be recycled or degraded through the multivesicular-body pathway. Actions of the ubiquitin ligases Deltex (purple) and Itch/NEDD4/Su(dx) (pink) regulate trafficking, although their precise roles are not yet clear. Other proteins (syntaxin, ESCRT complexes) that affect trafficking are indicated, but their sites of action are hypothetical and remain to be fully clarified. Ub, ubiquitin.

In the traditional model of <u>NICD regulating gene transcription</u>, CSL recruits corepressor proteins and histone deacetylases (HDACs) to repress the transcription of target genes without NICD binding. NICD binding can change the conformation of the CSL-repressing complex, dissociating repressive proteins and recruiting activating partners to promote the transcription. The transcriptional coactivator Mastermind-like protein (MAML) is one of the core activating partners that can recognize the NICD/CSL interface, after which it recruits other activating partners.

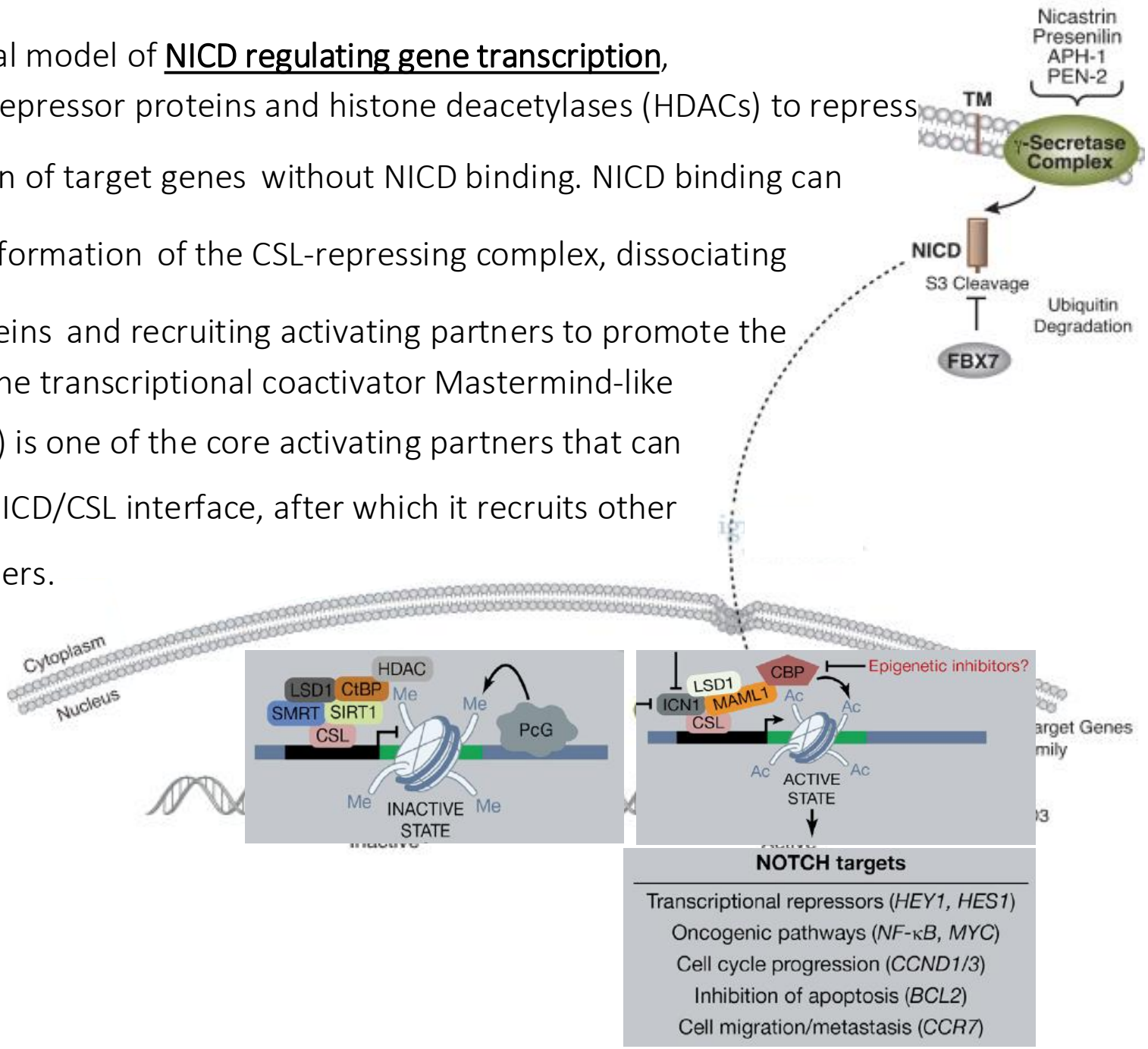

The canonical Notch Signaling Pathway

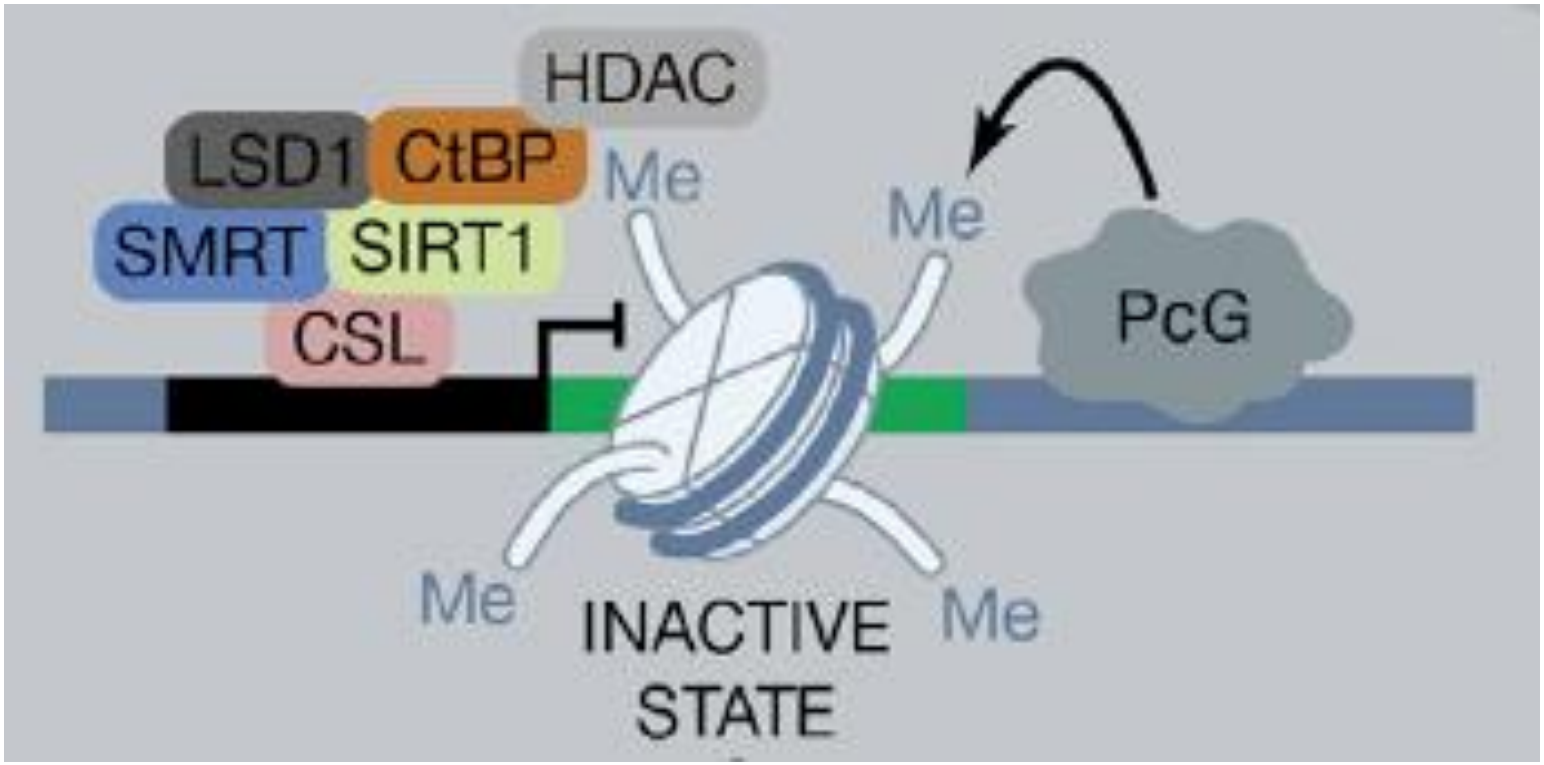

CSL (CBF-1/suppressor of hairless/Lag1 (CSL, also called recombination signal binding protein-J, RBPJ) is a DNA binding protein that functions as either a repressor or an activator of transcription, depending upon whether it is complexed by transcriptional corepressor or coactivator proteins, respectively. The classical model proposes that, in the absence of NICD, CSL binds with corepressors to inhibit the transcription of target genes.

The canonical Notch Signaling Pathway

Once ICN is transported to the nucleus, it forms a ternary complex, with the DNA-binding protein CSL (RBP-Jκ/CBF-1) and the Mastermind family protein MAML1. Both CSL and MAML1 act as central components of Notch signalling by targeting nuclear ICN to Notch-responsive genes and by acting as coactivator, respectively. Indeed, ICN-CSL-MAML1 serves as platform for the assembly of transcriptional activating complex containing several classes of transcriptional regulators including histone modifiers and RNA polymerase II recruiter.

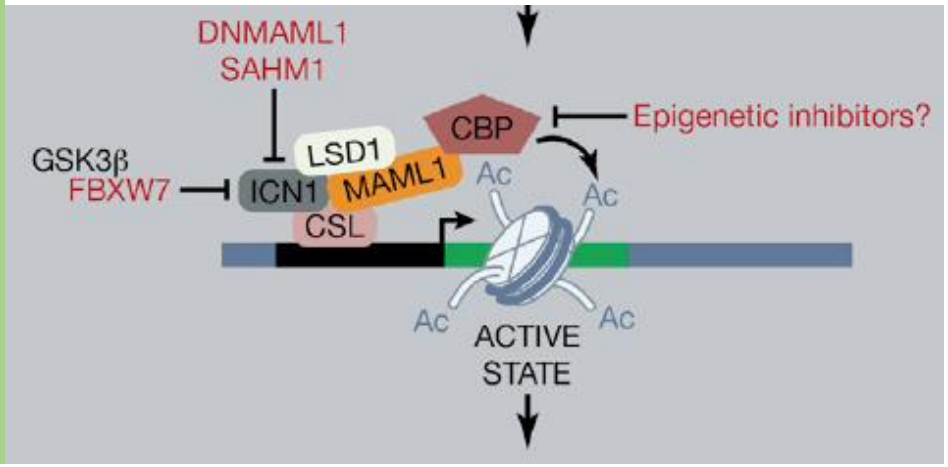

NOTCH targets

Transcriptional repressors (*HEY1, HES1*)

Oncogenic pathways (*NF-κB, MYC*)

Cell cycle progression (*CCND1/3*)

Inhibition of apoptosis (*BCL2*)

Cell migration/metastasis (*CCR7*)

HDAC, histone deacetylase; ICN1, intracellular part of NOTCH1; LSD1, lysine-specific demethylase 1; SMRT, Silencing-Mediator for Retinoid/Thyroid hormone receptors; GSK3b, glycogen synthase kinase 3 beta; DNMAML1, dominant-negative MAML1

SirT'N repression for Notch

SIRT1 deacetylase acts in concert with the LSD1 demethylase to repress Notch-induced transcription
Mulligan P. et al., 2011

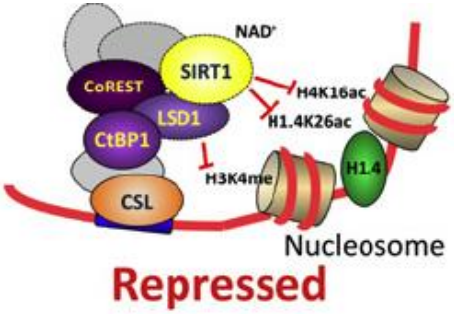

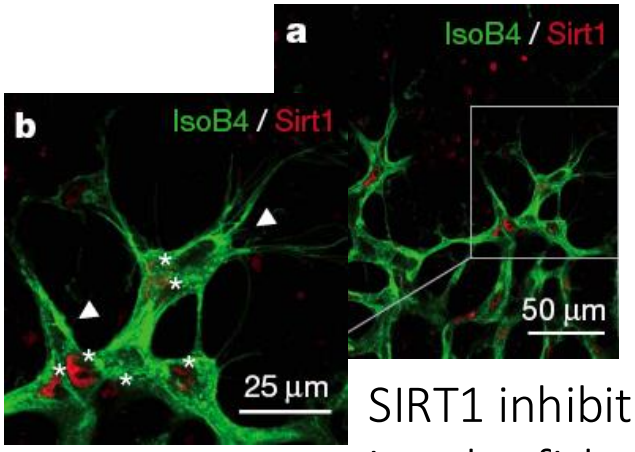

SIRT1 inhibits endothelial cell Notch signaling during angiogenesis in zebrafish and mice.
Guarani V. et al., 2012

Acetylation tightly controls the amplitude and duration of Notch signalling, extending the half-life of the protein, and enhancing its transcriptional activity. Sirt1 acts as a negative modulator of Notch1 signalling; its overexpression reverts Notch acetylation and dampens its stability (Collesi C., et al., 2018).

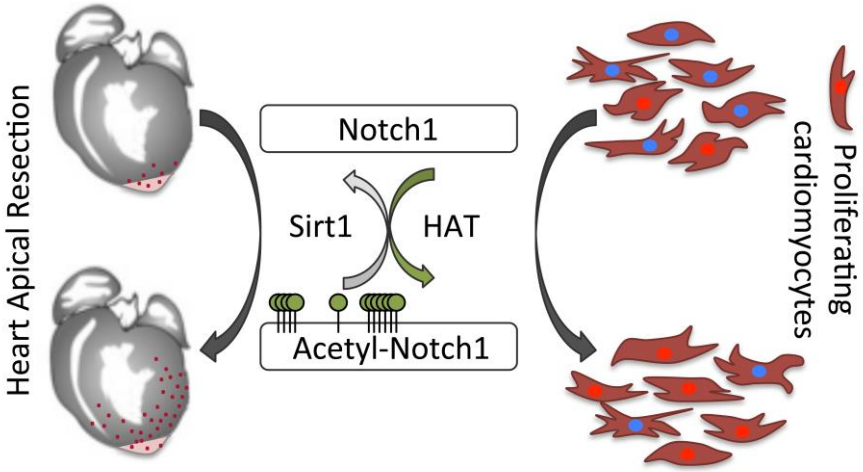

SCIENTIFIC REPORTS | (2018) 8:15515 | DOI:10.1038/s41598-018-33920-y

Src kinase phosphorylates Notch1 to inhibit MAML binding

Bryce LaFoya[1], Jordan A. Munroe[2], Xinzhu Pu[3] & Allan R. Albig[1,2]

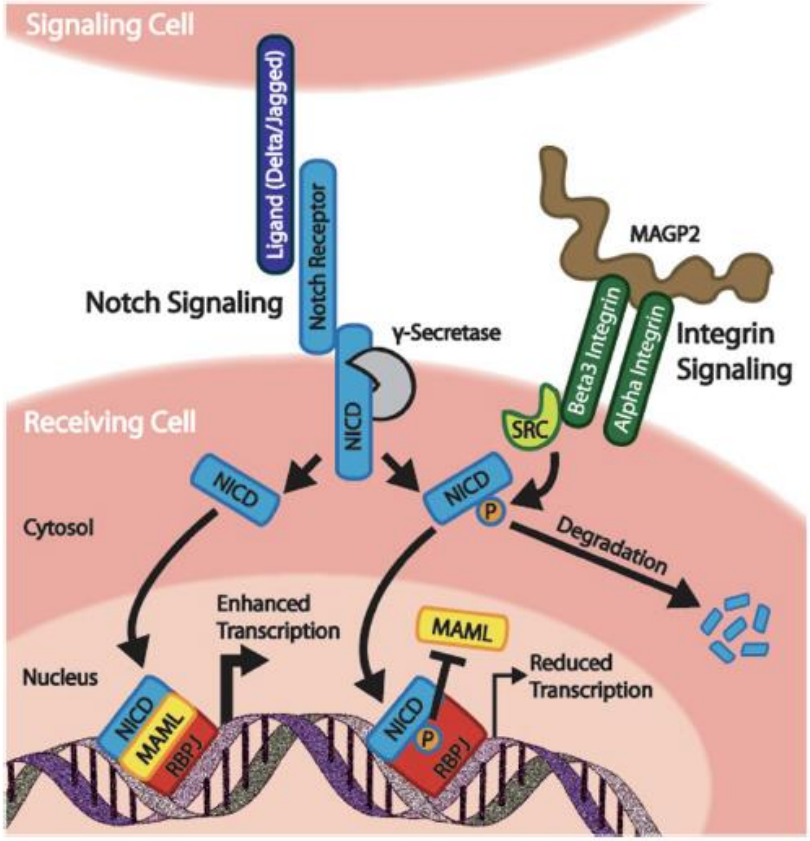

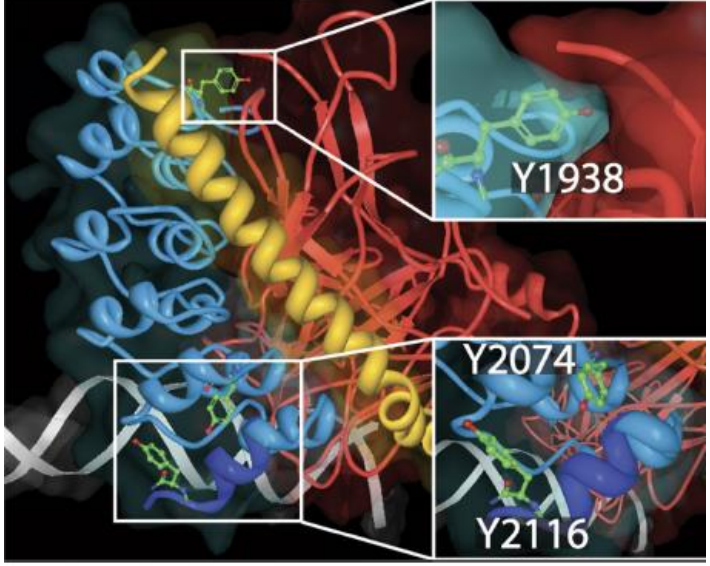

The tyrosine residues are within or in close proximity to the Notch ankyrin Domain. Y1938 may regulate RBPJ-NICD interactions. Y2074 and Y2116 may regulate the recruitment of p300 acetyltransferase to the N1ICD transcriptional complex

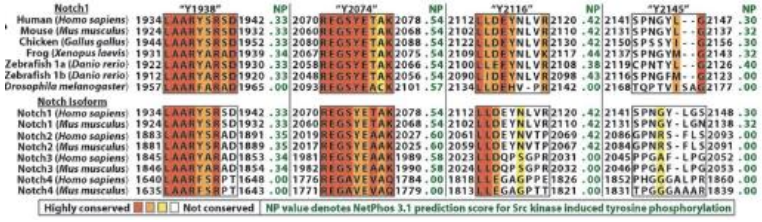

Integrin-induced c-src activity phosphorylates the Notch intracellular domain. This phosphorylation leads to decreased recruitment of MAML to the Notch transcriptional complex and subsequent reduction in target gene transcription. Phosphorylation of the Notch intracellular domain may lead to reduced half-life of the protein.

Mechanisms regulating NOTCH signaling

Glycosylation

O-fucosylation affects ligand binding.

O-glucose of NOTCH receptors is involved in S2 cleavage: alteration of O-glucosylation damages the proteolysis of NOTCH receptors after ligand binding

The sites of O-glycosylation are important regions for ligand binding, the loss of which decreases NOTCH signaling in T cells

Receptor trafficking

NOTCH receptors are constitutively endocytosed through a process modulated by ubiquitin ligases such as FBXW, NUMB, ASB, DTX1, NEDD4, ITCH, and CBL. Endocytosed NOTCH can be recycled to the cell membrane or trapped in the cytoplasm. Furthermore, the endocytosed NOTCH receptors in the cytoplasm can be degraded or activated.

Ligand ubiquitylation

Ubiquitylation of ligands (catalyzed by Neur and Mib) in signal-sending cells is necessary for signaling activation. The endocytosis of ligands promotes exposure of the NRR domain of the receptor for S2 cleavage.

Cis-inhibition

Receptors and ligands expressed on different cells can initiate signal transduction. However, receptors and ligands expressed on the same cell both inhibit and activate the whole signaling pathway, termed cis-inhibition and cis-activation.

The FEBS Journal

FEBS PRESS

REVIEW ARTICLE

Regulation of Notch signaling by E3 ubiquitin ligases

Debdeep Dutta*, Vartika Sharma, Mousumi Mutsuddi and Ashim Mukherjee

Department of Molecular and Human Genetics, Institute of Science, Banaras Hindu University, Varanasi, India

The FEBS Journal **289** (2022) 937–954

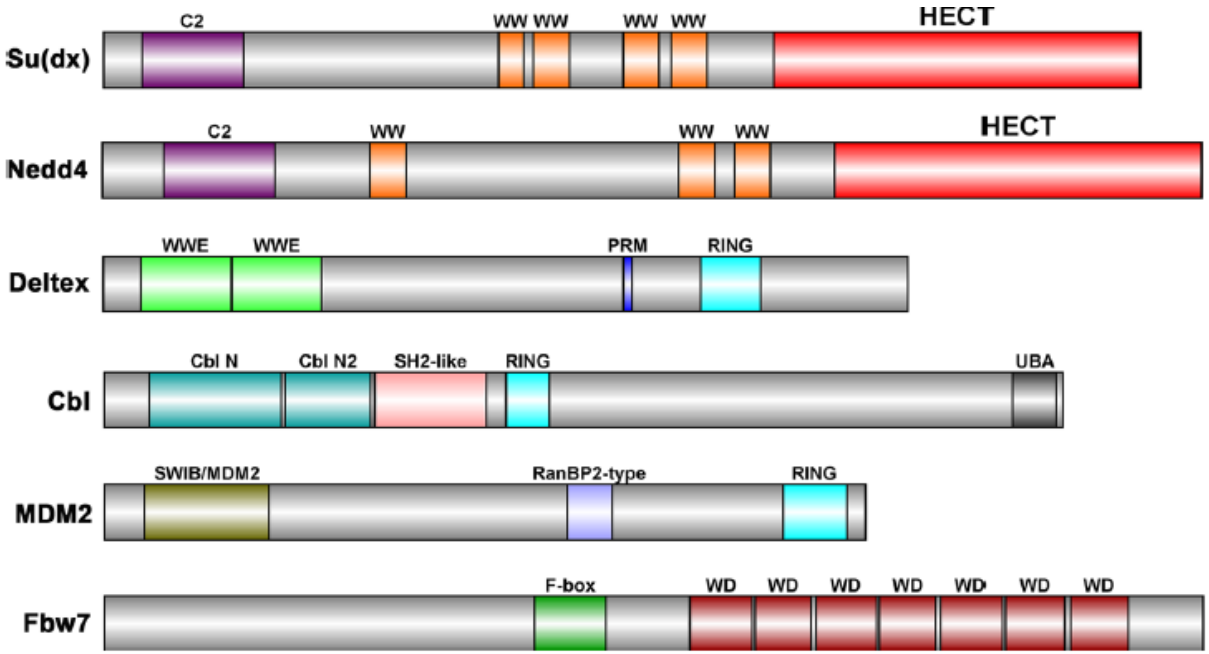

Fig. 3. Structural features of the major E3 ligases that act at the receptor level. HECT (homologous to E6AP COOH terminus), RING, and SCF (Skp1-Cul1-F-box) family E3 ligases are involved at the receptor-level regulation of Notch signaling.

THE JOURNAL OF BIOLOGICAL CHEMISTRY
Vol. 278, No. 25, Issue of June 20, pp. 23196–23203, 2003

Printed in U.S.A.

Mammalian Numb Proteins Promote Notch1 Receptor Ubiquitination and Degradation of the Notch1 Intracellular Domain*

Received for publication, March 19, 2003, and in revised form, April 3, 2003
Published, JBC Papers in Press, April 7, 2003, DOI 10.1074/jbc.M302827200

Melanie A. McGill‡ and C. Jane McGlade§

Numb recruits components of the ubiquitination machinery to the Notch receptor thereby facilitating Notch1 ubiquitination at the membrane, which in turn promotes degradation of the intracellular domain circumventing its nuclear translocation and downstream activation of Notch1 target genes.

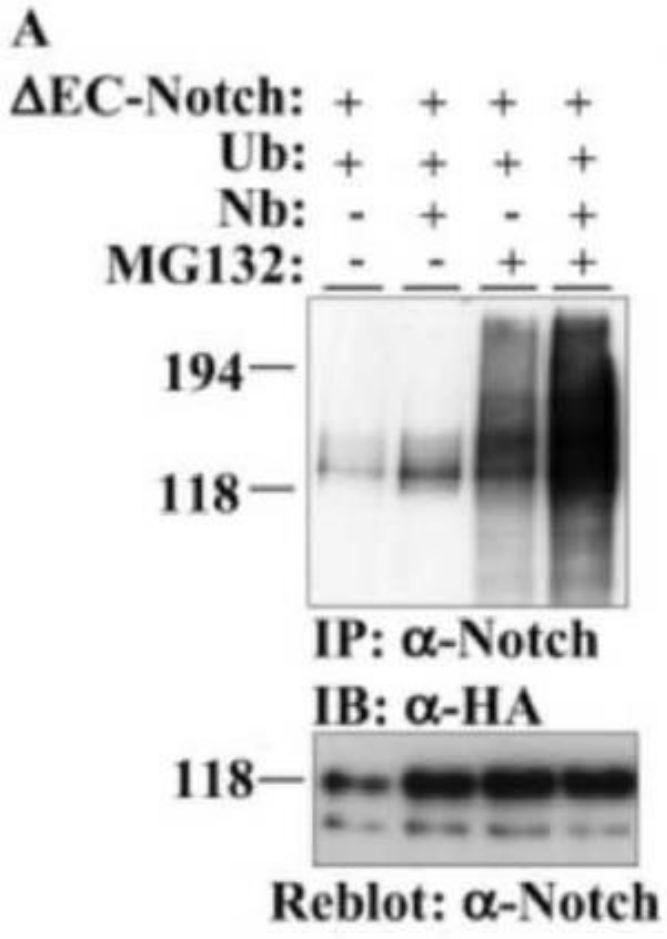

Numb

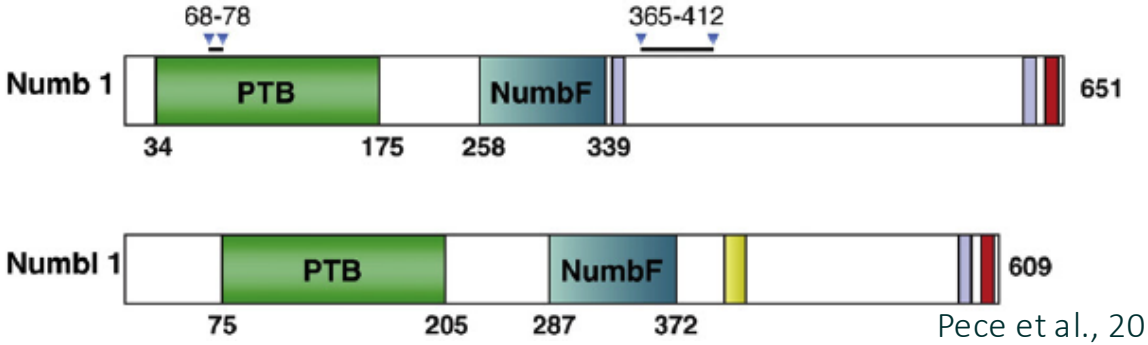

Pece et al., 2011

- Numb domains:
  - 1. PTB domain; N-terminal phosphotyrosine binding domain
  - 2. proline-rich C-terminal region.

- Numb binds directly to NICD. The Cterminal half of the PTB domain and the N-terminus of Numb are required to inhibit Notch. Numb also has two motifs associated with endocytic proteins.

- mammalian Numb (mNumb) localizes to clathrin coated pits and early endosomes, might target endocytosed NICD for proteosomal destruction.

- Numb acts either upstream of S3 cleavage site of Notch or inhibit the endocytosis of membrane-bound activated Notch.

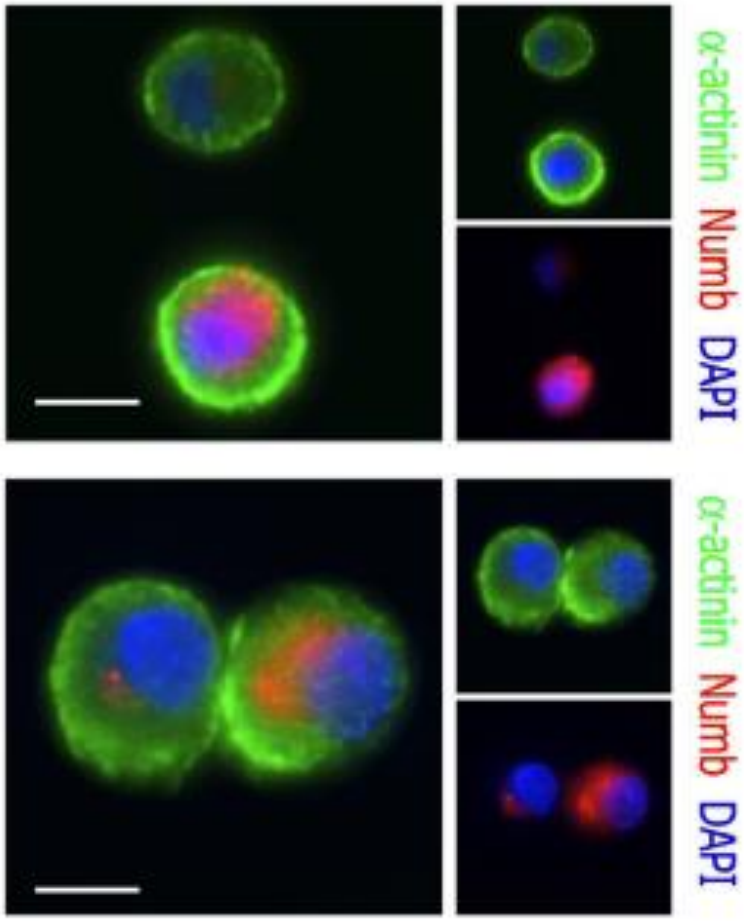

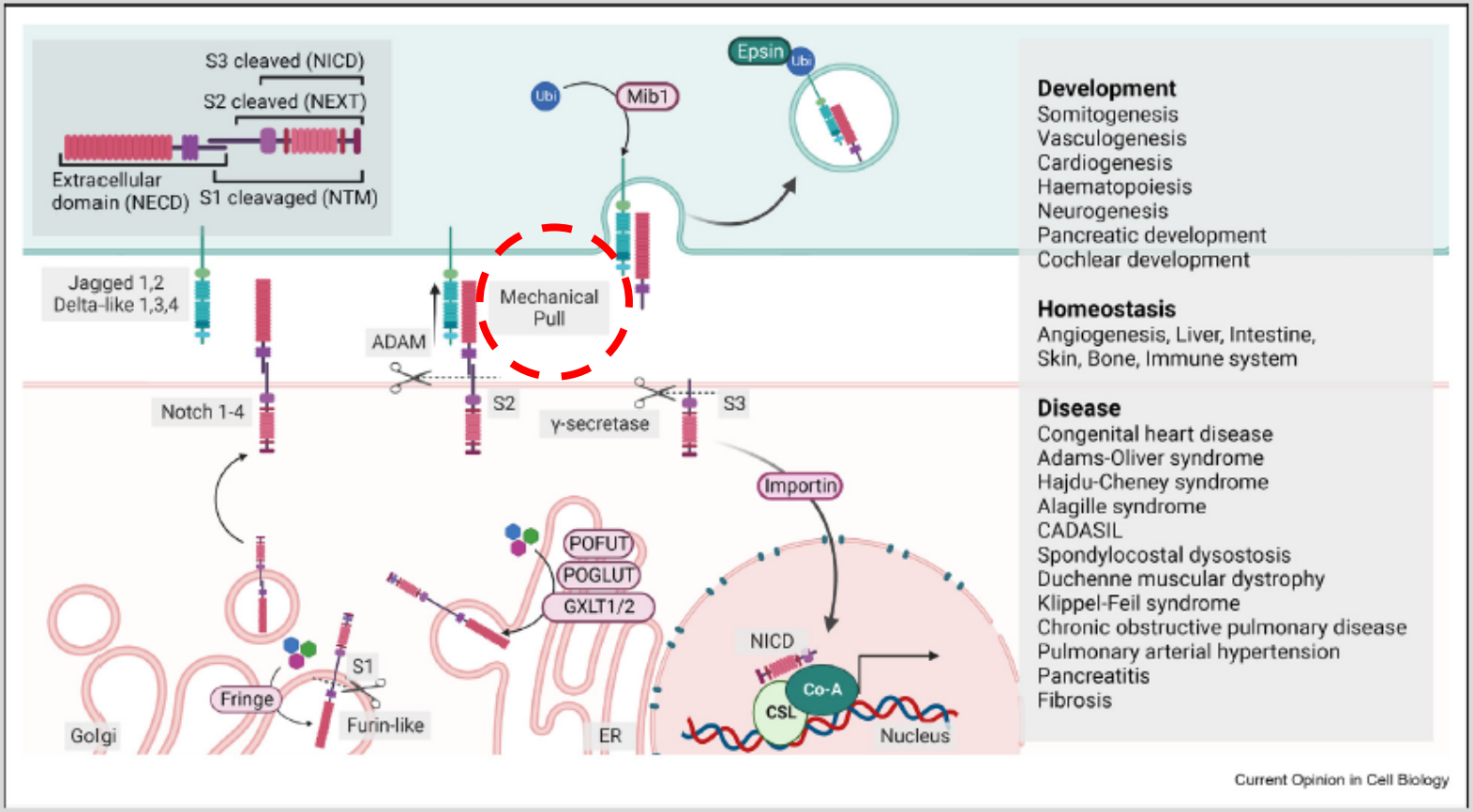

Notch is a contact-dependent pathway, that involves two neighboring cells expressing the Notch receptors (Notch1-4) and ligands (Jagged1,2 and Delta-like 1,3,4). The full-length Notch receptor (NFL) is synthesized as a single polypeptide and modified with sugar groups by e.g., POFUT, POGLUTand GXYLT in the endoplasmic reticulum. In the Golgi, the receptor is further modified by fringe glycosyl-transferases and goes through its first cleavage, S1, catalyzed by furin-like convertase yielding two fragments, the Notch transmembrane-intracellular domain (NTM), and Notch extracellular domain (NECD). On the membrane, once the receptor interacts with a ligand presented by a neighboring cell, it is subjected to a mechanical pull, which leads to two consecutive proteolytic cleavages, S2 and S3, on the NTM. These are catalyzed by metalloprotease ADAM and the γ-secretase complex (NTM) and yield the Notch extracellular truncated domain (NEXT) and the Notch intracellular domain (NICD), respectively. NICD translocates to the nucleus, where it interacts with CSL (CBF1, Suppressor of Hairless, Lag-1) and other transcriptional factors and drives gene transcription. The conversion of the NICD signal into transcription is dependent on its complex interactions with the hetero-chromatin. In the ligand-presenting cell, the ligand is endocytosed together with the receptor extracellular domain (NECD) and processed for further signaling or targeted for degradation. Notch signaling regulates development, homeostasis and diseases as reviewed by Siebel and Lendahl [1], some of which are directly related to mechanical stress [5].

*In the signal-sending cells, when the ligand interacts with the receptor, a **pulling force** is generated.*

As a result, the ligand-NECD complex undergoes transendocytosis mediated by the E3 ligases Neuralized and Mindbomb. After this transendocytosis, the ligand is recycled back to the cell membrane.

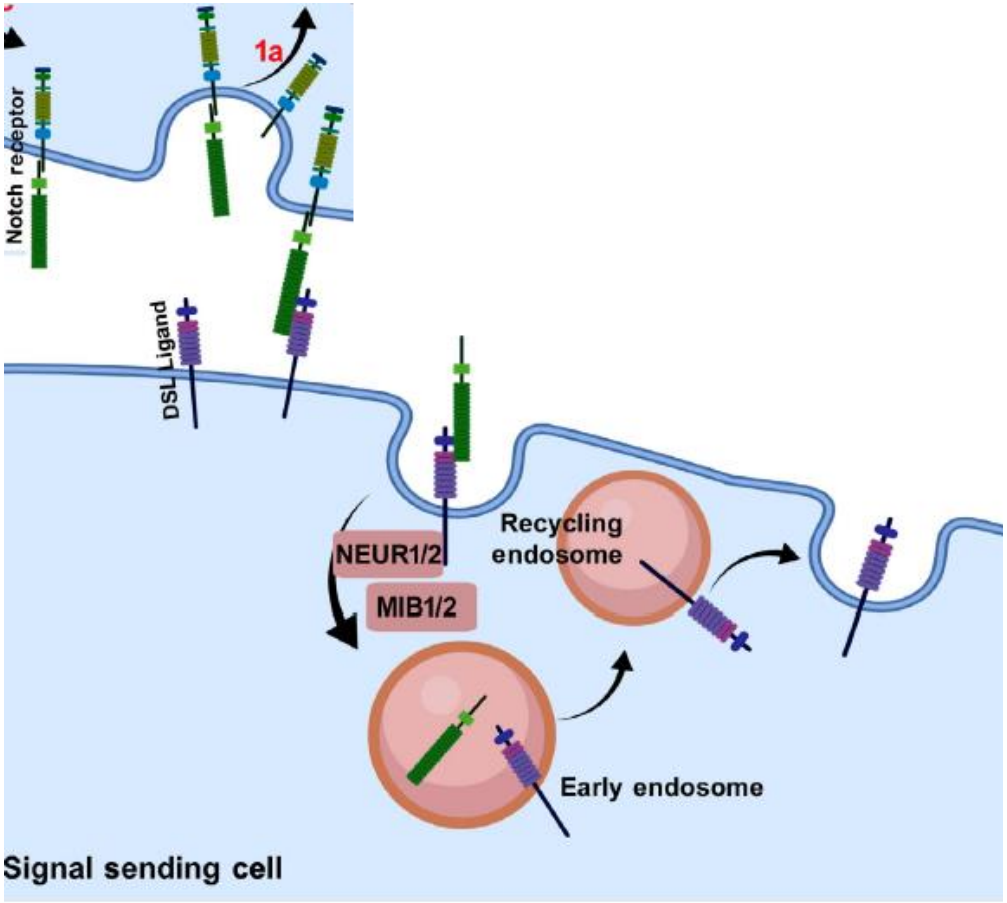

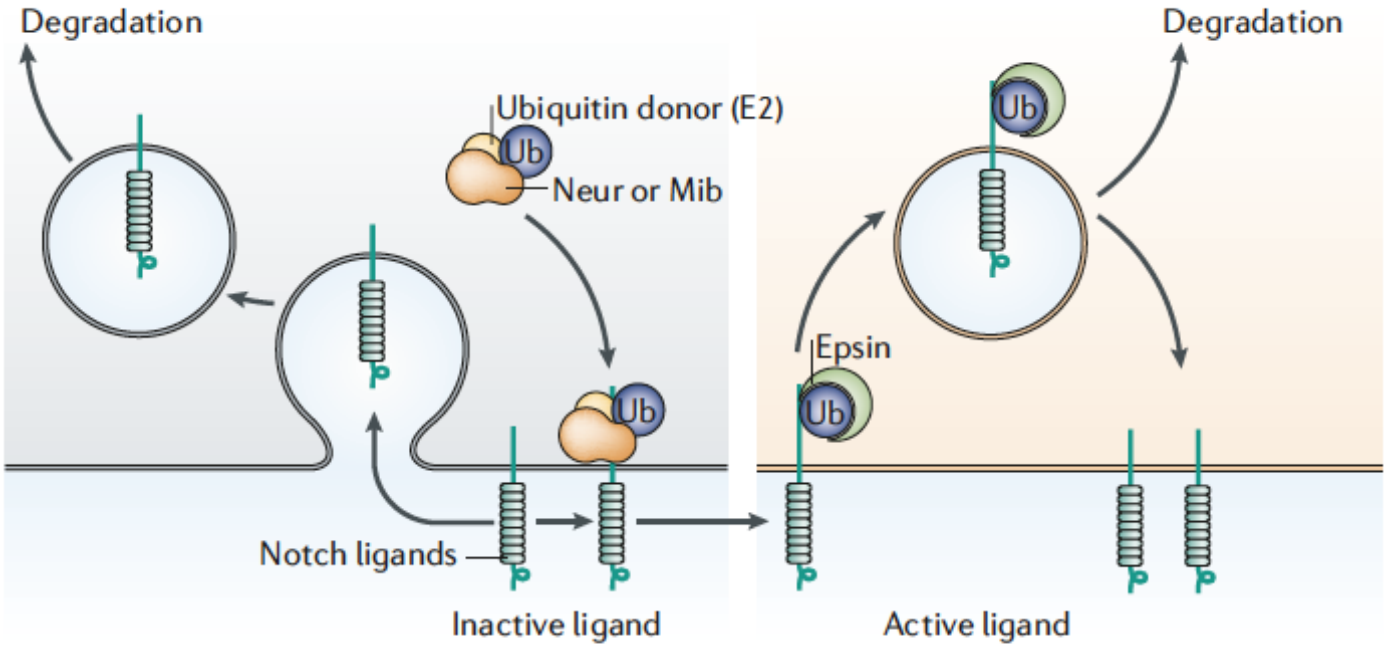

Figure 2 | **Ligand activation entails ubiquitylation.** The E3 ubiquitin (Ub) ligases Neuralized (Neur) and Mind bomb (Mib) interact directly with Notch ligands. Prior to modification by Neur or Mib, ligands are inactive, and can be endocytosed and degraded. Neur- or Mib-mediated ubiquitylation of Notch ligands is required for Epsin-mediated endocytosis. Ligands (in the light orange area) are then competent to signal either because endocytosis is directly associated with receptor activation or because it allows entry into a specific compartment or membrane domain that renders ligands active. They can also be targeted for degradation. E2, ubiquitin-conjugating enzyme.

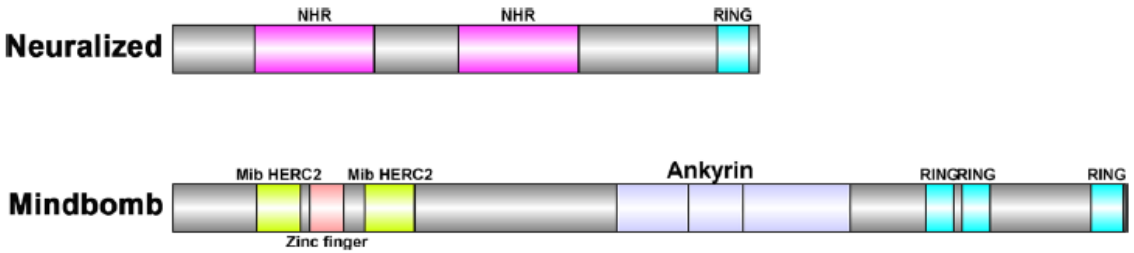

MINDBOMB

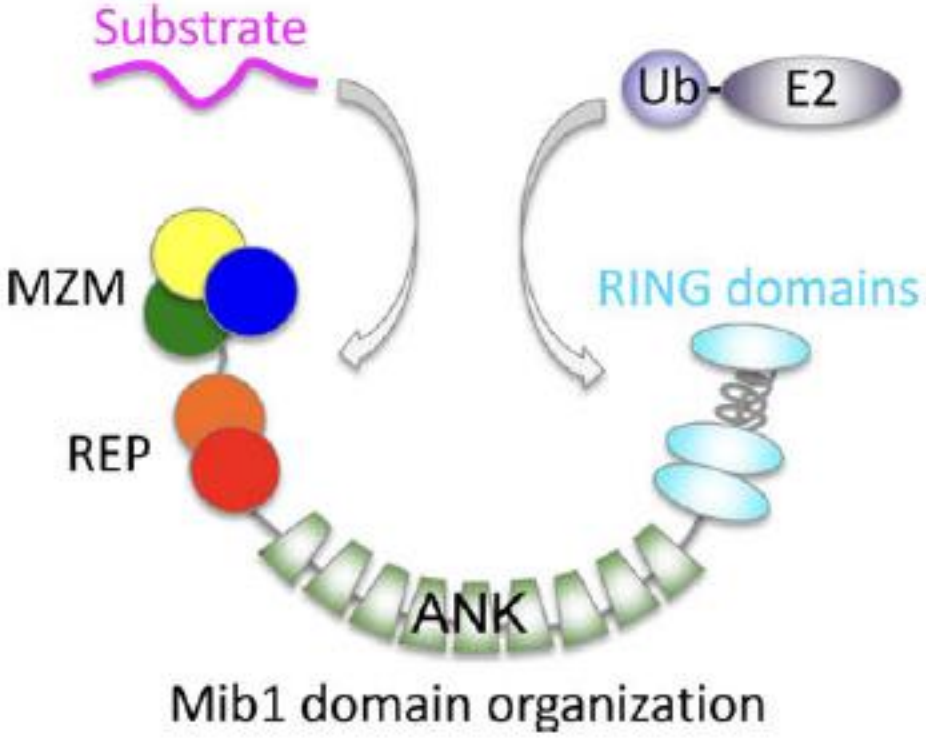

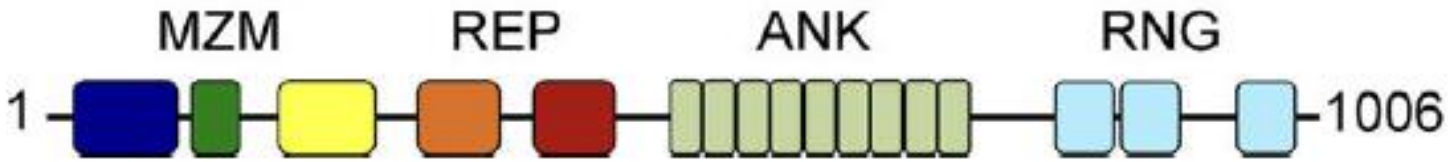

Domain organization of Mib1 highlighting the MZM, REP, ANK, and RNG regions of the protein. The MZM domain contains two Mib-Herc2 domains (blue and yellow) flanking a ZZ Zinc finger (green). The REP domain contains two tandem “Mib repeat” elements (orange and red). The ANK domain is composed of nine ankyrin-type repeats (light green), and the C-terminal RNG domain is composed of three RING elements (cyan).

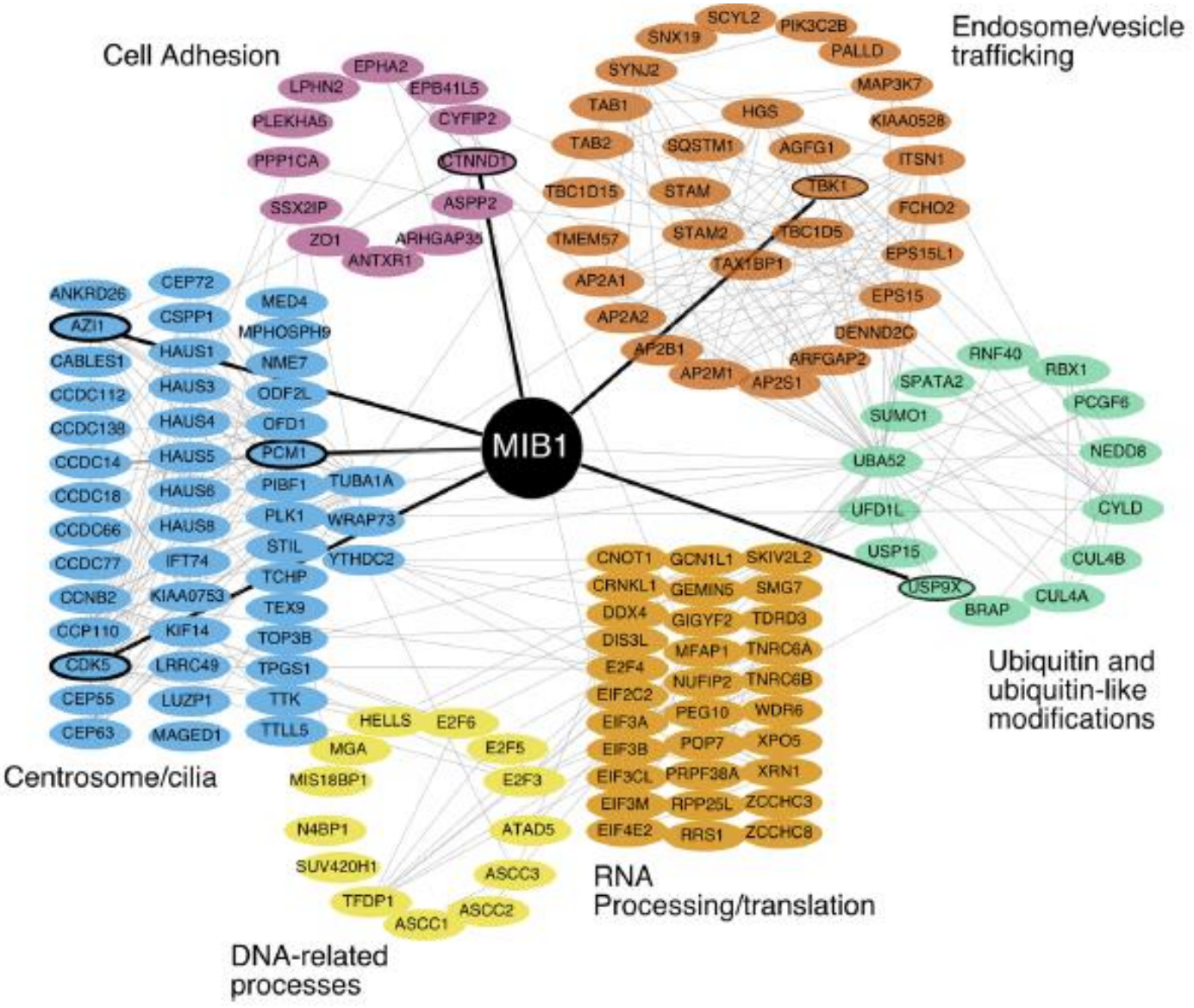
Cell Adhesion
EPHA2
LPHN2
EPB41L5
PLEKHA5
CYFIP2
PPP1CA
CTNND1
SSX2IP
ASPP2
ZO1
ARHGAP35
ANTXR1
Endosome/vesicle trafficking
SCYL2
PIK3C2B
SNX19
PALLD
SYNJ2
MAP3K7
TAB1
HGS
KIAA0528
TAB2
SQSTM1
AGFG1
ITSN1
TBC1D15
STAM
TBK1
FCHO2
TMEM57
STAM2
TBC1D5
EPS15L1
TAX1BP1
AP2A1
EPS15
AP2A2
DENND2C
AP2B1
ARFGAP2
AP2M1
AP2S1
MIB1
ANKRD26
AZI1
CABLES1
CCDC112
CCDC138
CCDC14
CCDC18
CCDC66
CCDC77
CCNB2
CCP110
CDK5
CEP55
CEP63
CEP72
CSPP1
HAUS1
HAUS3
HAUS4
HAUS5
HAUS6
HAUS8
IFT74
KIAA0753
KIF14
LRRC49
LUZP1
MAGED1
MED4
MPHOSPH9
NME7
ODF2L
OFD1
PCM1
PIBF1
PLK1
STIL
TCHP
TEX9
TOP3B
TPGS1
TTK
TTLL5
TUBA1A
WRAP73
YTHDC2
Centrosome/cilia
RNF40
RBX1
SPATA2
PCGF6
SUMO1
NEDD8
UBA52
CYLD
UFD1L
CUL4B
USP15
CUL4A
USP9X
BRAP
Ubiquitin and ubiquitin-like modifications
CNOT1
GCN1L1
SKIV2L2
CRNKL1
GEMIN5
SMG7
DDX4
GIGYF2
TDRD3
DIS3L
MFAP1
TNRC6A
E2F4
NUFIP2
TNRC6B
EIF2C2
EIF3A
PEG10
WDR6
EIF3B
POP7
XPO5
EIF3CL
PRPF38A
XRN1
EIF3M
RPP25L
ZCCHC3
EIF4E2
RRS1
ZCCHC8
RNA Processing/translation
HELLS
E2F6
MGA
E2F5
MIS18BP1
E2F3
N4BP1
ATAD5
SUV420H1
ASCC3
TFDP1
ASCC2
ASCC1
DNA-related processes

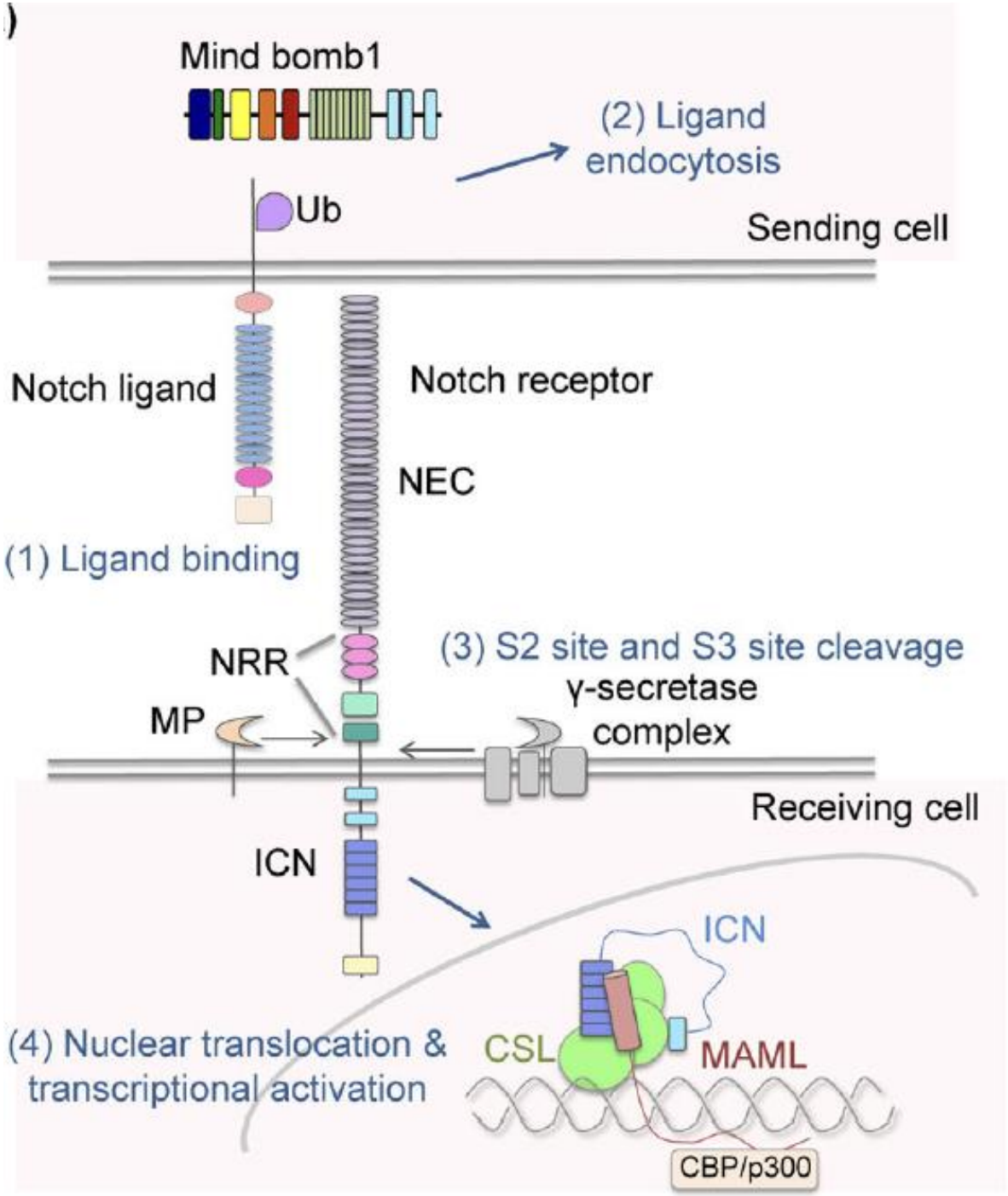

Notch signaling initiates upon transcellular engagement of a Notch ligand with a Notch receptor, and relies on ubiquitin-dependent internalization of the ligand. In vertebrates, ubiquitination is dependent on the E3 ligase **Mind bomb 1 (Mib1).** Transcellular delivery of force is thought to expose a site (S2) within the Notch negative regulatory region (NRR) for cleavage by ADAM-family metalloproteases. S2 cleavage is followed by cleavage at site S3 by gamma secretase, leading to release and entry of of the intracellular Notch (ICN) domain into the nucleus

Review

The NHR domains of Neuralized and related proteins: Beyond Notch signalling

Sili Liu [a,b], Gabrielle L. Boulianne [a,b,*]

S. Liu, G.L. Boulianne / Cellular Signalling 29 (2017) 62–68

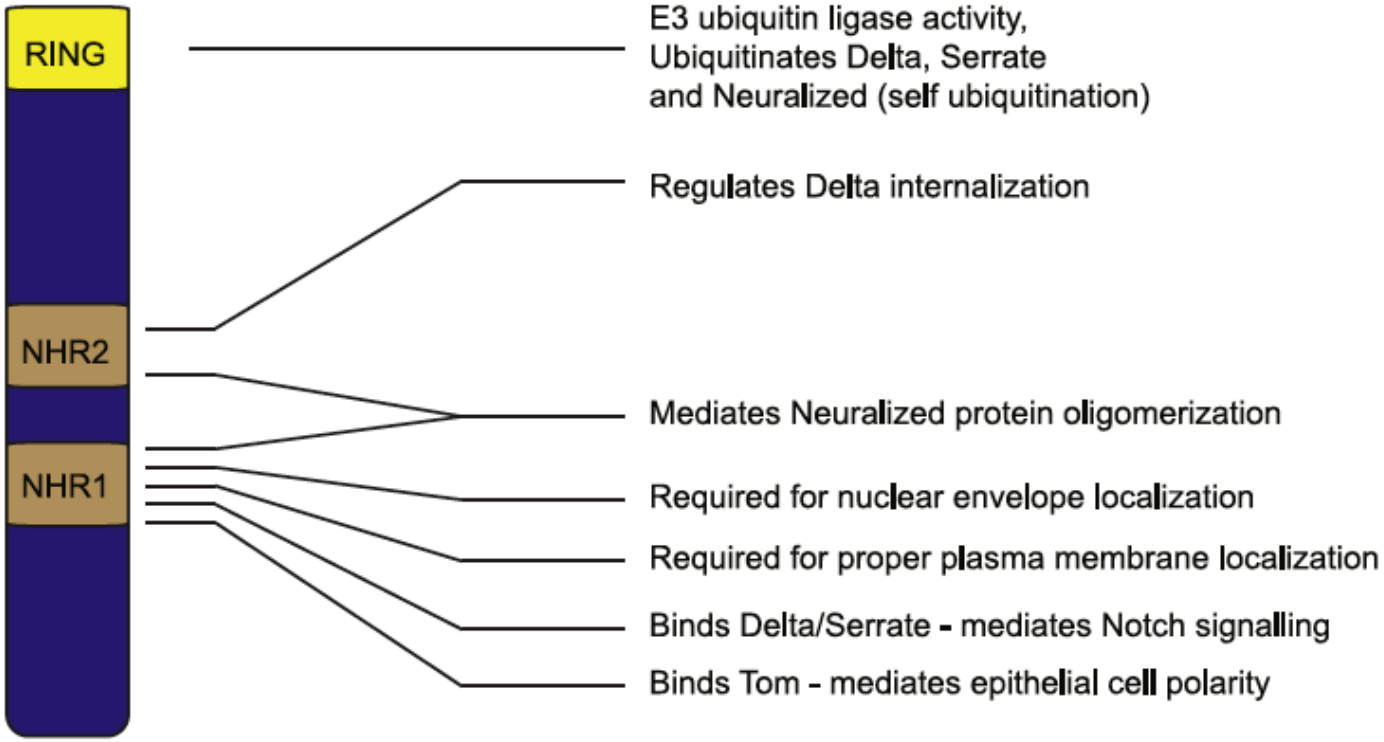

Non-canonical Notch Signaling Pathway

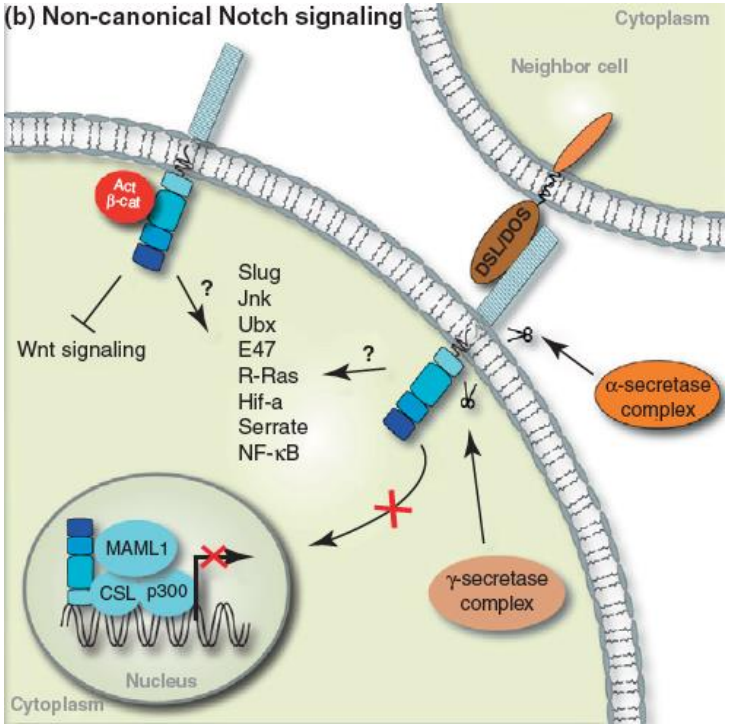

Non-canonical Notch signaling is CSL-independent and can be either ligand-dependent or independent.

The most well-studied and conserved effect of non-canonical Notch function is regulation of **Wnt/β-catenin signaling**: Notch binds and titrate levels of the active β-catenin. Therefore, active β-catenin activity is a readout for non-canonical Notch signals.

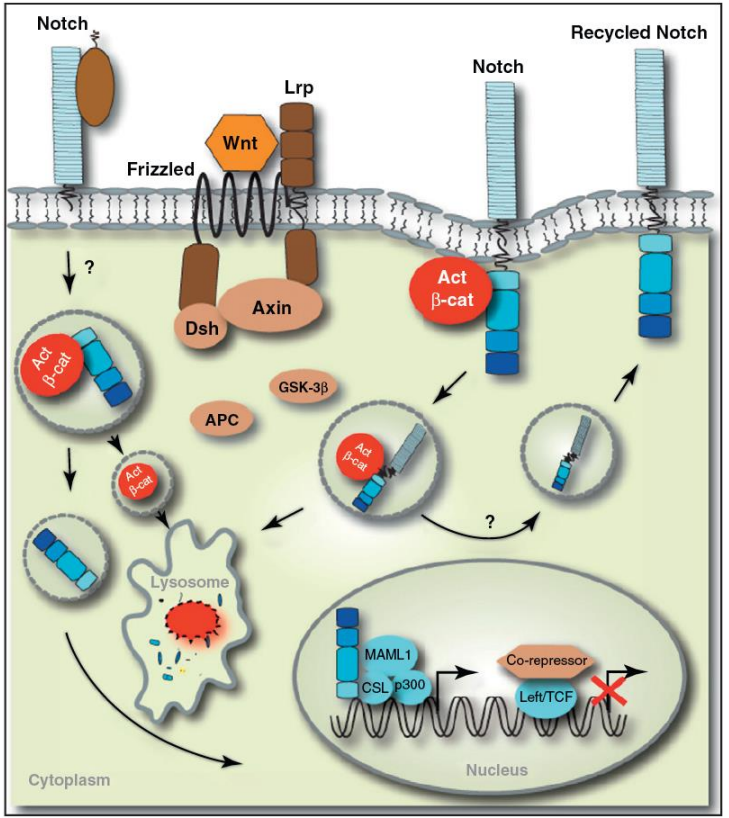

In the presence of Wnts, membrane-bound Notch forms a complex with active β-catenin and degrades active β-catenin through an endo-lysosomal pathway. The degradation is independent of GSK3β-dependent destruction complex.

Whether Notch is recycled back to the membrane is unclear.

Numb regulation of Notch and β-catenin

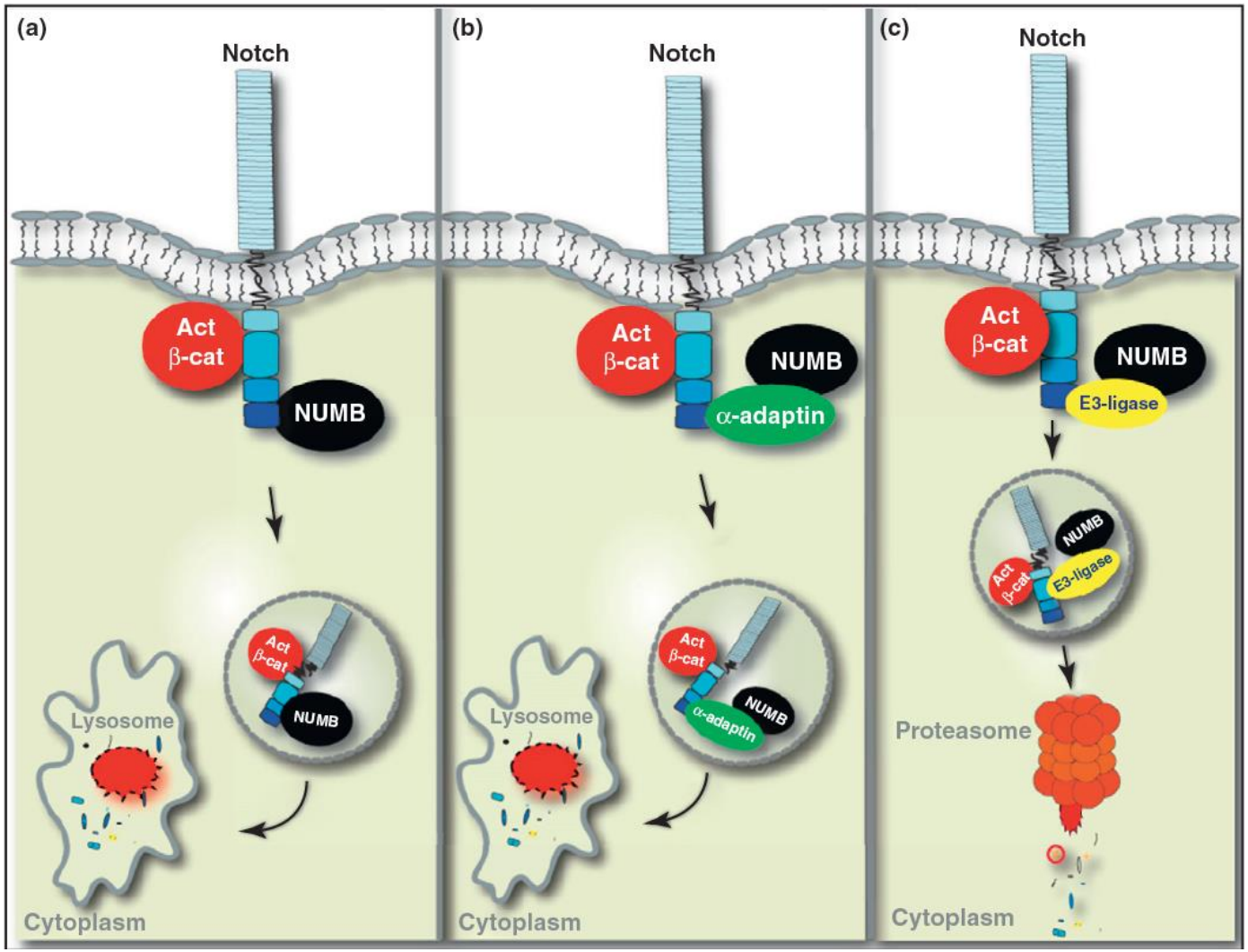

Numb could bind to Notch either directly (a) or dependently from α-adaptin (b), with targeting of the Numb-Notch complex for lysosomal degradation. In both cases it might be possible that activated β-catenin could be targeted for lysosomal destruction. Downregulation of Notch may occur through proteasome-mediated degradation (c).

Notch signaling has effects in many different organs

- Notch signalling can maintain stem cells or precursor populations in an undifferentiated state
- Notch signalling influences binary cell-fate decisions via lateral or inductive signalling
- Notch is able to influence differentiation and cell-cycle progression

Notch signaling and cell-fate decisions

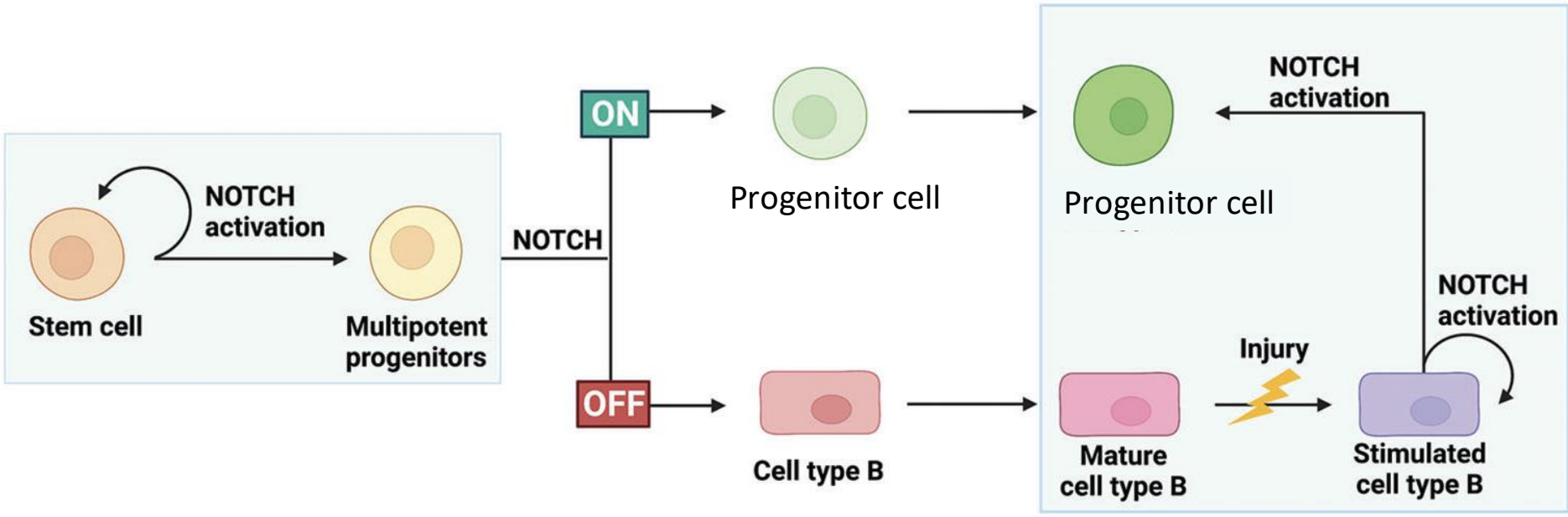

NOTCH signaling is involved in regulating the differentiation and function of stem cells, affecting organ production and damage repair

Notch function in the developing nervous system of vertebrates.

Development 140, 689-704 (2013) doi:10.1242/dev.080614

Stem cells living with a Notch

Ute Koch, Rajwinder Lehal and Freddy Radtke*

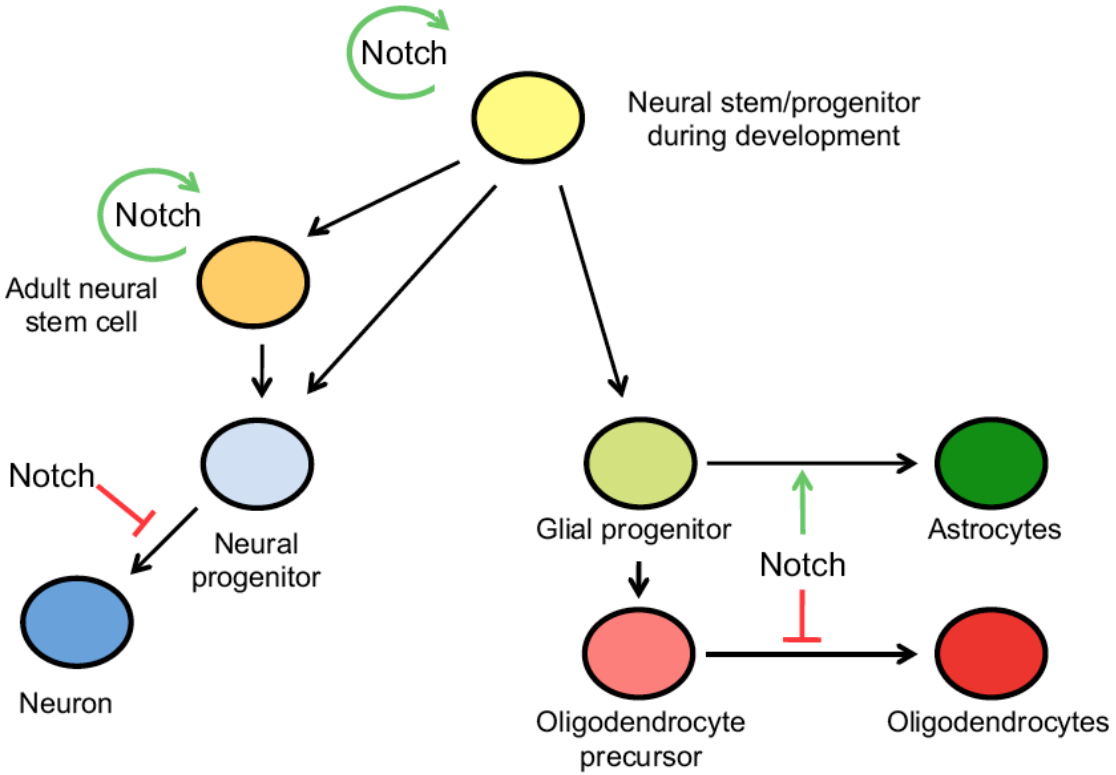

Notch signaling regulates self-renewal (curved green arrows) of developing and adult neural stem cells, preserving the neural stem cell pool. Notch also promotes gliogenesis (straight green arrow), whereas oligodendrocyte and terminal differentiation of neurons are inhibited (red capped bars).

LINEAGE DECISION

The NICD-RBP-Jk complex up-regulates expression of target genes of Notch signaling such as HES and HERP in mammals.

The HES family is a basic helix-loop-helix (bHLH) type trancriptional repressor and acts as Notch effectors by negatively regulating expression of downstream target genes such as tissue-specific transcription factors.

HES1 and HES5, for instance, were shown to be upregulated by NICD and necessary to prevent neuronal differentiation of neural precursor cells from mouse embryos

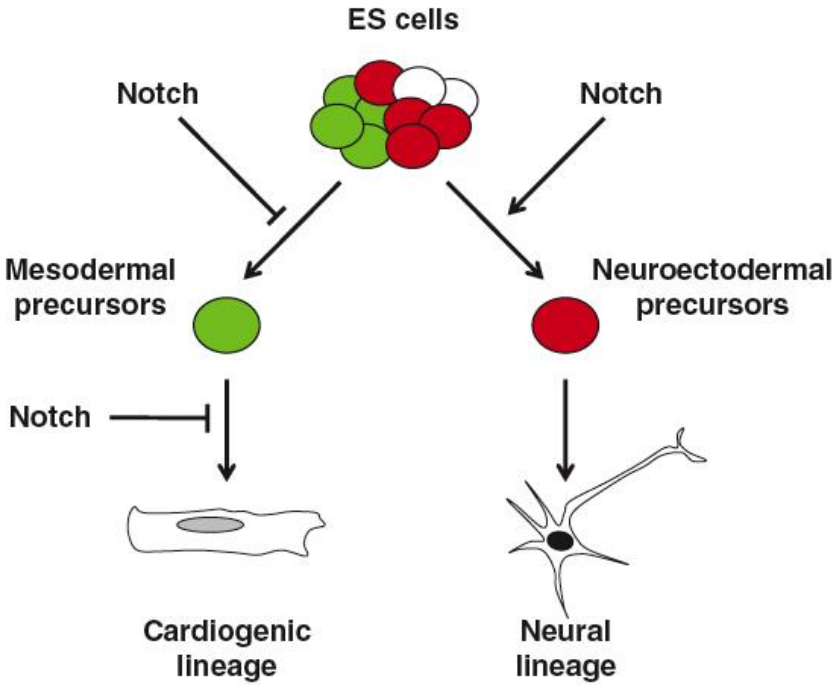

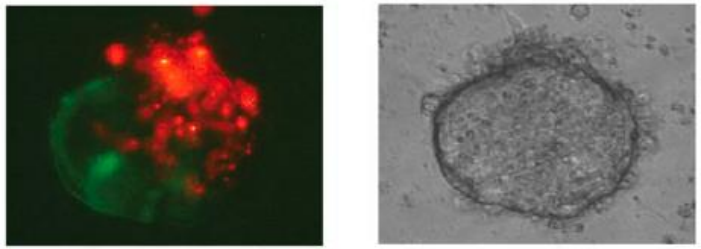

Pedrazzini et al., 2007

May 2012 | Volume 7 | Issue 5 | e37365

Notch2 and Notch3 Function Together to Regulate Vascular Smooth Muscle Development

Qingqing Wang[1], Ning Zhao[1,2], Simone Kennard[3], Brenda Lilly[1,2]*

Embryos lacking both Notch2 and Notch3 have disrupted blood vessels

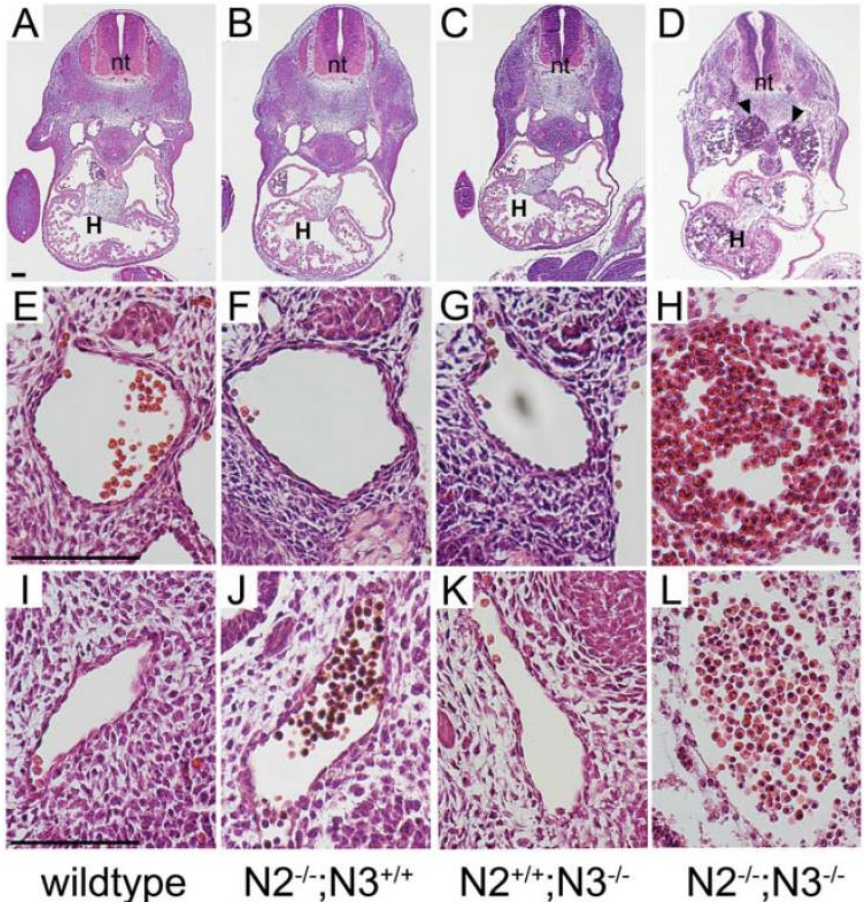

Yolk sac

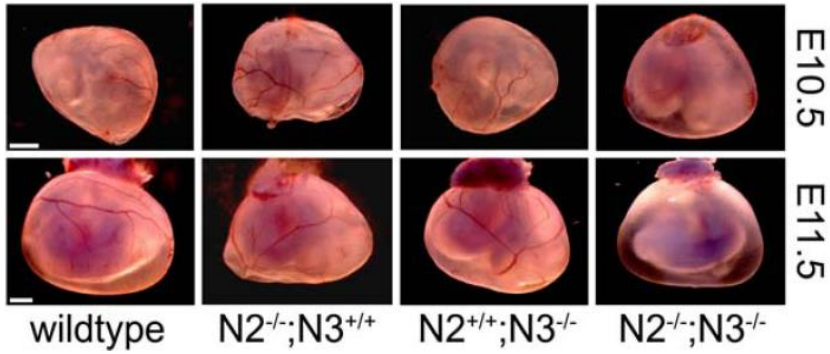

Embryos

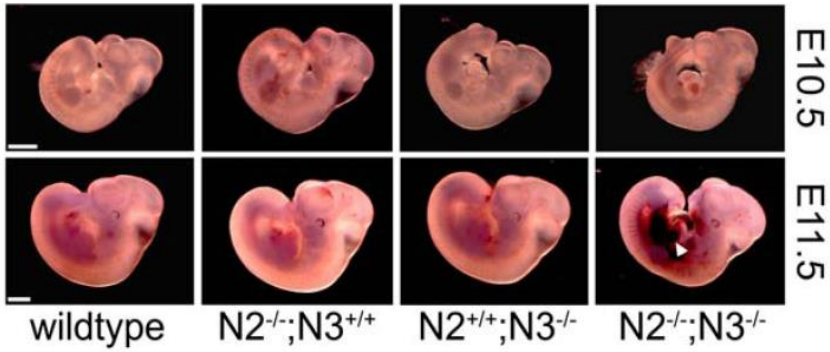

At E10.5, Notch2-/-;Notch3-/-; (N2-/-;N3-/-) embryos exhibit a decrease in yolk sac blood vessels, while the embryo is relatively normal in appearance.

At E11.5, Notch2-/-;Notch3-/- mice show severe vascular defects in both yolk sac and embryo. Yolk sac blood vessels are not visible and extensive hemorrhaging is seen in the embryo (arrowhead).

Active Notch signaling during angiogenesis

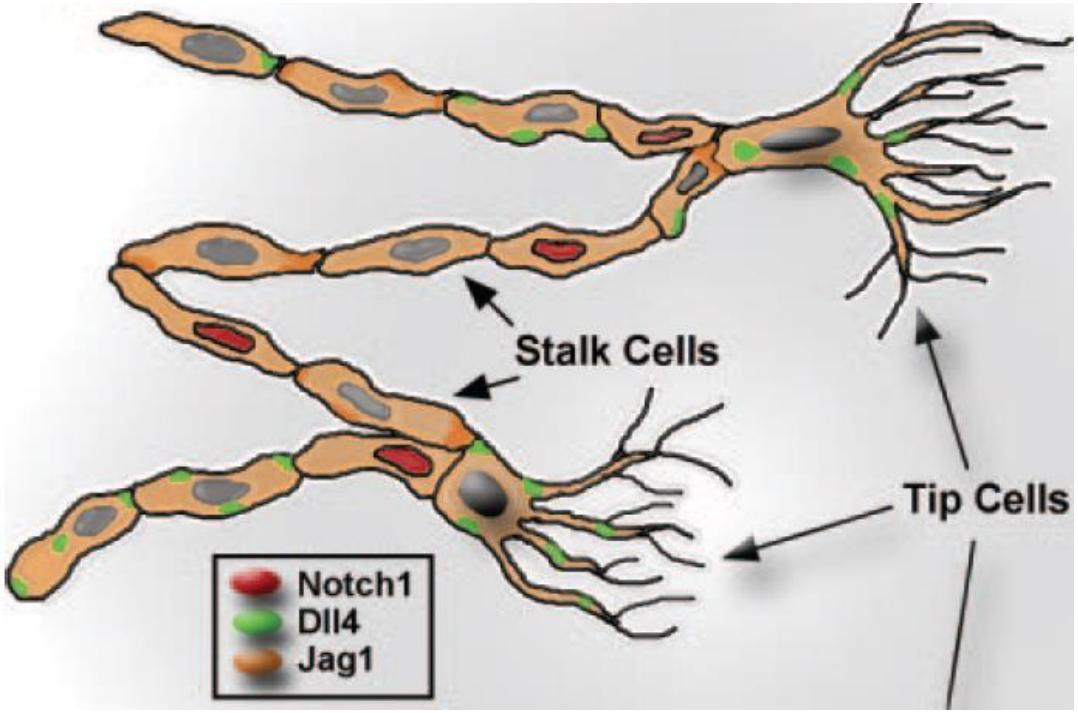

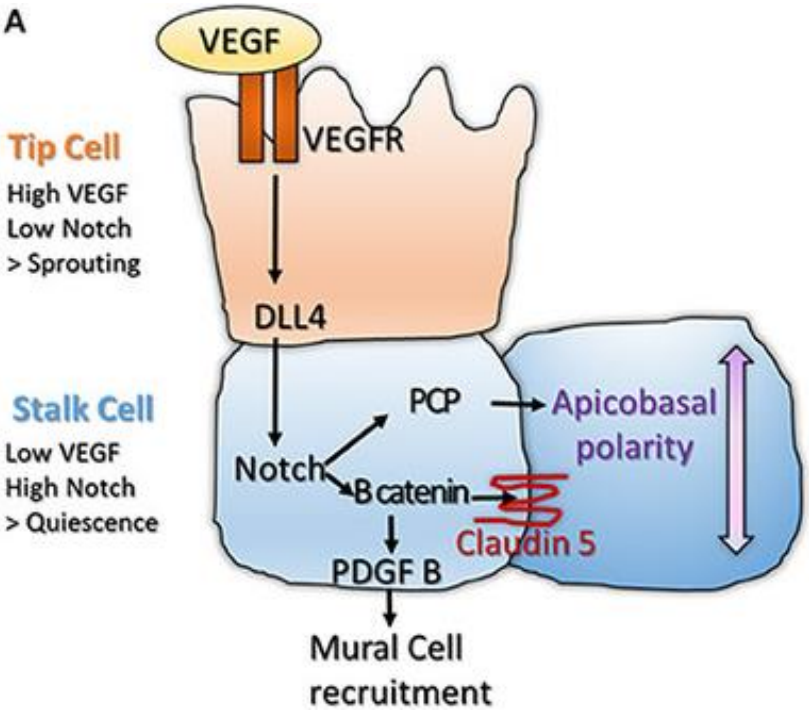

Relative distribution of active Notch1 (red), Delta-like4 (Dll4) (green), and Jagged1 (Jag1) (orange) in tip and stalk cells of angiogenic sprouts.

The pattern of active Notch is scattered in stalk cells.

In contrast, Dll4 expression solely marks the tip cells at the leading edge of the vascular front.

Table 1. Relationship between Notch signaling and congenital heart disease.

Congenital heart disease	Gene mutation
Aortic valve degenerative disease	RBP-Jκ
Left ventricular outflow tract defects	Notch 1
Bicuspid aortic valve disease	Notch 1-4, Jagged 1, Hes 1, Hey 1, Hey 2
Aortic valve calcification	Notch 1, Hey 1, Hey 2
Pulmonic stenosis	Jagged 1
Tetralogy of Fallot	Jagged 1
Mitral valve disease	HRT 2
Tricuspid valve disease	HRT 2
Ventricular septal defect	HRT 2
Atrial septal defect	HRT 2
Pericardial distension	Notch 1, RBP-Jκ
Alagille syndrome	Notch 2, Jagged 1, HRT 2, Hey 2

RBP-Jκ: recombination signal binding protein for immunoglobulin Jκ region; Hes: hairy and enhancer of split: Hey: hairy/enhancer of split-related with YRPW motif; HRT: hairy-related transcription.

Regulatory role of Notch signaling for myocardial regeneration.

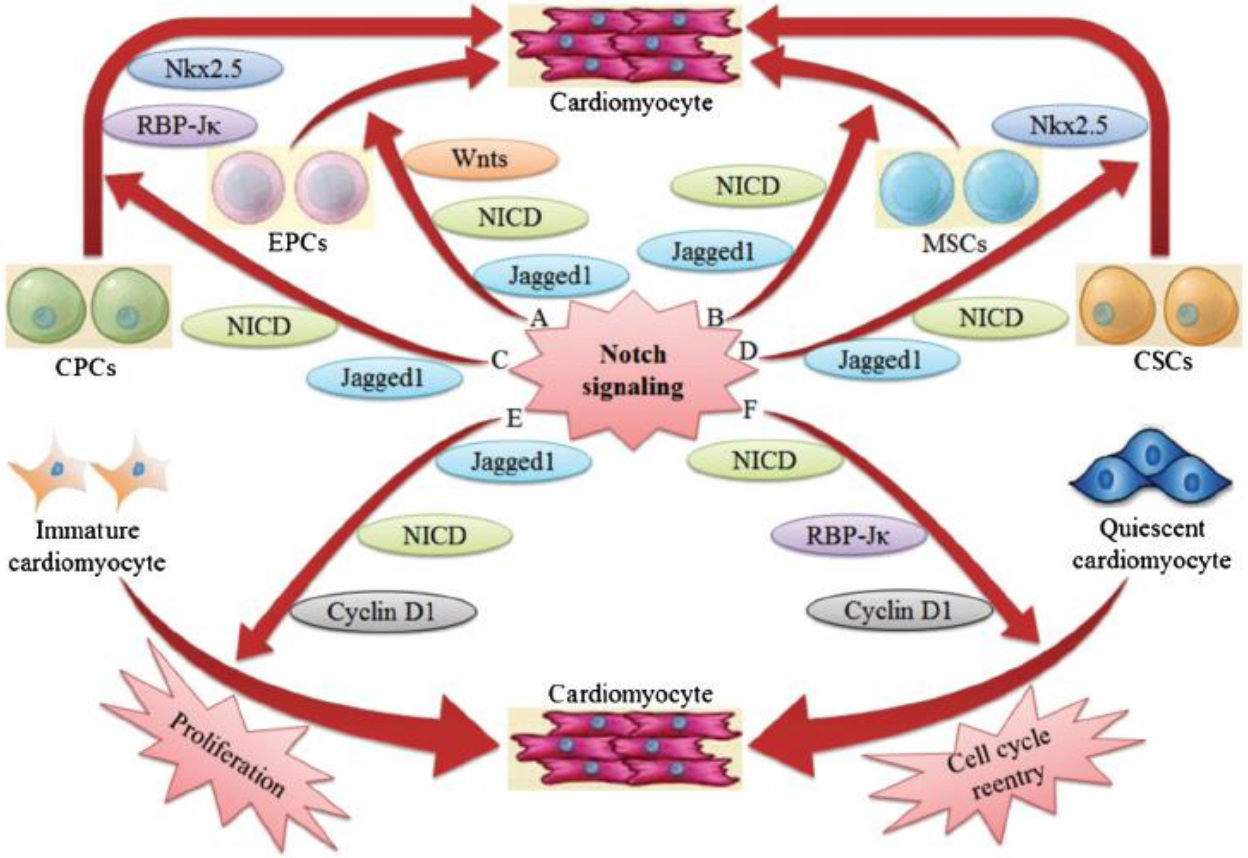

A, Notch signaling amplifies EPC differentiation into cardiomyocytes through Jagged 1, NICD and Wnts.
B, MSCs enhance cardiomyocyte proliferative capacity through Jagged 1 and NICD.
C, Notch signaling promotes the differentiation of CPCs into cardiomyocytes through Jagged 1, NICD, RBP-Jk, and Nkx2.5.
D, Notch signaling expands the proportion of CSCs differentiating into cardiomyocytes through Jagged 1, NICD, and Nkx2.5.
E, Notch 1 signaling stimulates proliferation of immature cardiomyocytes through Jagged1, NICD, and cyclin D1.
F, Notch signaling activates cell cycle reentry of quiescent cardiomyocytes through NICD, RBP-Jk, and cyclin D1.

The proliferative potential of adult cardiomyocytes is extremely limited or null

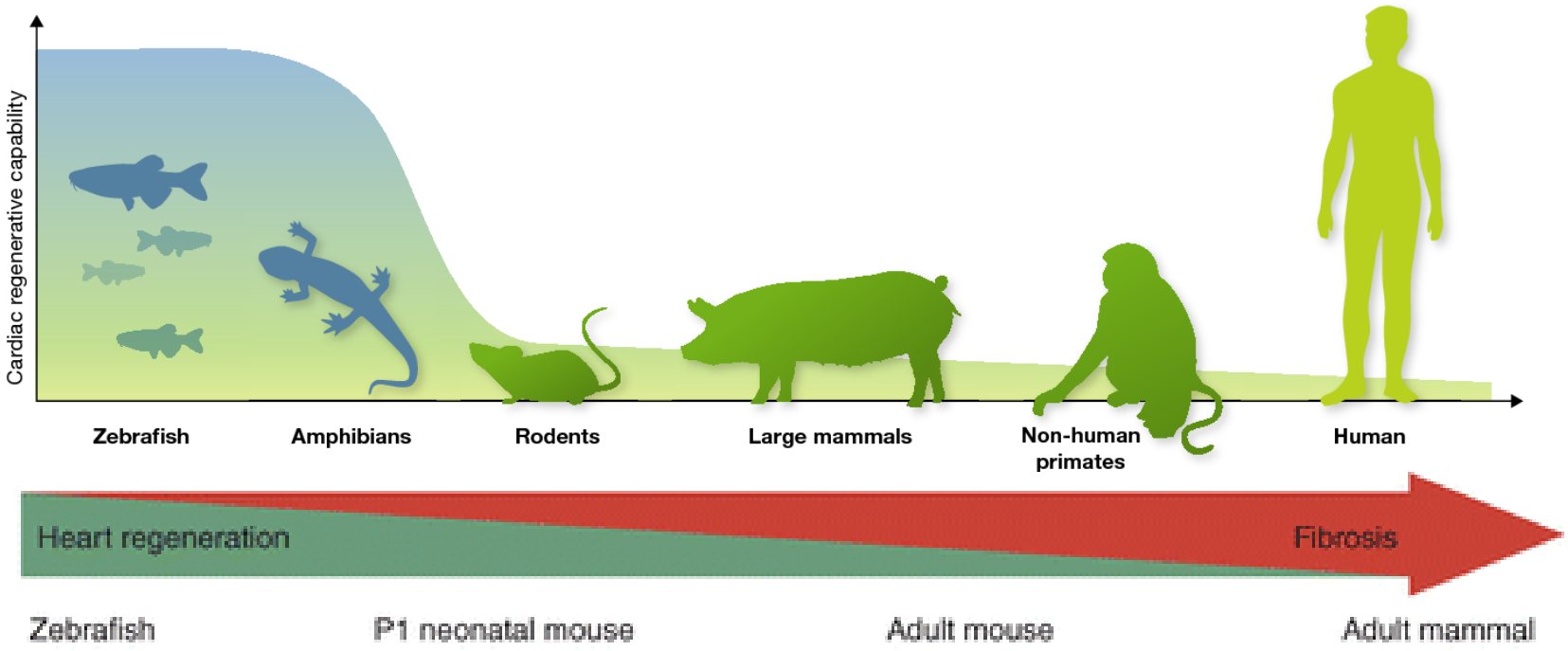

Regeneration genetics in Zebrafish

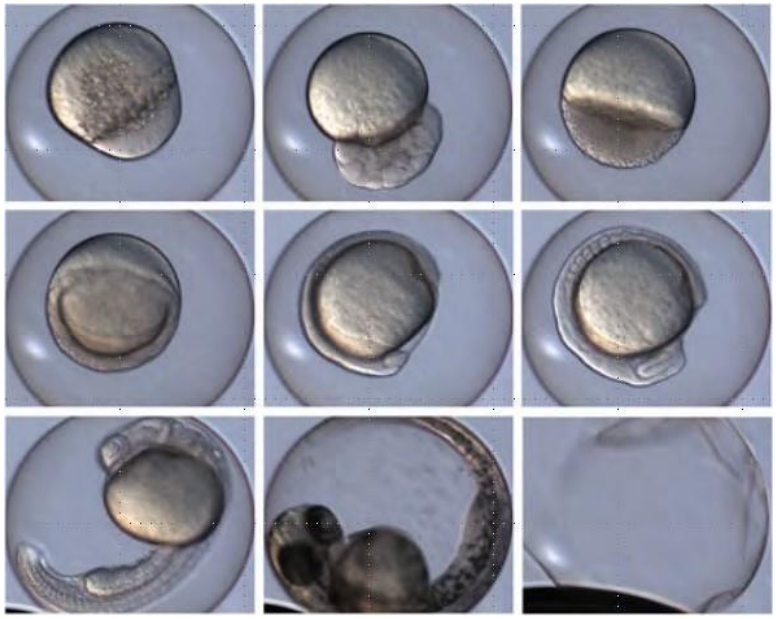

- Its fecundity makes it an optimal candidate for genetic and genomic analysis
- Eggs are fertilized outside the mother body - easy harvest and manipulation
- The embryo is transparent
- Thousands of mutations generated and characterized
- It regenerates fins, spinal cord, and optic nerve

Tales of Regeneration in Zebrafish

Kenneth D. Poss, Mark T. Keating, and Alex Nechiporuk*

DEVELOPMENTAL DYNAMICS 226:202–210, 2003

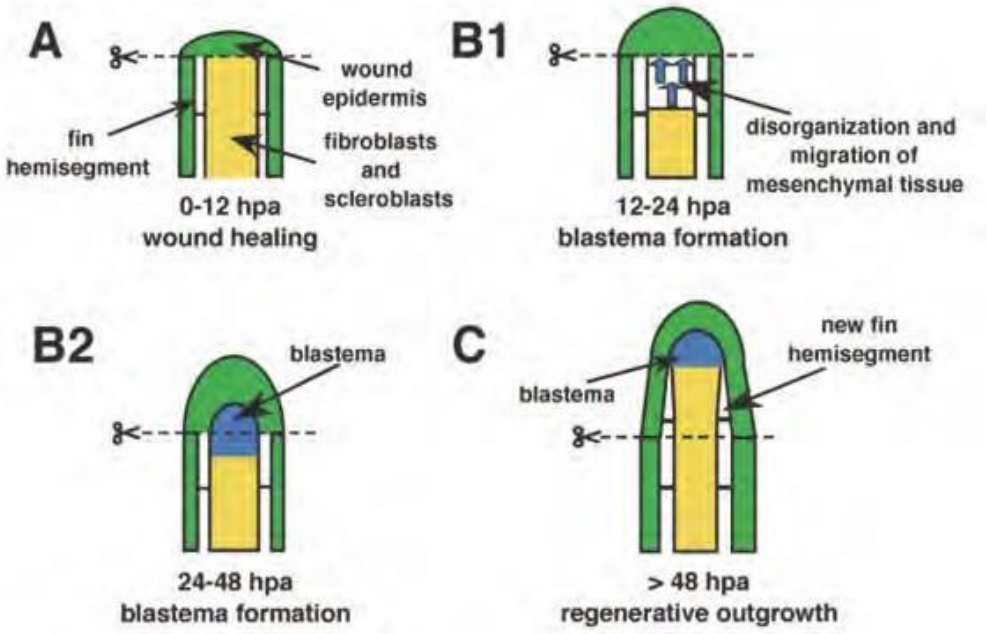

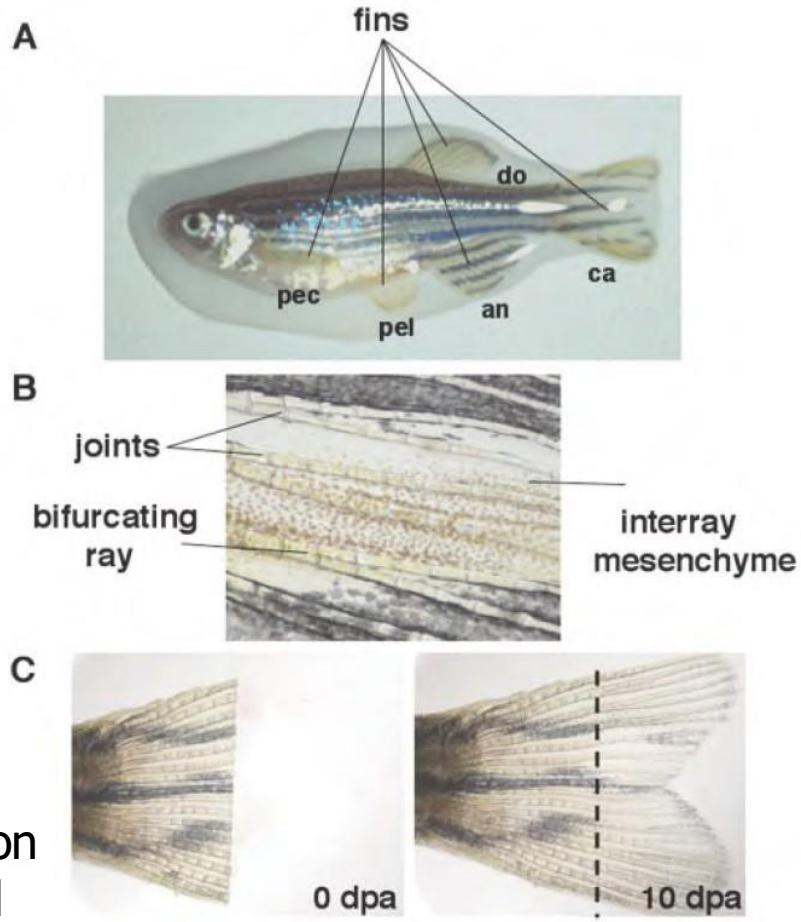

A hallmark of epimorphic limb or fin regeneration is formation of the **blastema**, a developmental event that distinguishes regeneration from embryogenesis.

Heart Regeneration in Zebrafish

Kenneth D. Poss,* Lindsay G. Wilson, Mark T. Keating*

13 DECEMBER 2002 VOL 298 SCIENCE

Cardiac injury in mammals and amphibians typically leads to scarring, with minimal regeneration of heart muscle. Here, we demonstrate histologically that zebrafish fully regenerate hearts within 2 months of 20% ventricular resection. Regeneration occurs through robust proliferation of cardiomyocytes localized at the leading epicardial edge of the new myocardium. The hearts of zebrafish with mutations in the Mps1 mitotic checkpoint kinase, a critical cell cycle regulator, failed to regenerate and formed scars. Thus, injury-induced cardiomyocyte proliferation in zebrafish can overcome scar formation, allowing cardiac muscle regeneration. These findings indicate that zebrafish will be useful for genetically dissecting the molecular mechanisms of cardiac regeneration.

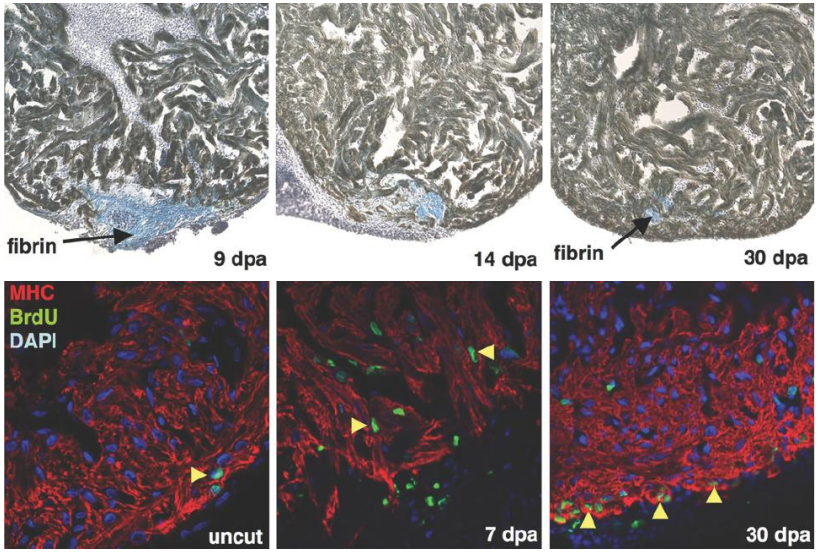

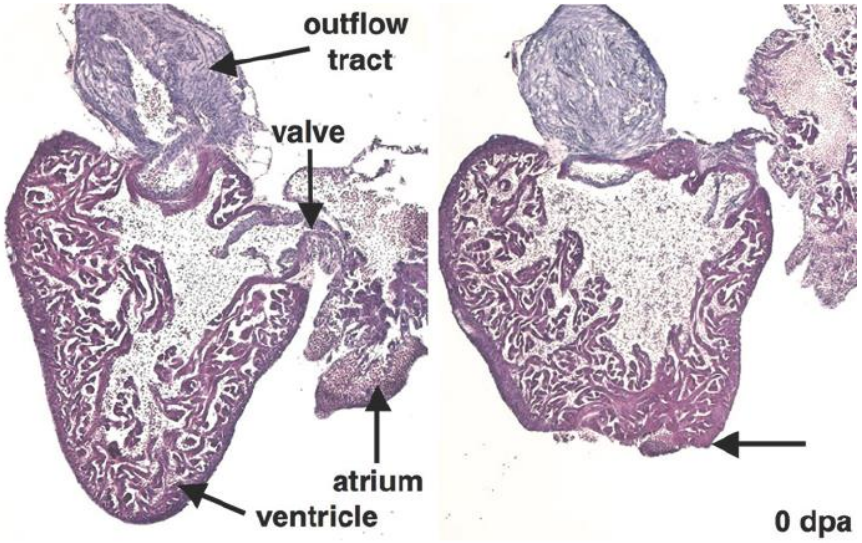

Primary contribution to zebrafish heart regeneration by *gata4*$^{+}$ cardiomyocytes

Kazu Kikuchi[1,2], Jennifer E. Holdway[1,2], Andreas A. Werdich[4], Ryan M. Anderson[5], Yi Fang[1,2], Gregory F. Egnaczyk[1,2,3], Todd Evans[6], Calum A. MacRae[4], Didier Y. R. Stainier[5] & Kenneth D. Poss[1,2]

NATURE | Vol 464 | 25 March 2010

Many different hypothesis for the BrdU labeling results:

- First, differentiated, contracting CMs in existing myofibers could be stimulated to enter the cell cycle, divide, and reform the apex.
- Second, regeneration could proceed through the recruitment of undifferentiated progenitor cells that form new, proliferative CMs.
- A third conceivable mechanism for the origin of regenerative muscle is a chimera of these two mechanisms called "dedifferentiation", in which existing muscle would downregulate contractile genes toward creation of undifferentiated or poorly differentiated cells.

How is organ size control achieved?

Primary contribution to zebrafish heart regeneration by *gata4*$^{+}$ cardiomyocytes

Kazu Kikuchi[1,2], Jennifer E. Holdway[1,2], Andreas A. Werdich[4], Ryan M. Anderson[5], Yi Fang[1,2], Gregory F. Egnaczyk[1,2,3], Todd Evans[6], Calum A. MacRae[4], Didier Y. R. Stainier[5] & Kenneth D. Poss[1,2]

NATURE | Vol 464 | 25 March 2010

Cardiomyocytes are the source of the regenerating tissues and expressed a marker of regeneration called *gata4*—a transcription factor involved in normal development of the heart

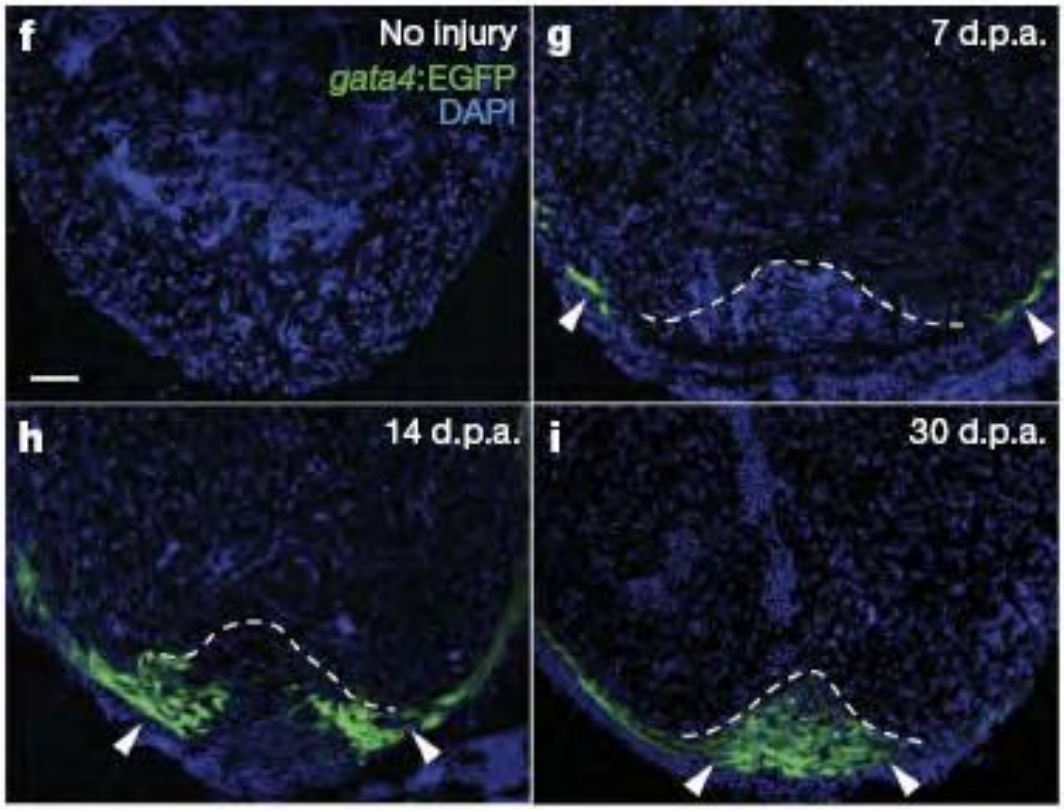

PNAS | September 30, 2003 | vol. 100 | suppl. 1 | 11889–11895

Activation of Notch signaling pathway precedes heart regeneration in zebrafish

Ángel Raya*†, Christopher M. Koth*†, Dirk Büscher*†, Yasuhiko Kawakami*†, Tohru Itoh*†, R. Marina Raya*, Gabriel Sternik*, Huai-Jen Tsai‡, Concepción Rodríguez-Esteban*, and Juan Carlos Izpisúa-Belmonte*§

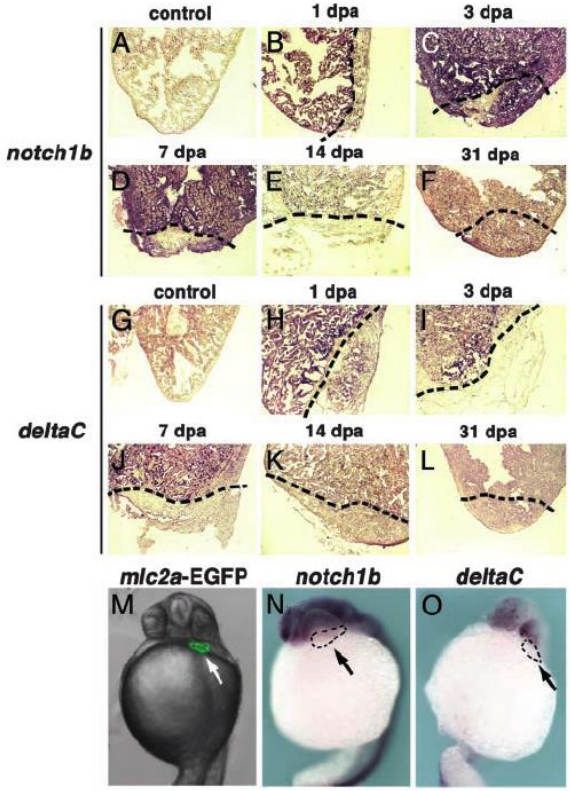

Heart regeneration in zebrafish is accompanied by up-regulation of components of the Notch pathway, followed by members of the Msx family.

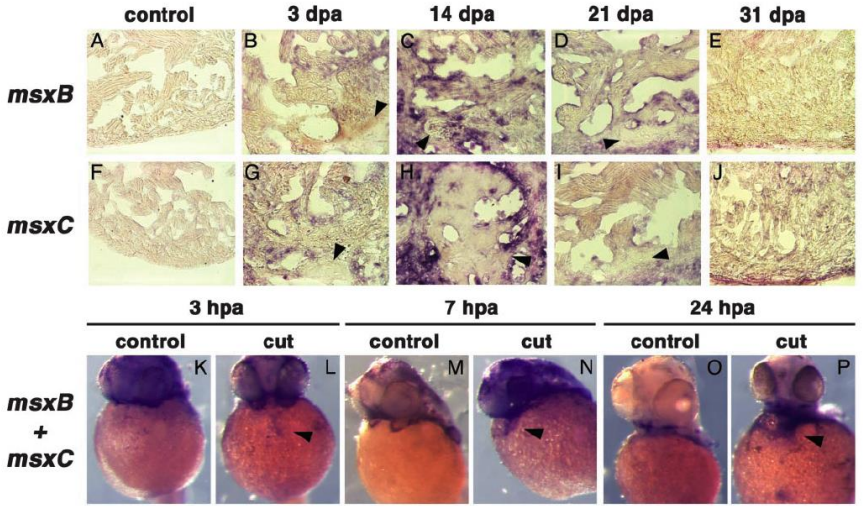

These genes are not expressed during zebrafish heart development, indicating that **regeneration** involves the execution of a specific genetic program, rather than redeployment of a developmental program.

Cell, Vol. 103, 1099–1109, December 22, 2000, Copyright ©2000 by Cell Press

Dedifferentiation of Mammalian Myotubes Induced by msx1

Shannon J. Odelberg,*§‖ Angela Kollhoff,† and Mark T. Keating*†‡‖#
*Division of Cardiology, Department of Internal Medicine

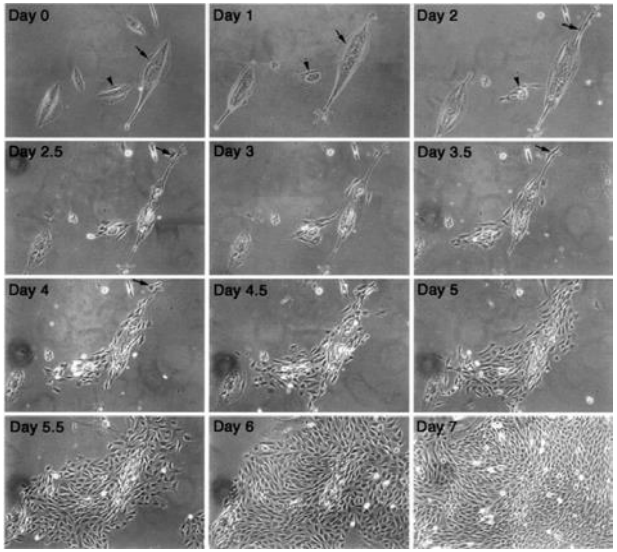

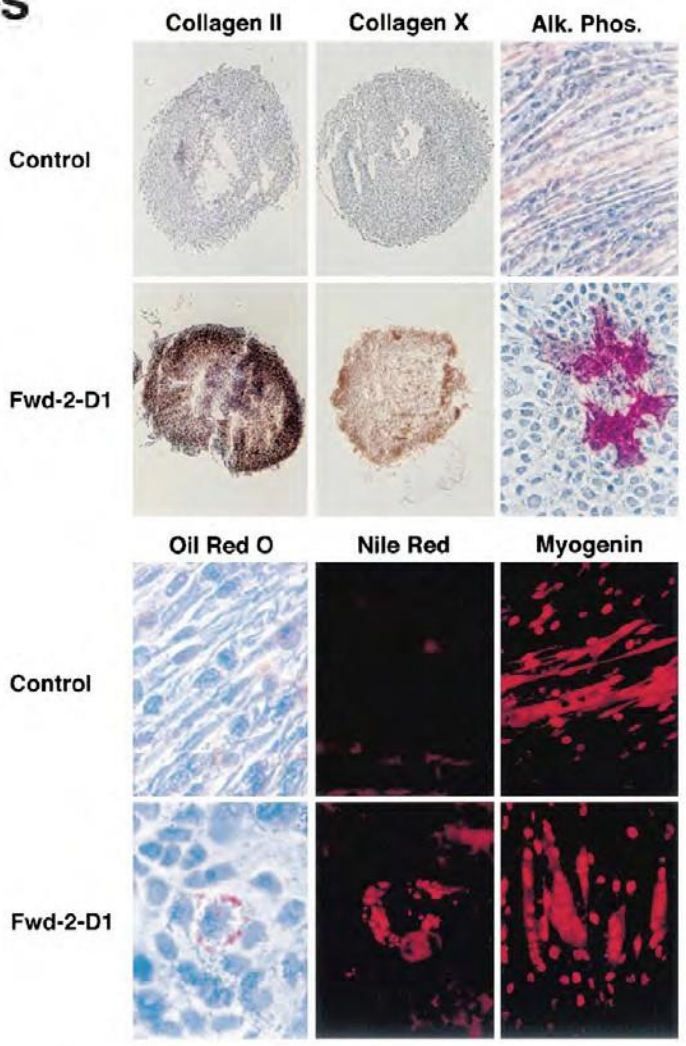

Mononucleated cells from dedifferentiated myotubes exhibit signs of pluripotency (subjected to chondrogenic, osteogenic, adipogenic, and myogenic inducing signals)

Mammalian cells might maintain the pathways required to respond to the proper “pro-regeneration” signals

Several factors could explain the absence of cellular dedifferentiation in mammals:

1. The extracellular factors that initiate dedifferentiation are not adequately expressed following amputation
2. The intrinsic cellular signaling pathways for dedifferentiation are absent
3. Differentiation factors are irreversibly expressed in mammalian cells
4. Structural characteristics of mammalian cells make dedifferentiation impossible

Mammalian myotube dedifferentiation induced by newt regeneration extract

Christopher J. McGann*†, Shannon J. Odelberg*†‡, and Mark T. Keating‡§¶||

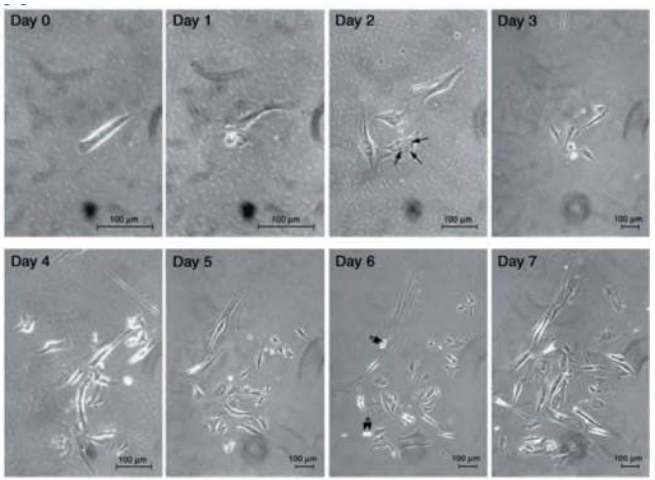

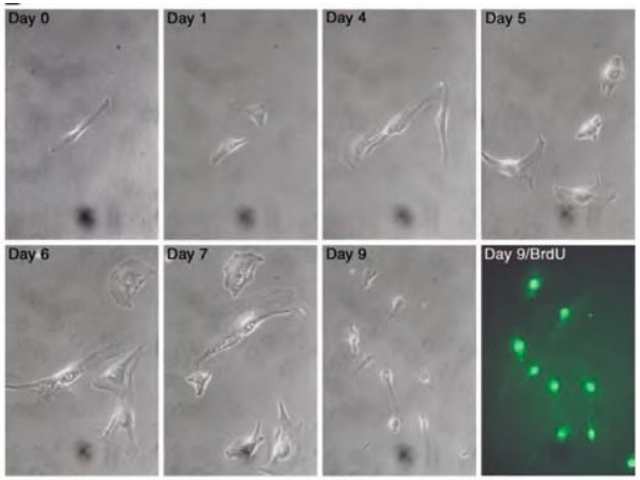

Mammalian cells retain the intracellular signaling pathways required for dedifferentiation, suggesting that mammals fail to exhibit *in vivo* cellular dedifferentiation because they lack the signals (proteins!) that initiate the process

PNAS | November 20, 2001 | vol. 98 | no. 24 | 13699–13704

nature Vol 464|25 March 2010|doi:10.1038/nature08899

LETTERS

Zebrafish heart regeneration occurs by cardiomyocyte dedifferentiation and proliferation

Chris Jopling[1], Eduard Sleep[1,2]†, Marina Raya[1]†, Mercè Martí[1], Angel Raya[1,2,3]† & Juan Carlos Izpisúa Belmonte[1,2,4]

Although mammalian hearts show almost no ability to regenerate, there is a growing initiative to determine whether existing cardiomyocytes or progenitor cells can be coaxed into eliciting a regenerative response. In contrast to mammals, several non-mammalian vertebrate species are able to regenerate their hearts[1–3], including the zebrafish[4,5], which can fully regenerate its heart after amputation of up to 20% of the ventricle. To address directly the source of newly formed cardiomyocytes during zebrafish heart regeneration, we first established a genetic strategy to trace the lineage of cardiomyocytes in the adult fish, on the basis of the Cre/*lox* system widely used in the mouse[6]. Here we use this system to show that regenerated heart muscle cells are derived from the proliferation of differentiated cardiomyocytes. Furthermore, we show that proliferating cardiomyocytes undergo limited dedifferentiation characterized by the disassembly of their sarcomeric structure, detachment from one another and the expression of regulators of cell-cycle progression. Specifically, we show that the gene product of *polo-like kinase 1* (*plk1*) is an essential component of cardiomyocyte proliferation during heart regeneration. Our data provide the first direct evidence for the source of proliferating cardiomyocytes during zebrafish heart regeneration and indicate that stem or progenitor cells are not significantly involved in this process.

NATURE | Vol 464 | 25 March 2010

Regenerated cardiomyocytes are derived from differentiated, pre-existing cardiomyocytes

has been regenerated by cardiomyocytes. The exact source of these new cardiomyocytes is not yet known definitively. To address this question we developed and successfully implemented the 4-hydroxy-tamoxifen (4-OHT)-inducible Cre/*lox* approach in zebrafish to label regenerating cardiomyocytes genetically (for a detailed description of the lines generated and/or methodologies, see Methods and Supplementary Figs 1–9).

genetically labelled 48 h after fertilization. About 20% of the ventricle was removed, and cardiac regeneration was subsequently assessed at 7, 14 and 30 days after amputation. At 7 days after amputation, the remaining cardiac tissue was uniformly positive for green fluorescent protein (GFP) (Fig. 1a, b), with much of the missing tissue now replaced by a fibrin/collagen clot ($n = 5$ hearts) (Fig. 1c). At 14 days

($n = 7$ hearts; Fig. 1f). These results suggest that the regenerated cardiomyocytes arise from differentiated GFP-positive cardiomyocytes. These findings were substantiated at 30 days after amputation, when regeneration is nearly complete; all of the cardiomyocytes within the

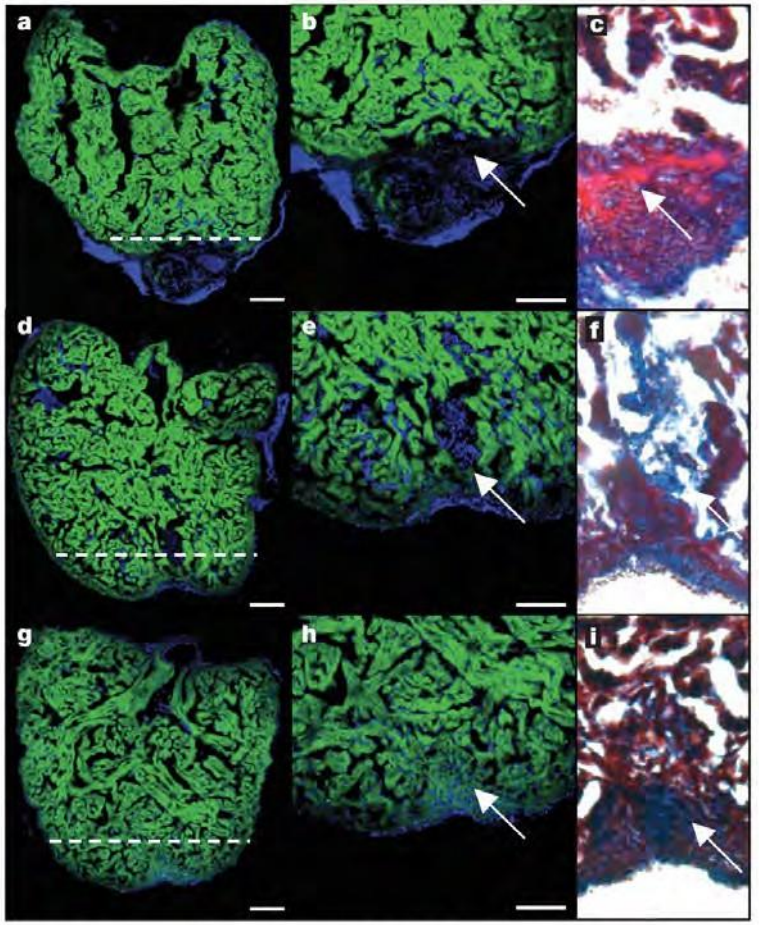

Figure 1 | Regenerated cardiomyocytes are derived from differentiated cardiomyocytes. Cardiomyocytes in transgenic zebrafish (tg-cmlc2a-Cre-Ert2: tg-cmlc2a-LnL–GFP) were genetically labelled at 48 h after fertilization by inducing Cre activity with tamoxifen. These embryos were then grown to adulthood (3 months or sexually mature), at which point the heart was amputated and allowed to regenerate for 7 (**a**–**c**), 14 (**d**–**f**) or 30 (**g**–**i**) days. The dashed white line represents the plane of amputation. At 7 days after amputation (**a**; enlargement in **b**) relatively little regeneration has occurred. Trichromic staining indicates that a fibrin clot has formed adjacent to the wound (**c**). By 14 days after amputation, GFP-positive cardiomyocytes have regenerated a substantial amount of new cardiac tissue (**d**; enlargement in **e**) and the fibrin clot was decreased in size (**f**). At 30 days after amputation, heart regeneration is virtually complete (**g**; enlargement in **h**) and all of the regenerated tissue is composed of GFP-positive cardiomyocytes. The clot has been replaced by a small scar (**h**). Scale bars, 100 μm (**a**, **d**, **g**) and 75 μm (**b**, **e**, **h**). Panels **c**, **f** and **i** are ×2 magnifications of the areas indicated with a white arrow in **b**, **e** and **h**.

Differentiating cardiomyocytes re-enter the cell cycle

We next sought to determine whether GFP-positive cardiomyocytes had re-entered the cell cycle. Adult GFP-positive transgenic zebrafish were treated with bromodeoxyuridine (BrdU) for 7 days after amputation (Fig. 2a–f). Subsequently, at 14 days after amputation, we found a significant increase in the number of BrdU-positive/GFP-positive cardiomyocytes in regenerating hearts compared with non-amputated controls (Fig. 2g). From this we conclude that differentiated GFP-positive cardiomyocytes had re-entered the cell cycle and engaged in DNA replication. We also analysed the position of BrdU-labelled GFP-positive cardiomyocytes within the regenerating heart (Fig. 2h and inset). Whereas most BrdU-positive/GFP-positive labelled cardiomyocytes were concentrated around the wound, a proportion could also be found in regions far from the site of amputation. This suggests that the response to the injury affects the heart in a global manner.

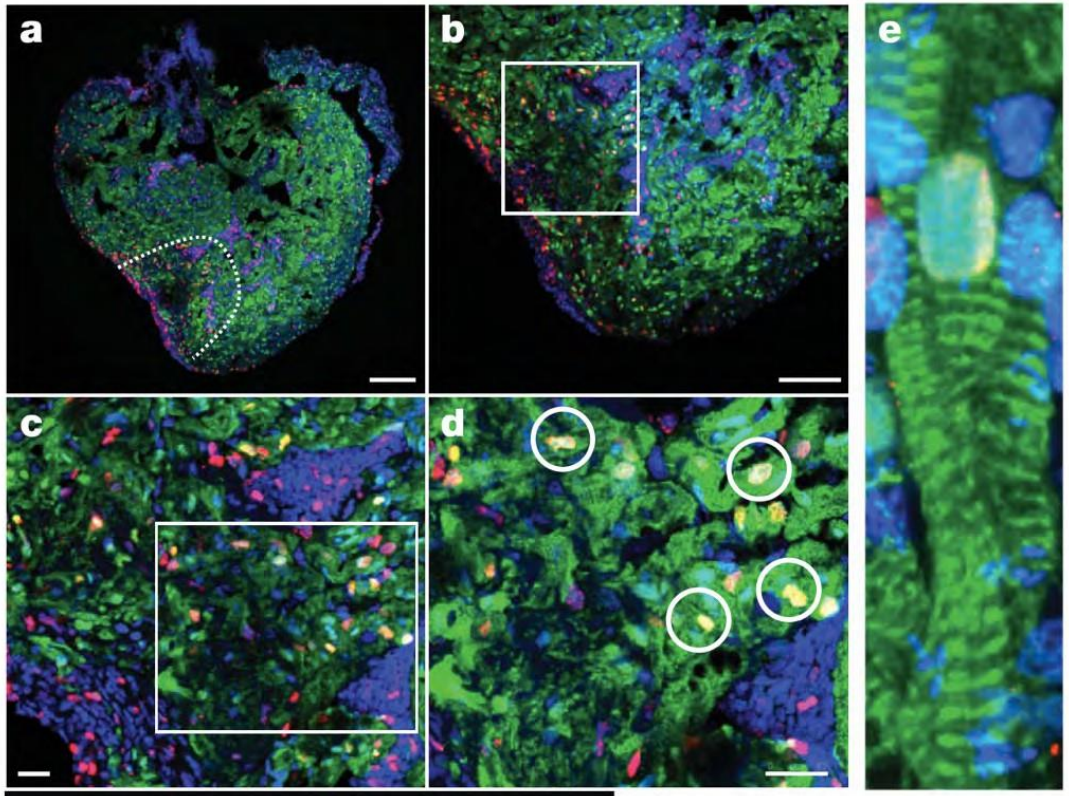

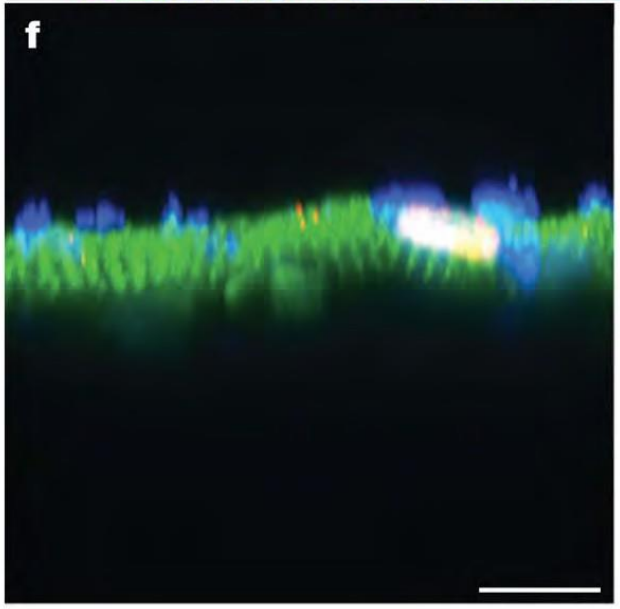

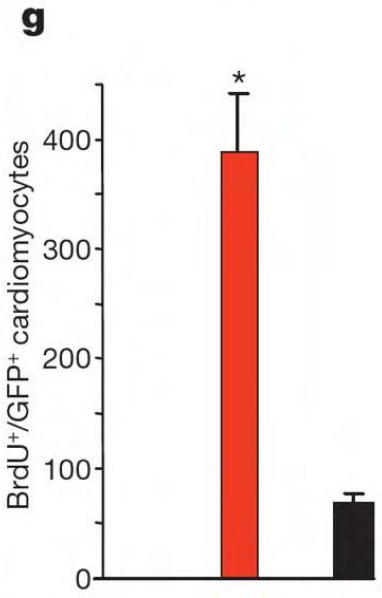

Figure 2 | Differentiated cardiomyocytes re-enter the cell cycle. (**a**–**f**) Transgenic zebrafish (tg-cmlc2a-Cre-Ert2: tg-cmlc2a-LnL–GFP) genetically labelled at 48 h after fertilization and grown to adulthood underwent cardiac amputation and were then treated with BrdU for 7 days after amputation. Hearts were isolated and processed at 14 days after amputation. Green, GFP-positive cardiomyocytes; red, BrdU-positive cells; blue, 4,6-diamidino-2-phenylindole stain for DNA; yellow, BrdU-positive/GFP-positive cardiomyocytes (white rings in **d**). **a**, Section of the entire heart, with a dashed white line representing the regenerating area. **b**, Enlargement of the regenerating area. **c**, **d**, Enlargements of the boxed areas in **b** and **c**, respectively. **e**, An *XY* reconstruction of an individual BrdU-positive/GFP-positive cardiomyocyte within a regenerating heart 14 days after amputation. **f**, An *XZ* reconstruction of the BrdU-positive/GFP-positive cardiomyocyte shown in **e**. **g**, The average number of BrdU-positive/GFP-positive cardiomyocytes per section (means and s.e.m.). Asterisk, $P < 0.01$ (*t*-test). Amputated (red bar), $n = 17$ sections from seven different animals; control (black bar), $n = 9$ sections from three different animals.

Regenerating cardiomyocyte partially disassemble the contractile apparatus but not revert to an embryonic stage

lineage they regress[7,8]. An increase in the expression of the cardiac-progenitor-associated genes *nkx2.5* and *hand2* during zebrafish heart regeneration has been reported[9]. However, our own *in situ* hybridization analyses failed to detect any significant upregulation of either transcript (data not shown), confirming previous results from our laboratory[5]. Furthermore, genome-wide transcriptome data[10,11] also failed to detect significant changes in the expression of either transcript during zebrafish heart regeneration. These results argue against an extensive dedifferentiation of cardiomyocytes as a prerequisite for their proliferation in the context of heart regeneration.

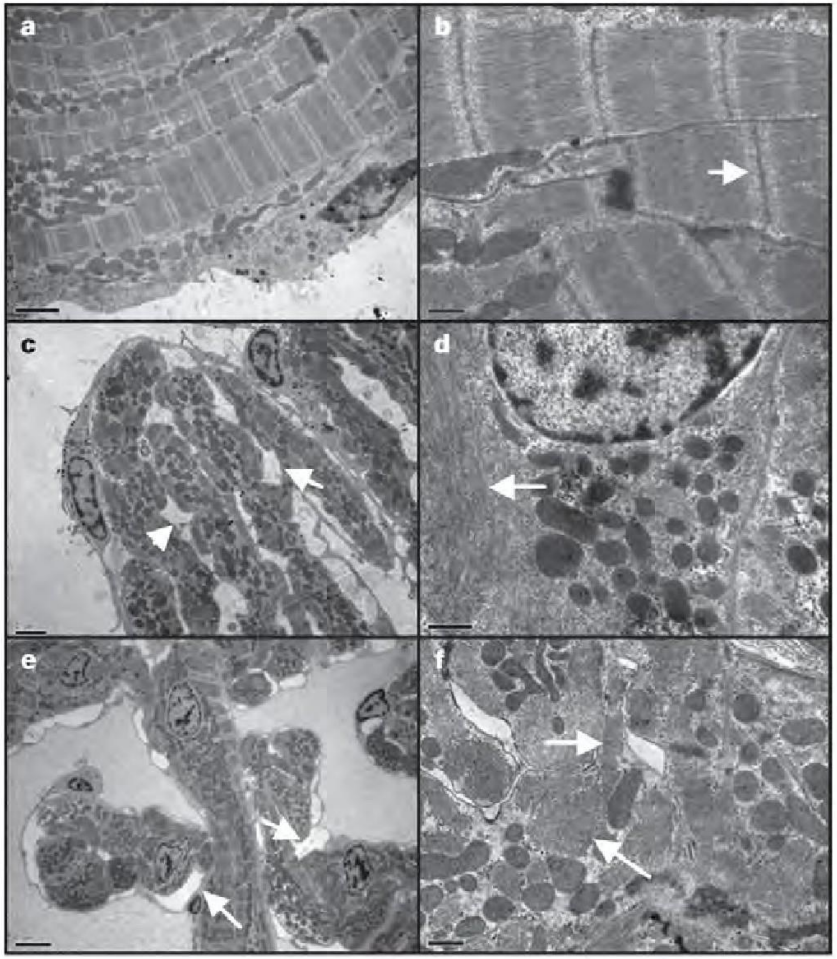

Figure 3 | Cardiomyocytes dedifferentiate, resulting in the disassembly of sarcomeric structure and detachment. Electron microscopy of sections of a control heart (**a**, **b**) and a regenerating heart at 5 days (**c**, **d**) and 7 days (**e**, **f**) after amputation. Cardiomyocytes in unamputated control samples show a tightly organized sarcomeric structure (**a**); at higher magnification (**b**) the Z-lines are clearly visible (arrow). At 5 days after amputation many of the cardiomyocytes have a disorganized sarcomeric structure (**c**) along with the appearance of intercellular spaces (arrows). Closer examination reveals a loss of Z-lines (**d**, arrow). At 7 days after amputation there is a similar loss of structure and appearance of intercellular spaces (**e**, arrows). At higher magnification (**f**) myosin fibres are visible (arrows); however, both longitudinal (upper arrow) and transverse (lower arrow) fibres are present within the same cardiomyocyte, indicating disorganized sarcomeric structure. Scale bars, 0.5 μm (**a**, **b**, **d**) and 2 μm (**c**, **e**, **f**).

What about mammals?

LETTER

doi:10.1038/nature11682

Mammalian heart renewal by pre-existing cardiomyocytes

Samuel E. Senyo[1], Matthew L. Steinhauser[1], Christie L. Pizzimenti[1], Vicky K. Yang[1], Lei Cai[1], Mei Wang[4,5], Ting-Di Wu[2,3], Jean-Luc Guerquin-Kern[2,3], Claude P. Lechene[4,5] & Richard T. Lee[1,6]

Although recent studies have revealed that heart cells are generated in adult mammals, the frequency of generation and the source of new heart cells are not yet known. Some studies suggest a high rate of stem cell activity with differentiation of progenitors to cardiomyocytes[1]. Other studies suggest that new cardiomyocytes are born at a very low rate[2–4], and that they may be derived from the division of pre-existing cardiomyocytes. Here we show, by combining two different pulse–chase approaches—genetic fate-mapping with stable isotope labelling, and multi-isotope imaging mass spectrometry—that the genesis of cardiomyocytes occurs at a low rate by the division of pre-existing cardiomyocytes during normal ageing, a process that increases adjacent to areas of myocardial injury. We found that cell cycle activity during normal ageing and after injury led to polyploidy and multinucleation, but also to new diploid, mononucleate cardiomyocytes. These data reveal pre-existing cardiomyocytes as the dominant source of cardiomyocyte replacement in normal mammalian myocardial homeostasis as well as after myocardial injury.

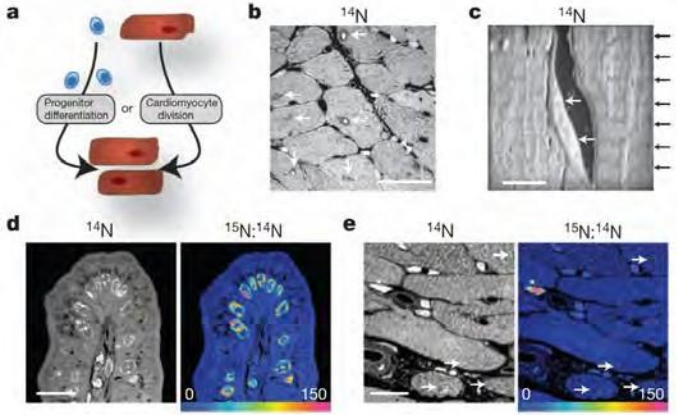

Figure 1 | Use of MIMS to study cardiomyocyte turnover. **a**, Primary question: are new cardiomyocytes derived from progenitors or from pre-existing cardiomyocytes? **b**, ^{14}N mass image. Subcellular details are evident, including cardiomyocyte nuclei (white arrows). Scale bar, 20 μm. **c**, MIMS resolves periodic sarcomeres (black arrows) in cardiomyocytes. Non-cardiomyocytes (white arrows) are seen outside cardiomyocyte borders. Scale bar, 5 μm. **d**, Right, ^{15}N:^{14}N hue–saturation–intensity image of small-intestinal epithelium after labelling with [^{15}N]thymidine. The scale ranges from blue, where the ratio is equivalent to natural ratio (0.37%, expressed as 0% above natural ratio (enrichment over natural ratio)), to red, where the ratio is 150% above natural ratio. ^{15}N labelling is concentrated in nuclei in a pattern resembling chromatin. Scale bar, 15 μm. **e**, Right, ^{15}N:^{14}N hue–saturation–intensity image of heart section (left ventricle). [^{15}N]Thymidine was administered for 1 week. Asterisk, rare $^{15}N^{+}$ interstitial cells. Cardiomyocyte nuclei (white arrows) are unlabelled. Scale bar, 15 μm.

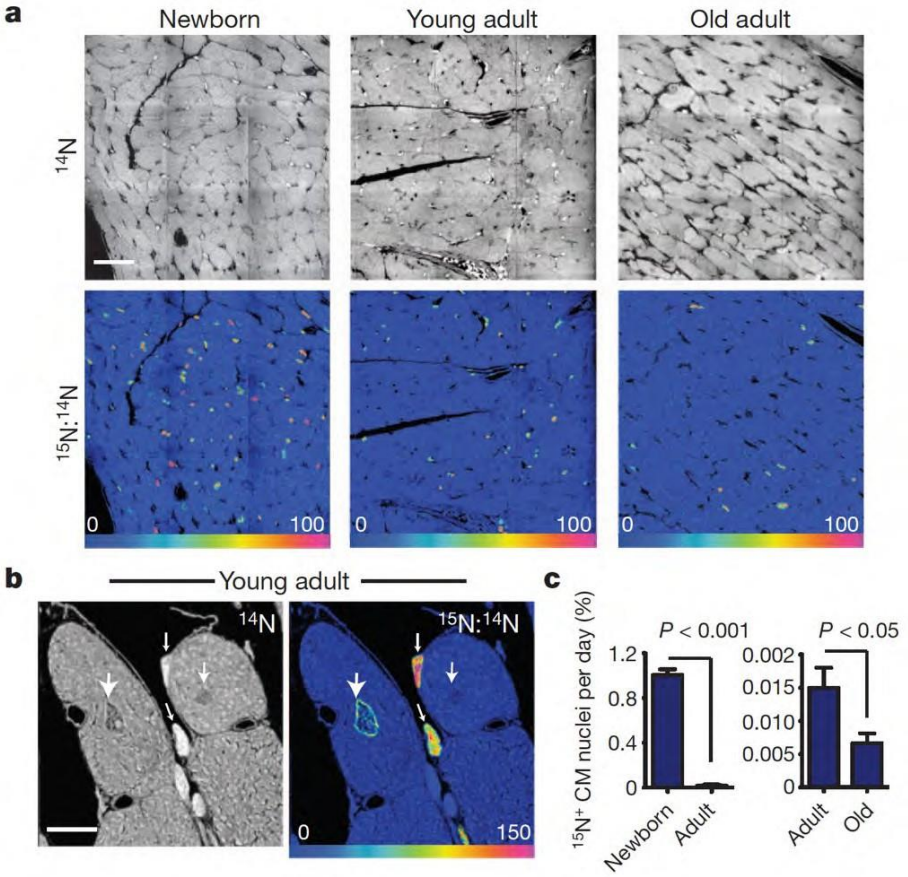

Figure 2 | Cardiomyocyte DNA synthesis decreases with age. **a**, [^{15}N]Thymidine was administered for 8 weeks to mice of different ages: newborn, starting at postnatal day 4; young adult, starting at 2 months; old adult, starting at 22 months. Top, ^{14}N mass images show histological details. Bottom, ^{15}N:^{14}N hue–saturation–intensity images show ^{15}N^{+} nuclei. Mosaics are constructed from nine tiles, 60 μm each. Scale bar, 30 μm. **b**, High-magnification analysis shows a cardiomyocyte from the young adult with nuclear ^{15}N labelling (large arrow), two labelled non-cardiomyocytes (small arrows) and an adjacent unlabelled cardiomyocyte nucleus (medium arrow). Scale bar, 10 μm. **c**, Age-related decline in cardiomyocyte DNA synthesis. Left, comparison of newborn with young adult. Right, scale reduced to compare young adult with old adult ($n = 3$ mice per group). Error bars indicate s.e.m.

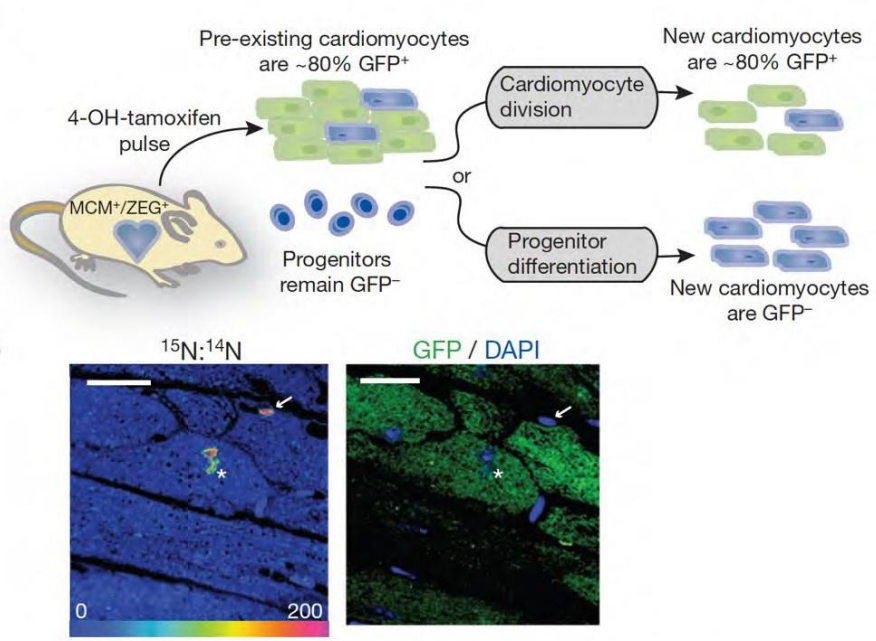

Figure 3 | New cardiomyocytes are derived from pre-existing cardiomyocytes during ageing. **a**, Experimental strategy. MerCreMer^{+}/ZEG^{+} (MCM^{+}ZEG^{+}) mice ($n = 4$) were treated for 2 weeks with 4-OH-tamoxifen to induce cardiomyocyte-specific GFP expression. [^{15}N]Thymidine was administered continuously during a 10-week chase, then cycling cells were identified by ^{15}N labelling. New cardiomyocytes (^{15}N^{+}) derived from pre-existing cardiomyocytes should express GFP at a rate similar to that of the surrounding quiescent (^{15}N^{-}) cardiomyocytes. New cardiomyocytes (^{15}N^{+}) derived from progenitors should be GFP^{-}. **b**, Left, ^{15}N:^{14}N hue–saturation–intensity image showing a [^{15}N]thymidine-labelled cardiomyocyte nucleus (white asterisk) and a ^{15}N^{+} non-cardiomyocyte (white arrow). Right, immunofluorescent image showing that the ^{15}N^{+} cardiomyocyte is GFP^{+}. Scale bars, 15 μm.

25 FEBRUARY 2011 VOL 331

Transient Regenerative Potential of the Neonatal Mouse Heart

Enzo R. Porrello,[1] Ahmed I. Mahmoud,[2] Emma Simpson,[3] Joseph A. Hill,[1,2] James A. Richardson,[1,3] Eric N. Olson,[1]* Hesham A. Sadek[2]*

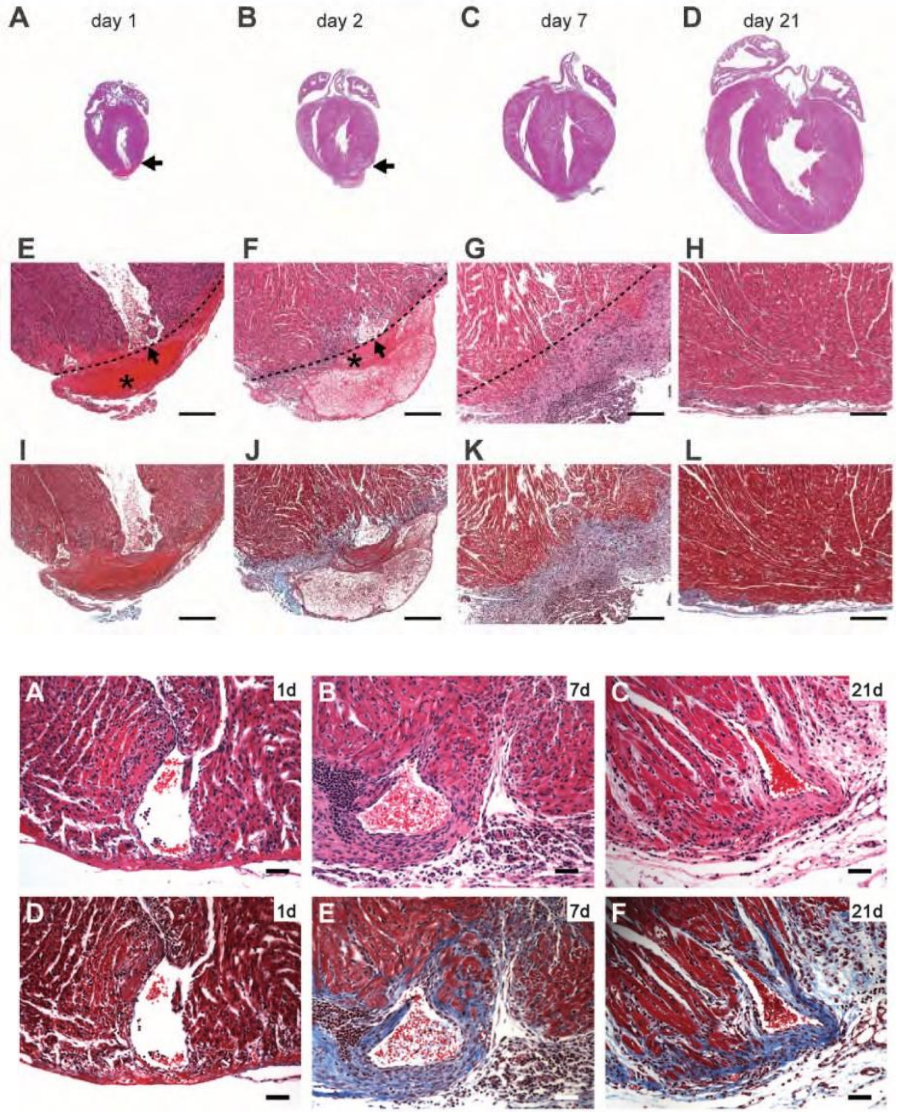

- Hearts of 1-day-old neonatal mice can regenerate after partial surgical resection, but this capacity is lost by 7 days of age.
- The regenerative response was characterized by cardiomyocyte proliferation with minimal hypertrophy or fibrosis.
- The majority of cardiomyocytes within the regenerated tissue originated from preexisting cardiomyocytes.

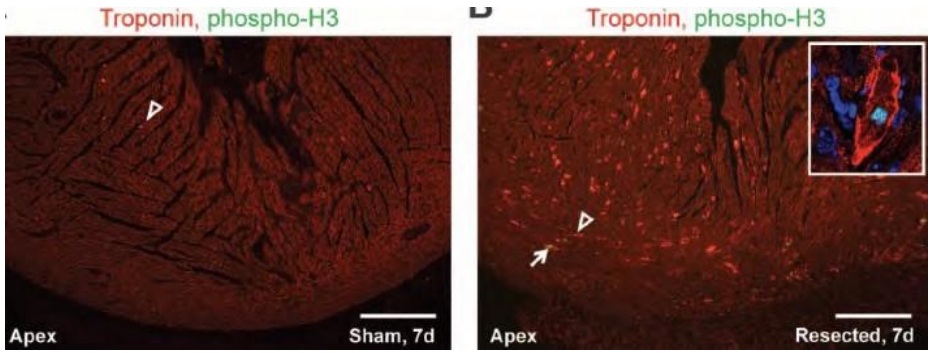

NATURE PROTOCOLS | VOL.9 NO.2 | 2014 | PROTOCOL

Surgical models for cardiac regeneration in neonatal mice

Ahmed I Mahmoud[1], Enzo R Porrello[2], Wataru Kimura[3], Eric N Olson[4] & Hesham A Sadek[3]

[1]Department of Medicine, Cardiovascular Division, Brigham and Women's Hospital and Harvard Medical School, Cambridge, Massachusetts, USA. [2]School of Biomedical Sciences, The University of Queensland, St. Lucia, Queensland, Australia. [3]Department of Internal Medicine, The University of Texas Southwestern Medical Center, Dallas, Texas, USA. [4]Department of Molecular Biology, The University of Texas Southwestern Medical Center, Dallas, Texas, USA. Correspondence should be addressed to H.A.S. (hesham.sadek@utsouthwestern.edu).

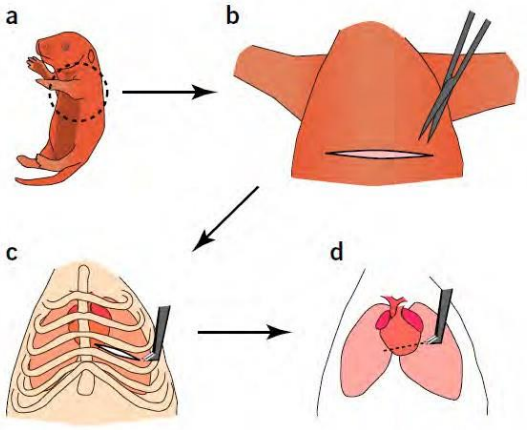

(Mahmoud et al., 2014)

Apical resection surgical model

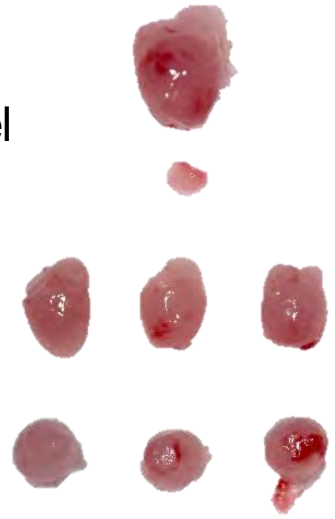

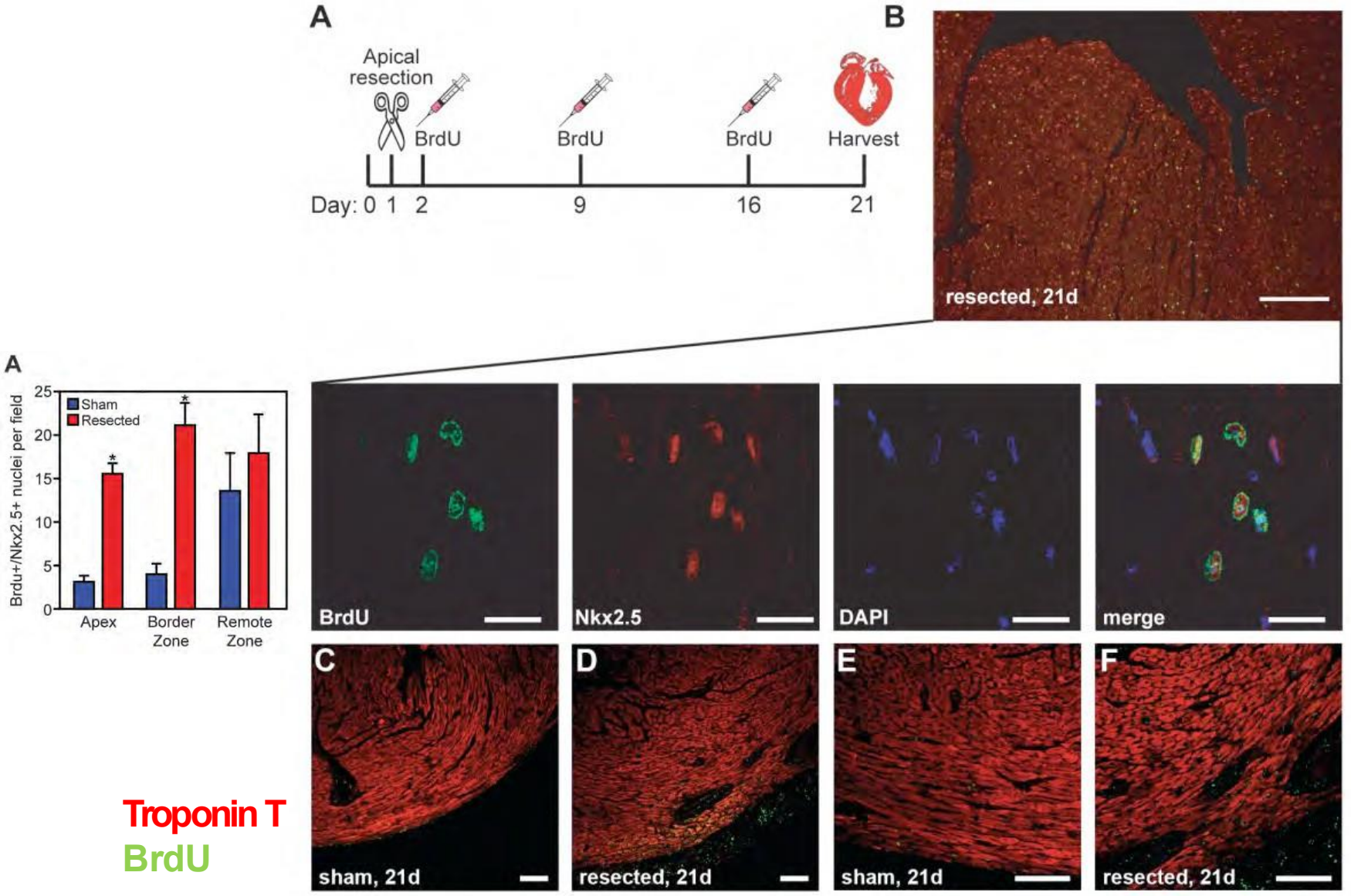

Newly formed cardiomyocytes

(Porrello et al., 2011)

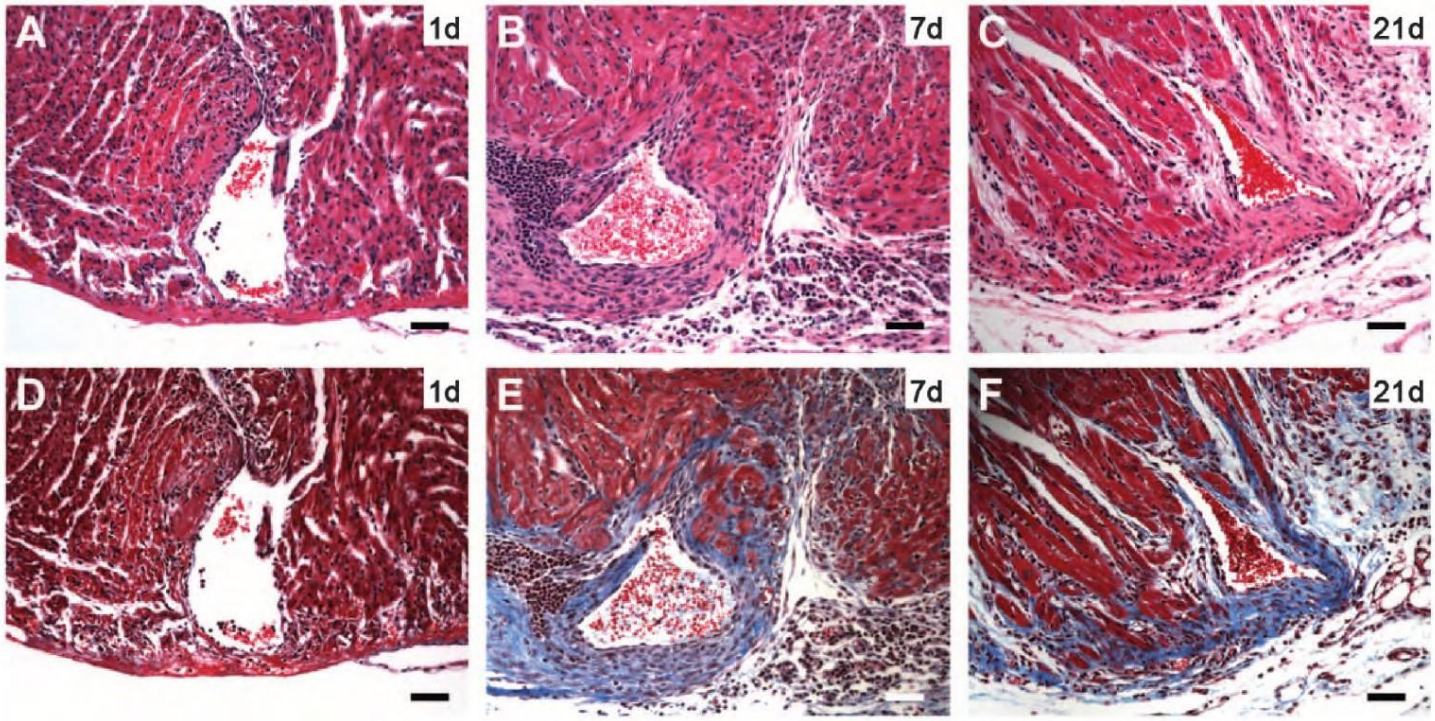

Fig. 4. Lack of regeneration after apical resection of 7-day-old mice. (**A** to **C**) H&E staining at 1, 7, and 21 dpr, respectively. (**D** to **F**) Trichrome staining at 1, 7, and 21 dpr. Note fibrotic scar (blue staining) surrounding resected ventricular chamber at 7 and 21 dpr [(E) and (F)]. Scale bars, 200 μm.

Which cells do they derive from ?

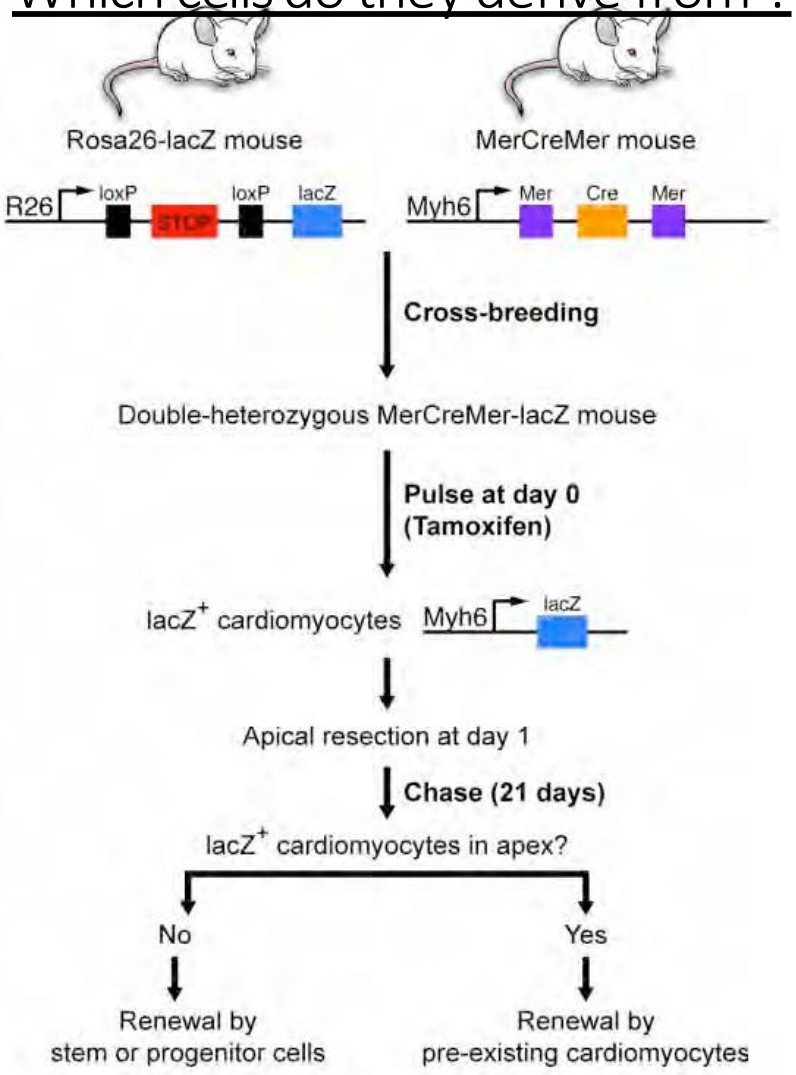

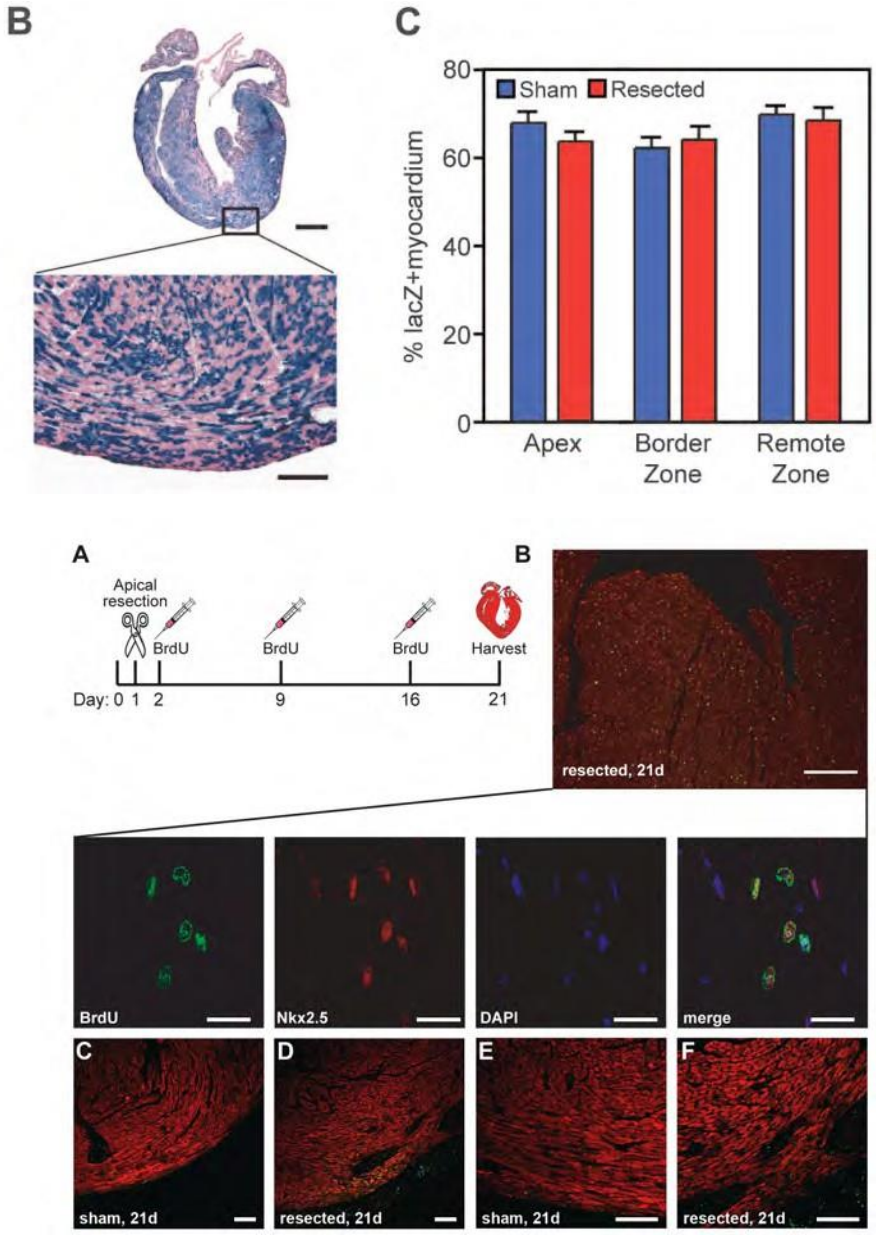

(Porrello et al., 2011)

Stem Cell Reports | Vol. 10 | 860–874 | March 13, 2018 | © 2018 The Author(s).

Stem Cell Reports
Article
ISSCR
OPEN ACCESS

Neonatal Apex Resection Triggers Cardiomyocyte Proliferation, Neovascularization and Functional Recovery Despite Local Fibrosis

Vasco Sampaio-Pinto,[1,2,3] Sílvia C. Rodrigues,[1,2] Tiago L. Laundos,[1,2,3] Elsa D. Silva,[1,2] Francisco Vasques-Nóvoa,[1,2,4] Ana C. Silva,[1,2,3,5] Rui J. Cerqueira,[4] Tatiana P. Resende,[1,2] Nicola Pianca,[6] Adelino Leite-Moreira,[4] Gabriele D'Uva,[6] Sólveig Thorsteinsdóttir,[7] Perpétua Pinto-do-Ó,[1,2,3,8] and Diana S. Nascimento[1,2,8,*]

SUMMARY

So far, opposing outcomes have been reported following neonatal apex resection in mice, questioning the validity of this injury model to investigate regenerative mechanisms. We performed a systematic evaluation, up to 180 days after surgery, of the pathophysiological events activated upon apex resection. In response to cardiac injury, we observed increased cardiomyocyte proliferation in remote and apex regions, neovascularization, and local fibrosis. In adulthood, resected hearts remain consistently shorter and display permanent fibrotic tissue deposition in the center of the resection plane, indicating limited apex regrowth. However, thickening of the left ventricle wall, explained by an upsurge in cardiomyocyte proliferation during the initial response to injury, compensated cardiomyocyte loss and supported normal systolic function. Thus, apex resection triggers both regenerative and reparative mechanisms, endorsing this injury model for studies aimed at promoting cardiomyocyte proliferation and/or downplaying fibrosis.

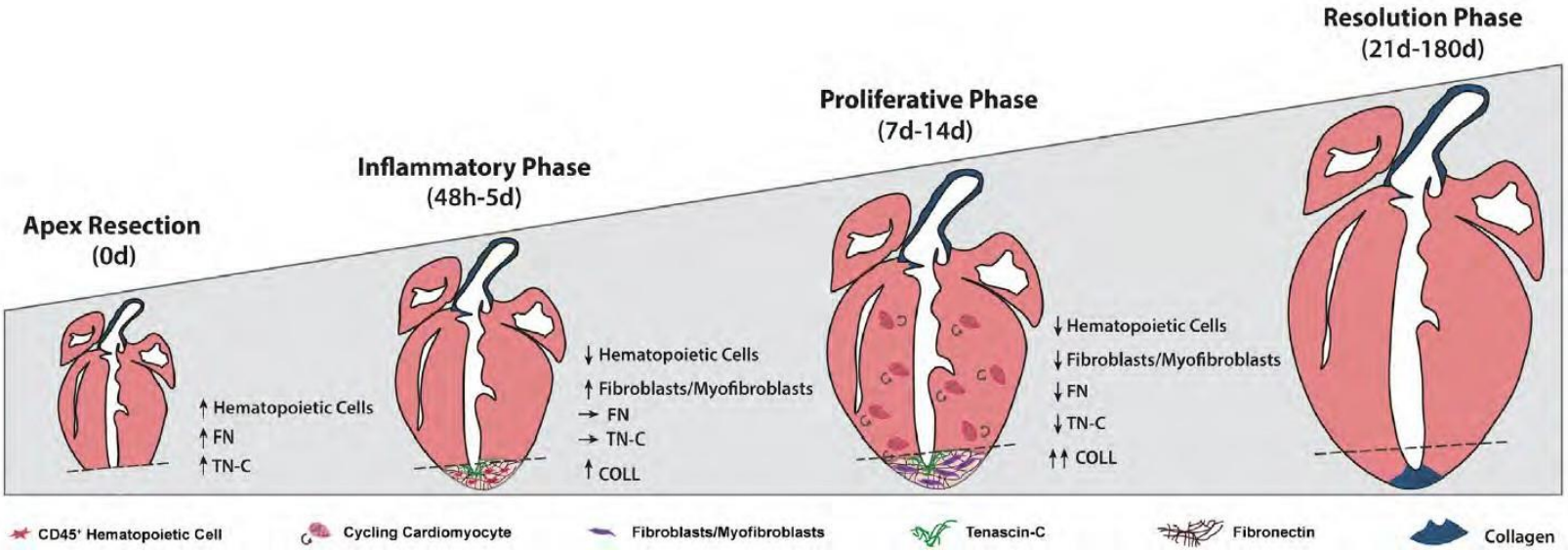

Apex resection promotes local infiltration of inflammatory cells in the first 48 hr, which leads to the deposition of a transient FN and TN-Crich ECM.

At 7 days post-injury, rates of CM proliferation are increased throughout the left ventricular myocardium and cardiac fibroblasts are activated at the injury site. These cellular dynamics result in a thickening of left ventricle walls, de novo vessel formation and deposition of a permanent fibrotic scar at the midpoint of the injured area.

Long-term evaluation showed preserved systolic function, shortened long-axis and thicker left ventricle, without hypertrophy and edema.

Is the heart really a post-mitotic organ?

Carbon dating of human tissues

After the Second World War, tests of nuclear bombs spewed carbon-14 pollution into the atmosphere. This isotope was incorporated into plants and the people who consumed them. After above-ground tests were stopped in 1963, levels of the isotope started to fall. The ^{14}C in a cell's DNA corresponds to the amount of the isotope in the atmosphere at the time it was dividing, providing a way to date a cell's birth.

People born before 1955 had levels of ^{14}C in their cardiomyocytes that were higher than was present in the atmosphere at the time of their birth, so some of these cells must have arisen later on in their lives. Further work and mathematical modelling allowed to calculate that a 50-year-old heart still contains more than half the cells it had at birth and that the turnover slows down with time. A 25-year-old heart replaces about 1% of all cardiomyocytes over a year; a 75-year-old about half that.

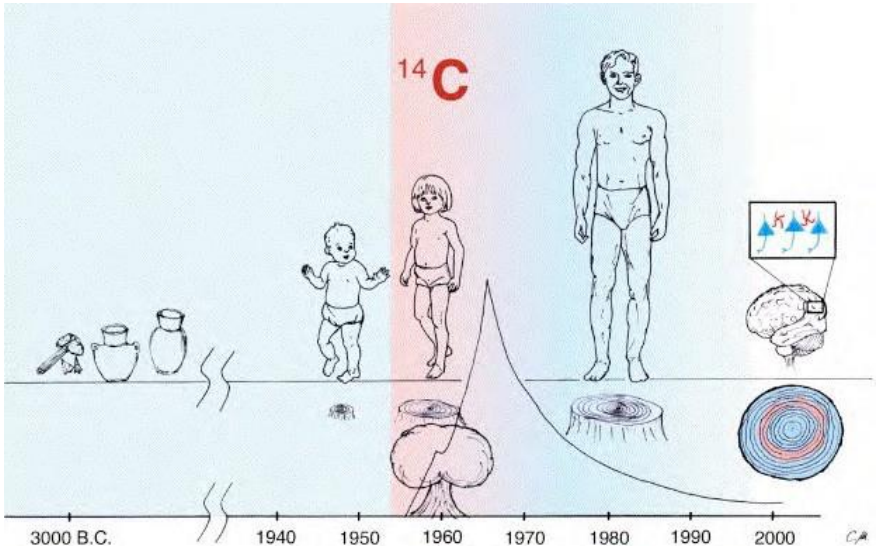

Although extensive regeneration is unlikely to occur in most of mammalian tissues, evidence has accumulated in recent years suggesting that mammalian cardiac myocytes do retain the capacity to divide. Carbon dating of cardiomyocytes in human hearts has been suggested to indicate a lifetime turnover rate of 50%.

Nevertheless, the ability of adult mammalian myocytes to regenerate injured tissue is limited. Perhaps during the course of evolution, mammalian hearts have simply lost the capacity for regeneration because it wasn't needed. After all, heart disease occurs later in life after we have reproduced. In addition, repair became more important. The mammalian heart works at high pressure, whereas the fish heart doesn't.

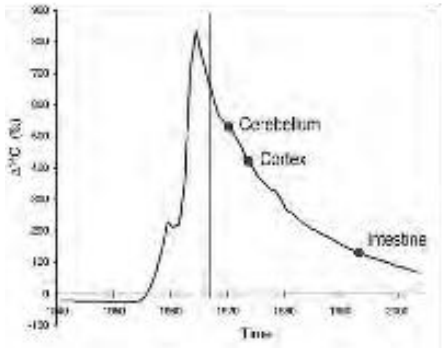

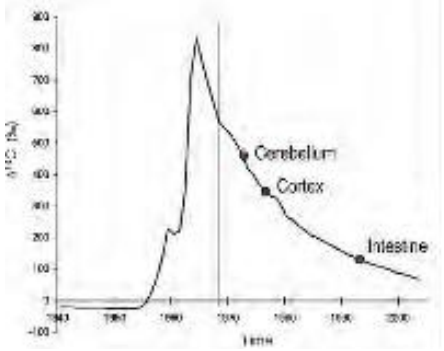

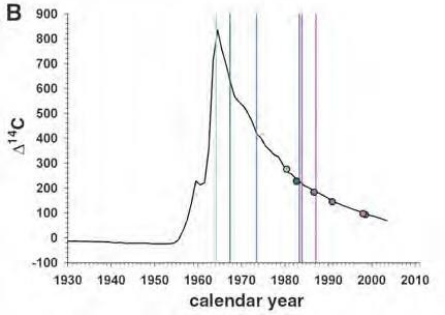

The vertical bar indicates the date of birth of each individual, and the similarly colored dots represent the ^{14}C data for the same individual.

3 APRIL 2009 VOL 324 SCIENCE

Evidence for Cardiomyocyte Renewal in Humans

Olaf Bergmann,[1]* Ratan D. Bhardwaj,[1]* Samuel Bernard,[2] Sofia Zdunek,[1] Fanie Barnabé-Heider,[1] Stuart Walsh,[3] Joel Zupicich,[1] Kanar Alkass,[4] Bruce A. Buchholz,[5] Henrik Druid,[4] Stefan Jovinge,[3,6] Jonas Frisén[1]†

It has been difficult to establish whether we are limited to the heart muscle cells we are born with or if cardiomyocytes are generated also later in life. We have taken advantage of the integration of carbon-14, generated by nuclear bomb tests during the Cold War, into DNA to establish the age of cardiomyocytes in humans. We report that cardiomyocytes renew, with a gradual decrease from 1% turning over annually at the age of 25 to 0.45% at the age of 75. Fewer than 50% of cardiomyocytes are exchanged during a normal life span. The capacity to generate cardiomyocytes in the adult human heart suggests that it may be rational to work toward the development of therapeutic strategies aimed at stimulating this process in cardiac pathologies.

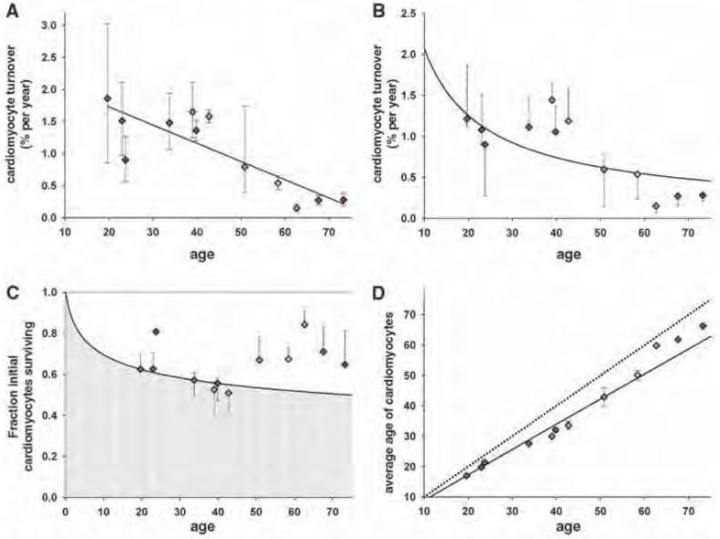

Fig. 4. Dynamics of cardiomyocyte turnover. (**A**) Individual data fitting assuming a constant turnover (see supporting online text) reveals an almost linear decline of cardiomyocyte turnover with age (R = −0.84; P = 0.001). A constant-turnover hypothesis might therefore not represent the turnover dynamics accurately. (**B**) Global fitting of all data points (see supporting online text, error sum of squares = 1.2×10^4) shows an age-dependent decline of cardiomyocyte turnover. (**C**) The gray area depicts the fraction of cardiomyocytes remaining from birth, and the white area is the contribution of new cells. Estimate is from the best global fitting. (**D**) Cardiomyocyte age estimates from the best global fitting. The dotted line represents the no-cell-turnover scenario, where the average age of cardiomyocytes equals the age of the individual. The black line shows the best global fitting. Colored diamonds indicate computed data points from ^{14}C-dated subjects. Error bars in (A) are calculated from the errors on ^{14}C measurements. Error bars in all other graphs are calculated for each subject individually and show the interval of possible values fitted with the respective mathematical scenario.

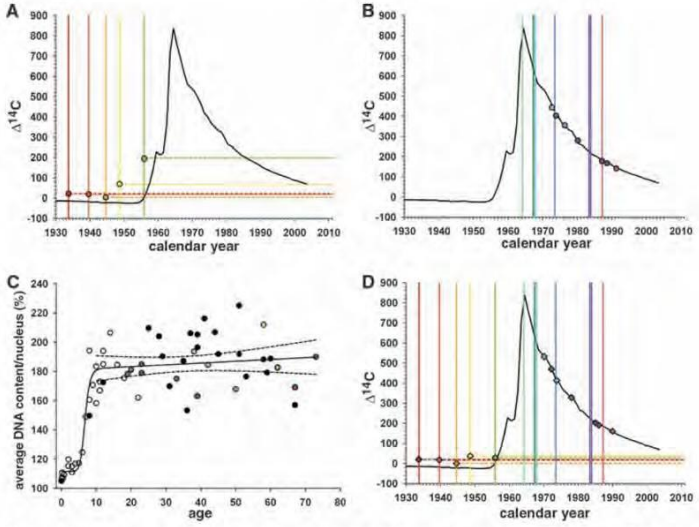

Fig. 3. Cardiomyocyte turnover in adulthood. (**A**) The ^{14}C concentrations in cardiomyocyte DNA from individuals born before the time of the atmospheric radiocarbon increase correspond to time points after the birth of all individuals. The vertical bar indicates year of birth, with the correspondingly colored data point indicating the Δ^{14}C value. (**B**) ^{14}C concentrations in cardiomyocyte DNA from individuals born after the time of the nuclear bomb test. (**C**) Average DNA content ($2n$ = 100%) per cardiomyocyte nucleus from individuals (without severe heart enlargement; see fig. S5) of different ages. Ploidy was measured by flow cytometry. Colored data points identify individuals analyzed for ^{14}C (n = 13). Black data points are from individuals analyzed only with regard to ploidy level (n = 23), and white data points are taken from Adler *et al.* (n = 26) (*24*, *26*). The dashed lines indicate the 95% confidence interval for the regression curve. (**D**) ^{14}C values corrected for the physiologically occurring polyploidization of cardiomyocytes during childhood for individuals born before and after the bomb-induced spike in ^{14}C concentrations, calculated on the basis of the individual average DNA content per cardiomyocyte nucleus. The ^{14}C content is not affected in individuals where the polyploidization occurred before the increase in atmospheric ^{14}C concentrations.

A considerable amount of cardiomyocyte division was shown in the failing and infarcted human myocardium (mitotic index of 0.015% and 0.08%, respectively)

The New England Journal of Medicine

EVIDENCE THAT HUMAN CARDIAC MYOCYTES DIVIDE AFTER MYOCARDIAL INFARCTION

ANTONIO P. BELTRAMI, M.D., KONRAD URBANEK, M.D., JAN KAJSTURA, PH.D., SHAO-MIN YAN, M.D., NICOLETTA FINATO, M.D., ROSSANA BUSSANI, M.D., BERNARDO NADAL-GINARD, M.D., PH.D., FURIO SILVESTRI, M.D., ANNAROSA LERI, M.D., C. ALBERTO BELTRAMI, M.D., AND PIERO ANVERSA, M.D.

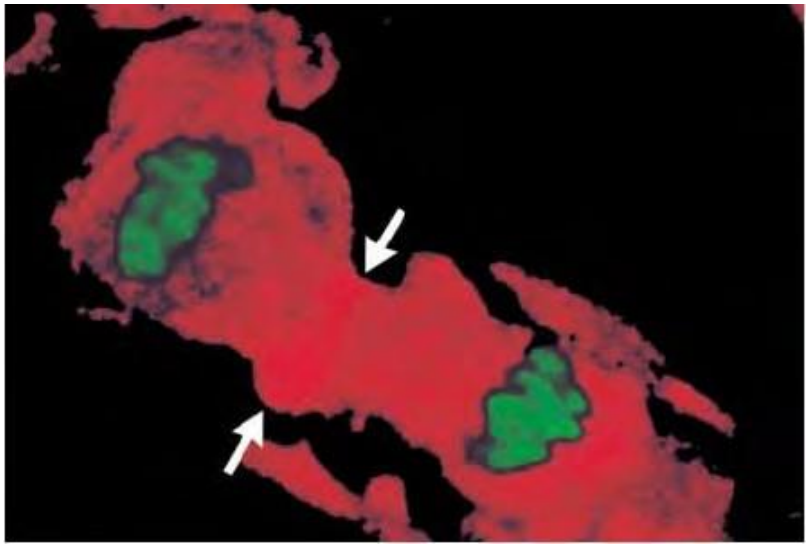

NEJM, 2001

When does cardiomyocyte proliferation stop?

Proliferating neonatal cardiomyocytes express Notch1

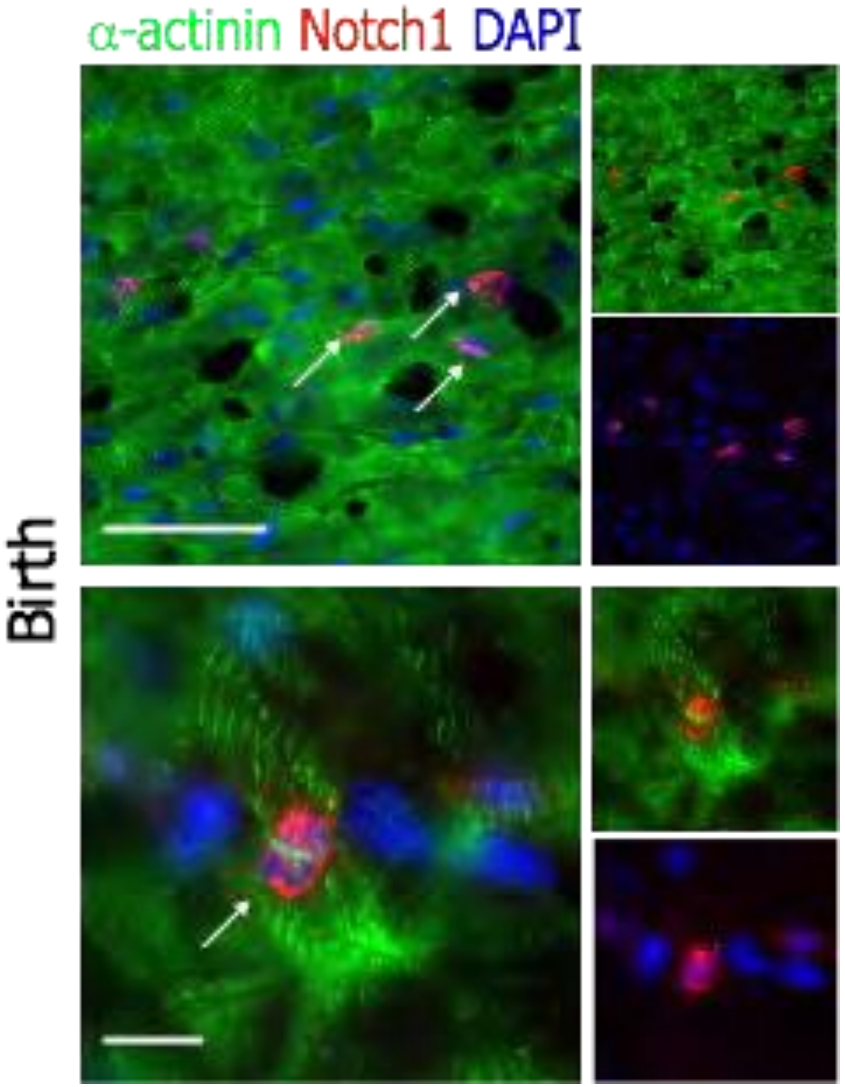

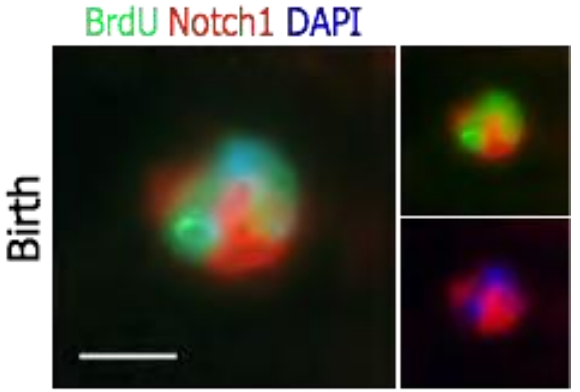

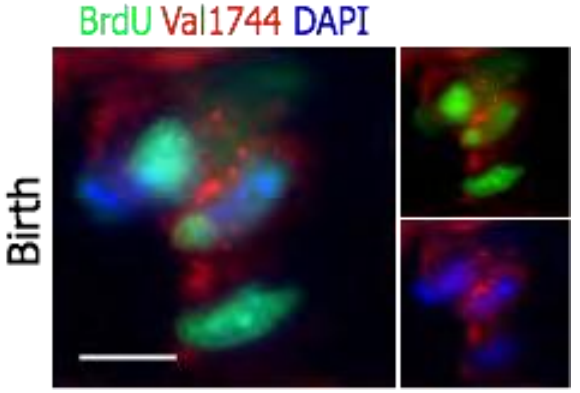

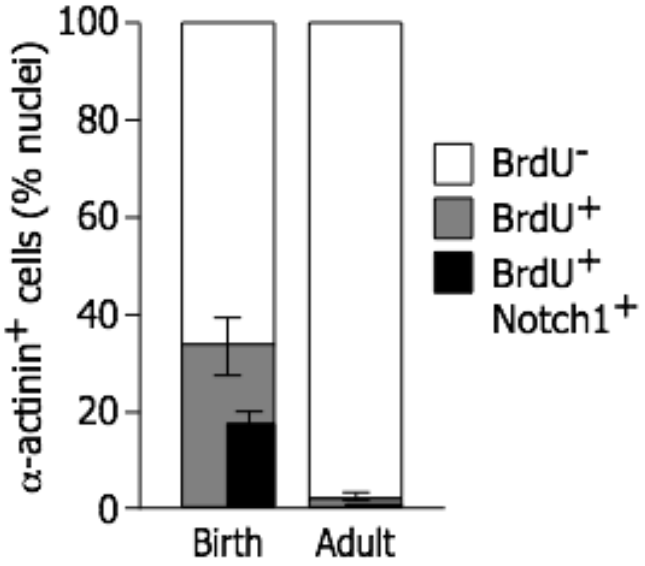

Proliferative potential of neonatal cardiomyocytes is rapidly lost in culture

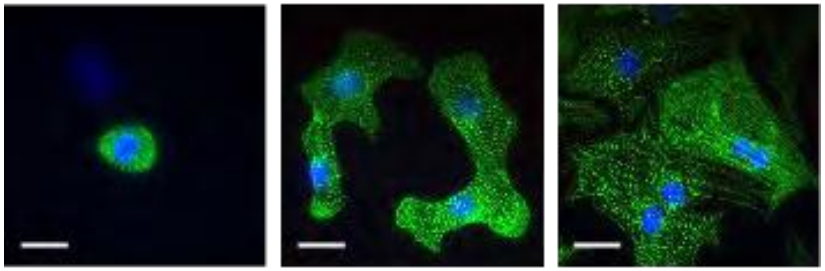

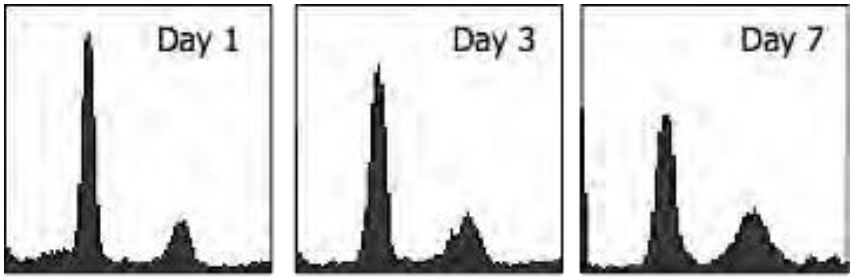

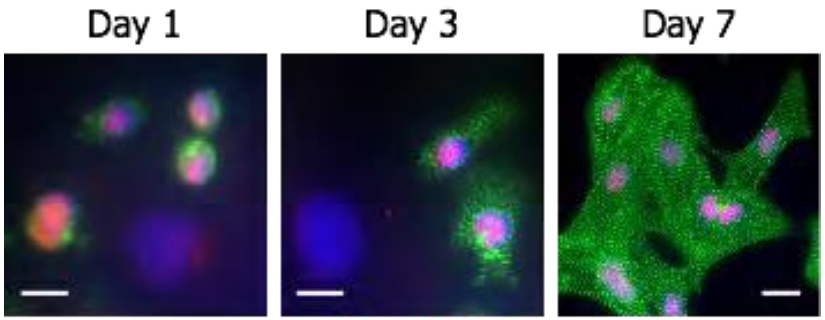

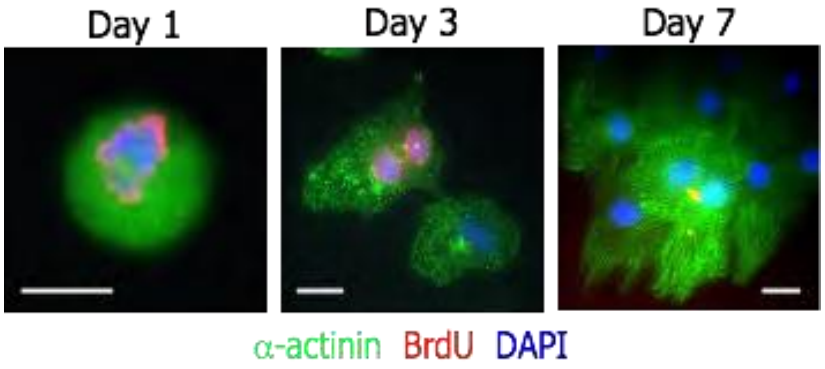

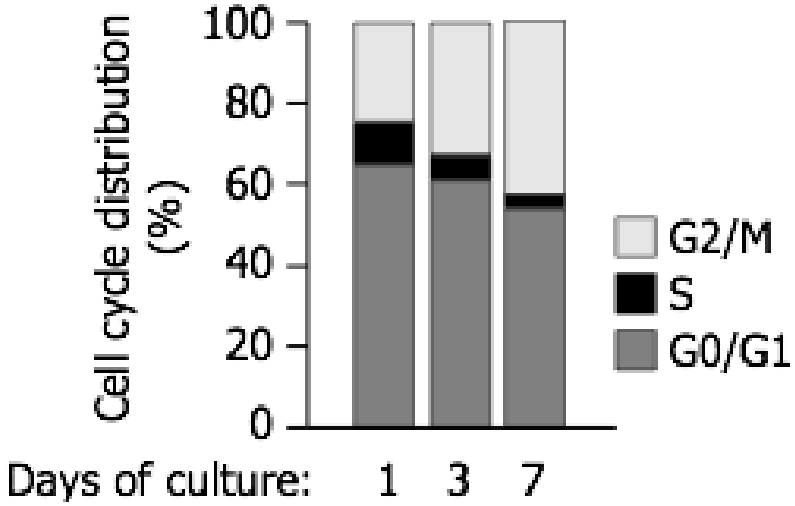

Loss of cardiomyocyte replicative potential correlates with loss of Notch1

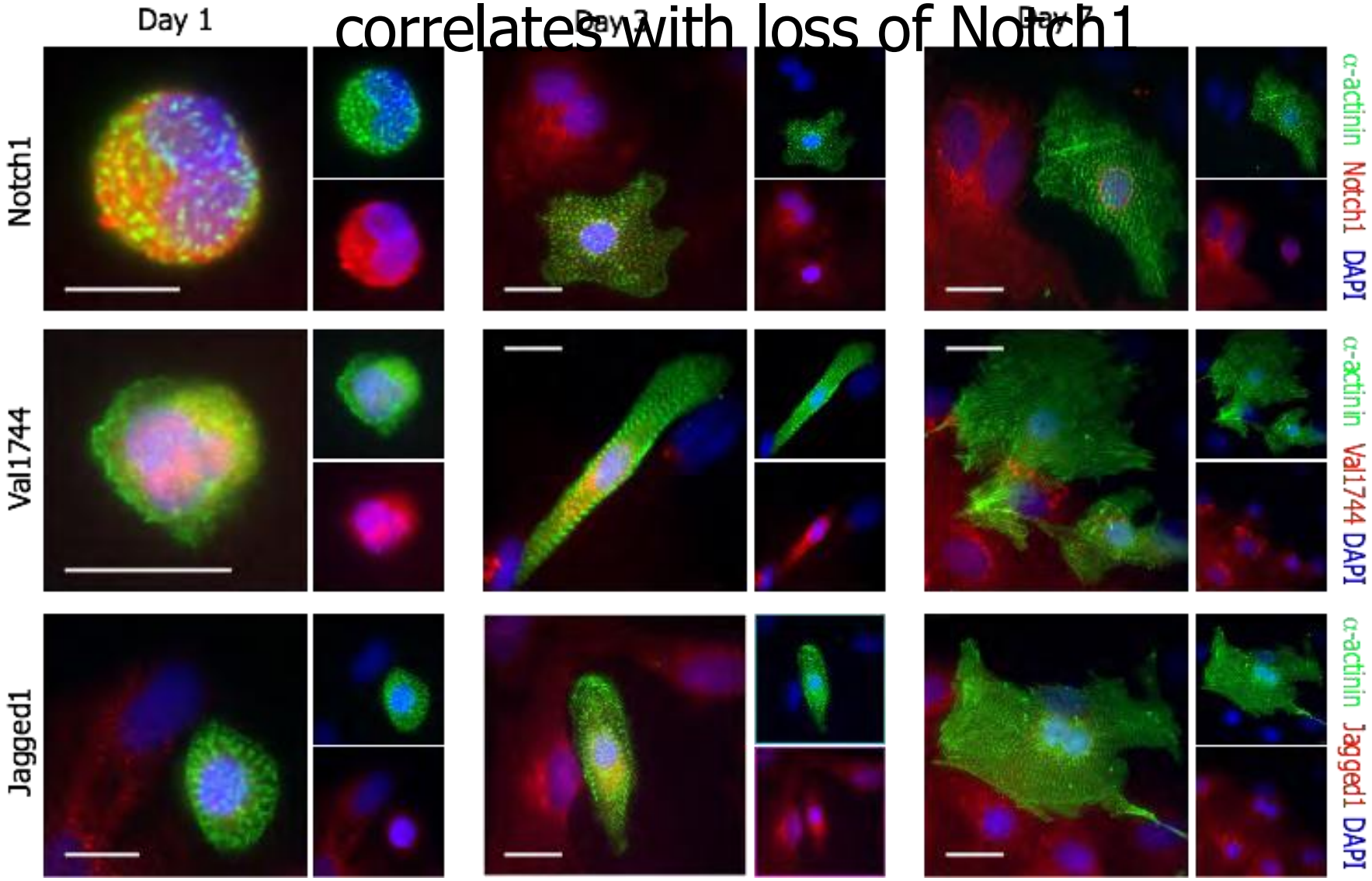

Published September 29, 2008

JCB: ARTICLE

Notch1 signaling stimulates proliferation of immature cardiomyocytes

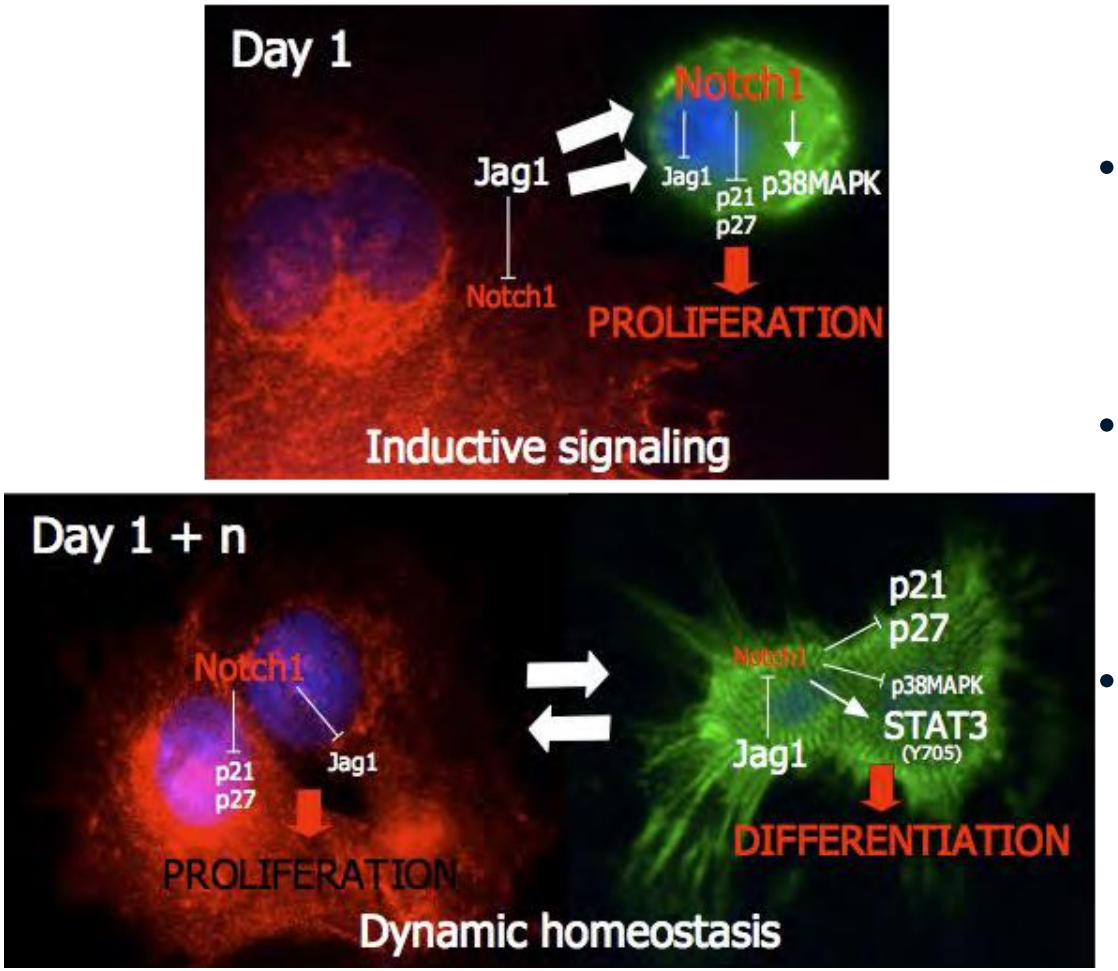

- Loss of cardiomyocyte proliferation after birth in vivo parallels loss of Notch signaling
- Neonatal cardiomyocyte proliferation in vitro requires activated Notch ICD
- Cardiomyocyte proliferation in vitro can be stimulated by Notch pathway stimulation
- In vivo, AAV9-N1ICD transduction induces the infiltration of the myocardium with BrdU+, proliferating cells.

Published October 6, 2008

Notch activates cell cycle reentry and progression in quiescent cardiomyocytes

Víctor M. Campa, Raquel Gutiérrez-Lanza, Fabio Cerignoli, Ramón Díaz-Trelles, Brandon Nelson, Toshiya Tsuji, Maria Barcova, Wei Jiang, and Mark Mercola

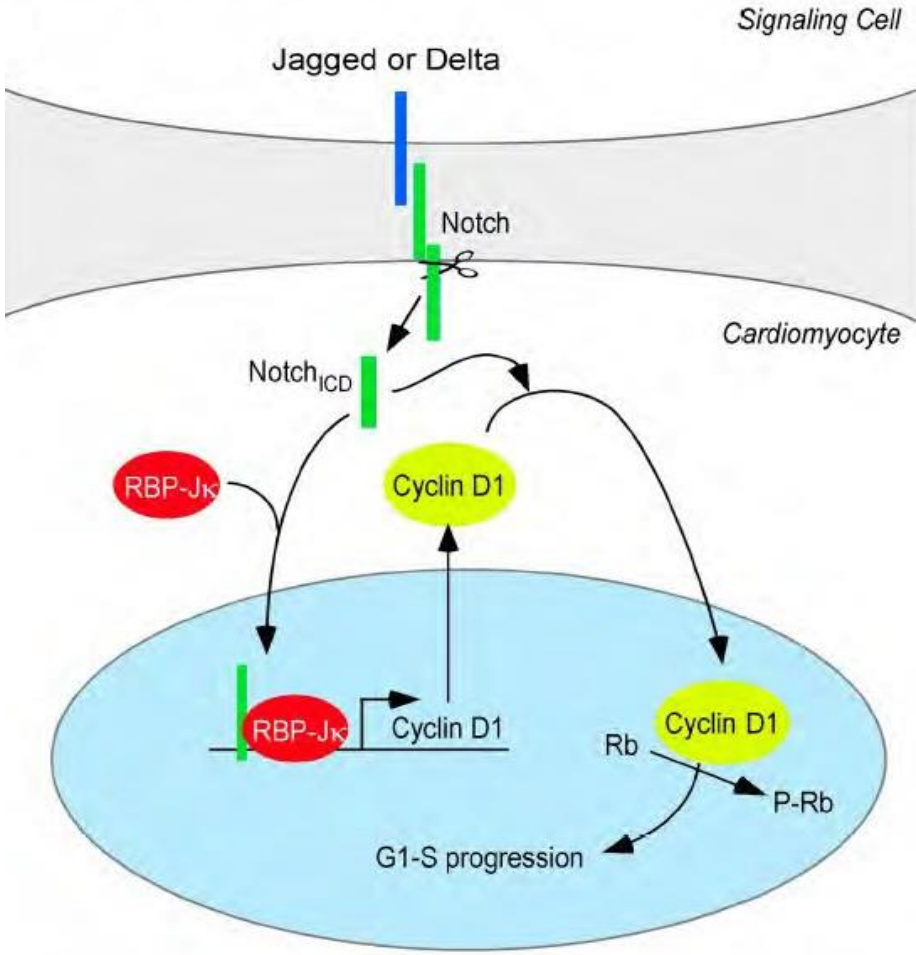

Figure 9. **Summary of Notch2-induced cell cycle entry.** RBP-Jκ–dependent transcription leads to accumulation of cyclin D1 in the cytosol. Notch ICD regulates entry into the cell cycle by controlling nuclear localization of cyclin D1 independently of RBP-Jκ.

What about adult cardiomyocytes?

Loss of cardiomyocyte proliferative potential correlates with downregulation of Notch1 and its target genes

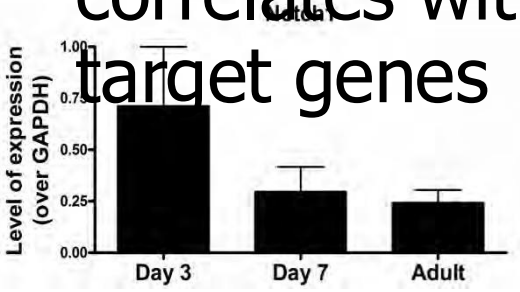

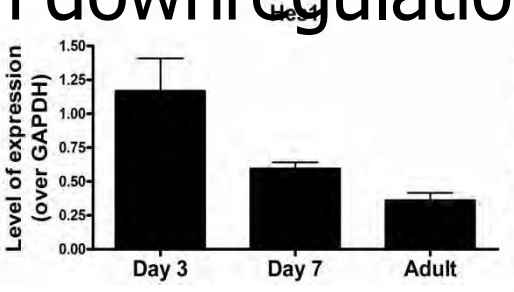

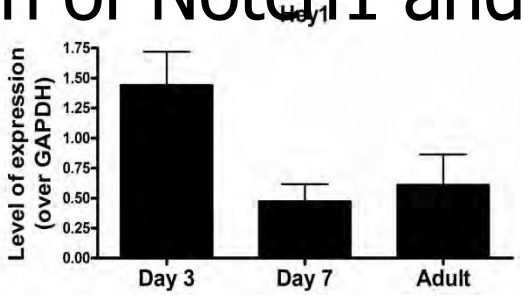

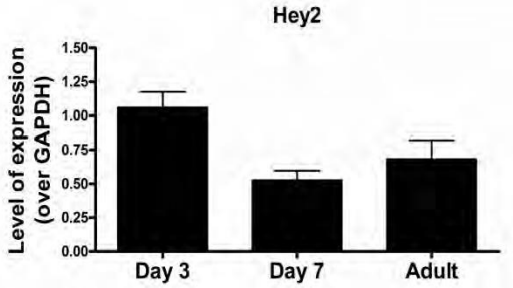

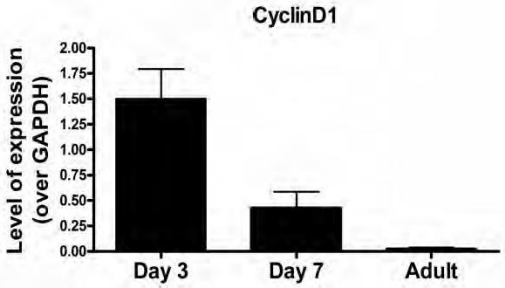

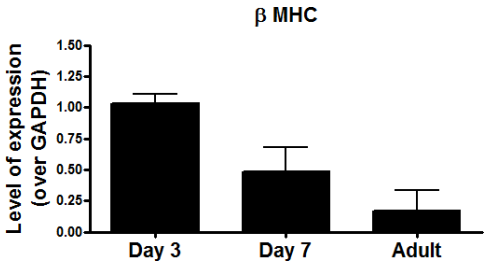

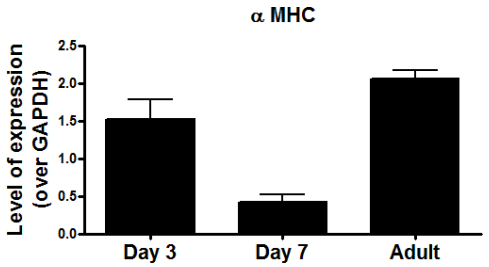

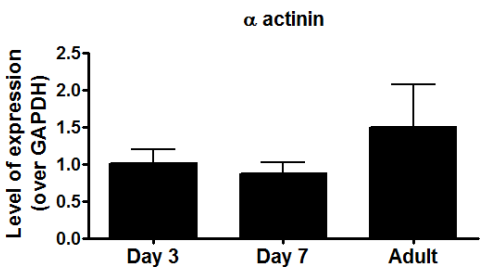

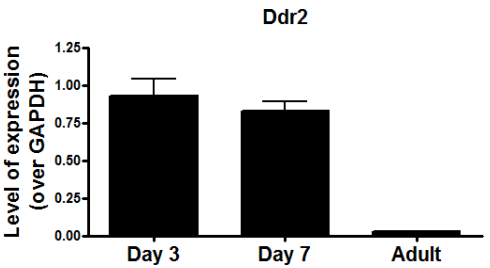

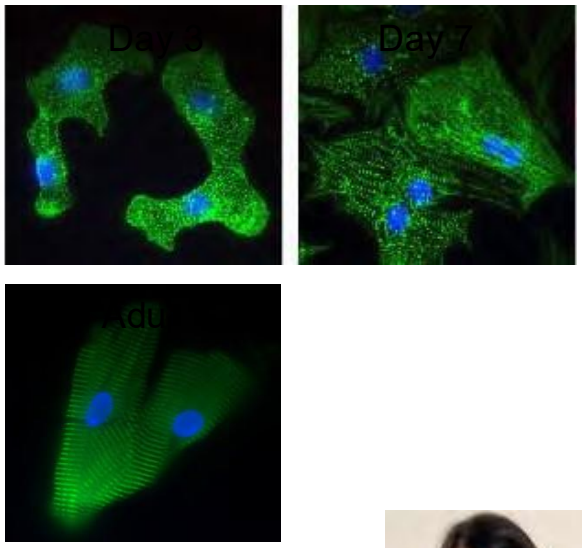

Giulia Felician

Methylation of promoters of Notch target genes impairs AAV9-sJagged1 and AAV9-N1ICD effect

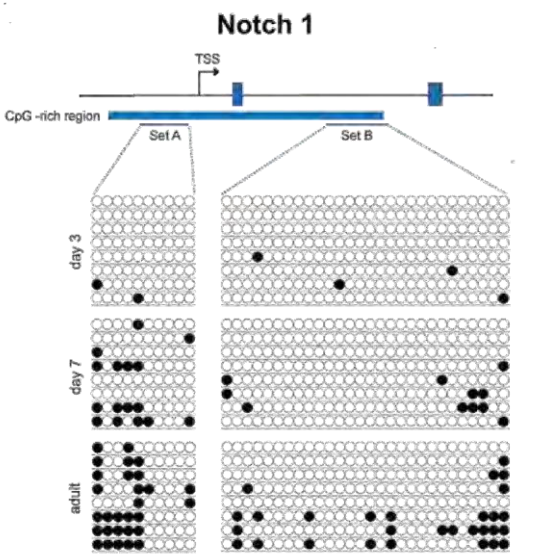

	day 3	day 7	adult
Set A	2/80 (2.5%)	16/80 (20.0%)	29/80 (36.2%)
Set B	4/224 (1.8%)	11/224 (4.9%)	29/224 (12.9%)

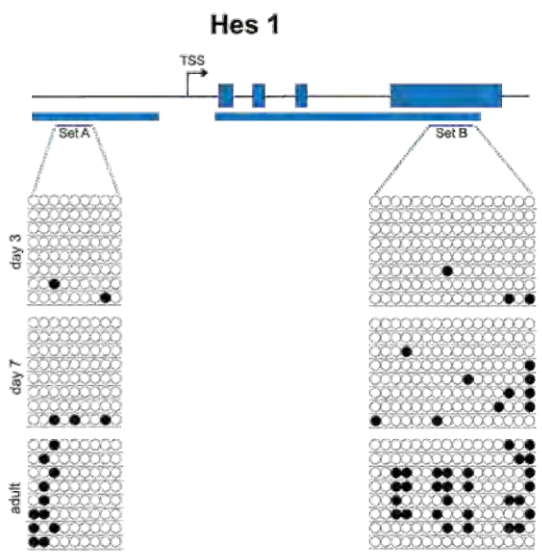

	day 3	day 7	adult
Set A	2/72 (2.7%)	3/72 (4.2%)	11/72 (15.3%)
Set B	3/128 (2.3%)	11/128 (8.6%)	29/128 (22.7%)

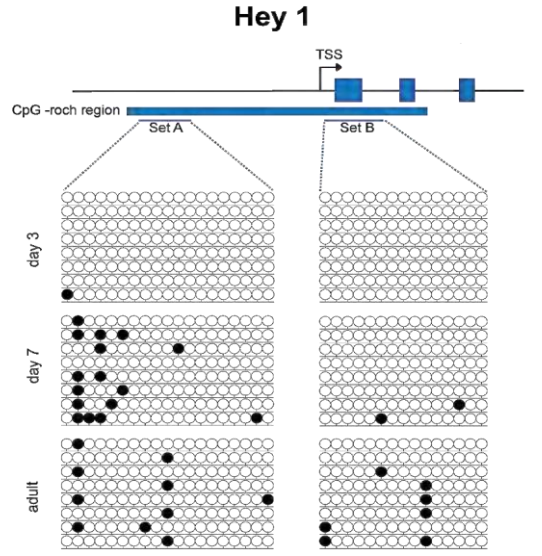

	day 3	day 7	adult
Set A	1/152 (0.6%)	16/152 (10.5%)	10/152 (6.6%)
Set B	0/120 (0%)	2/120 (1.7%)	7/120 (5.8%)

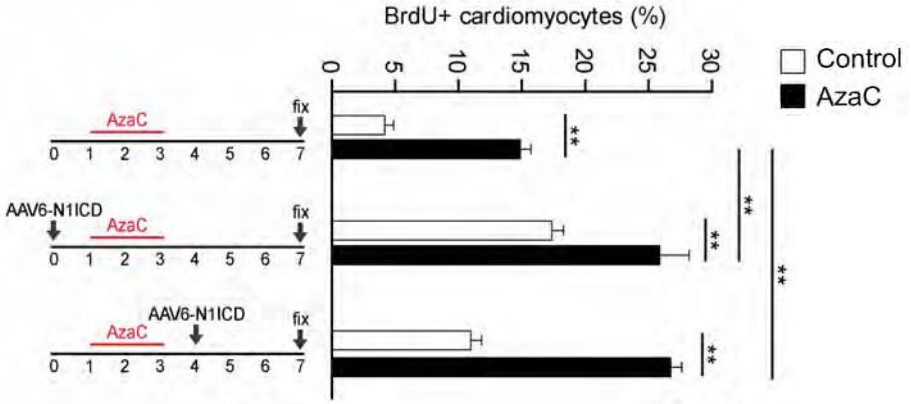

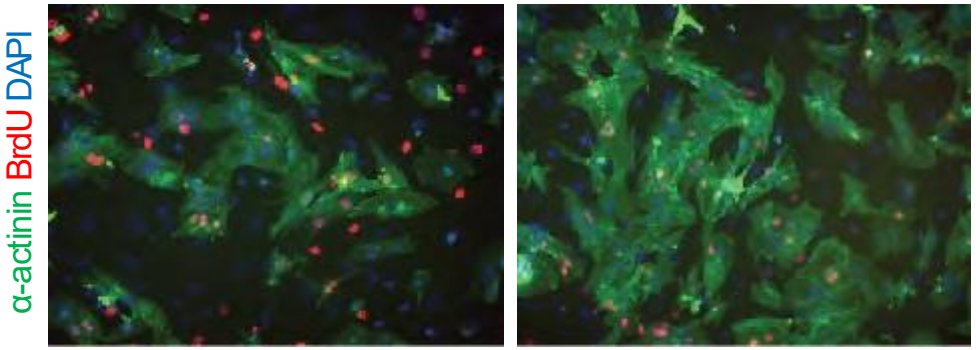

Felician G. et al., Circ. Res., 2014

Cardiac resident stem cells?

Cardiac stem cells (CSCs): do they exist?

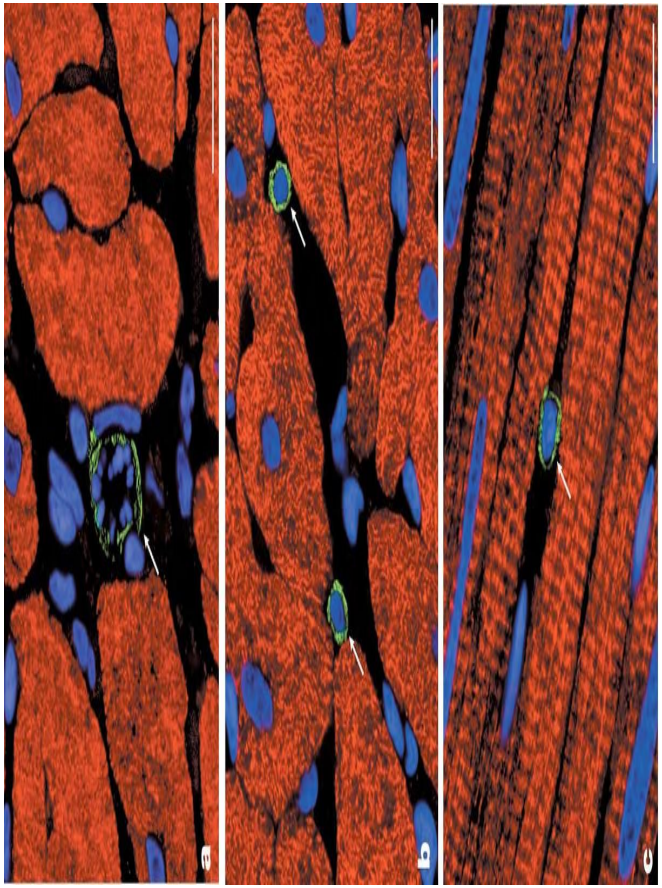

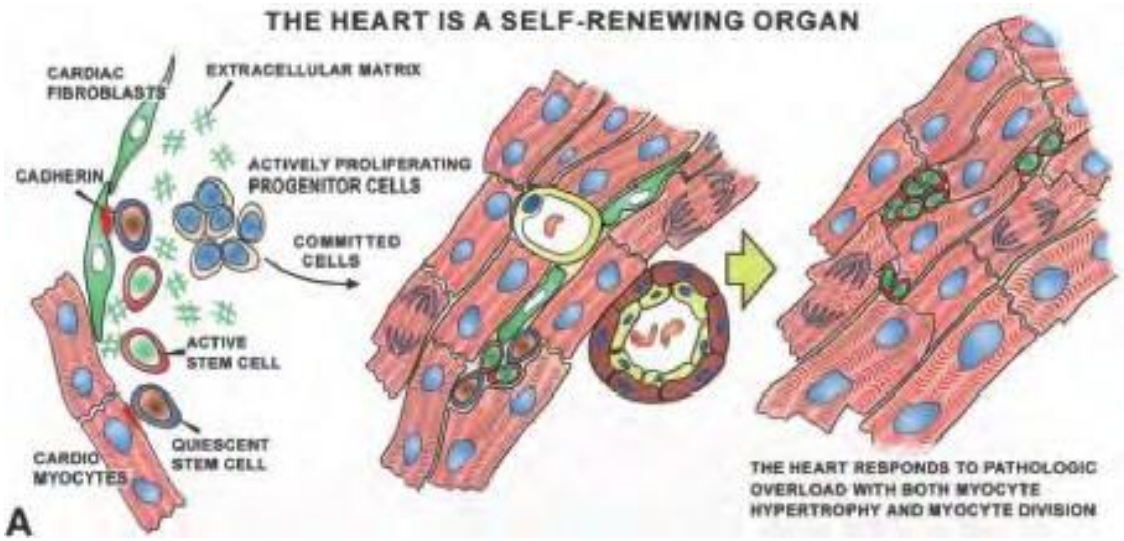

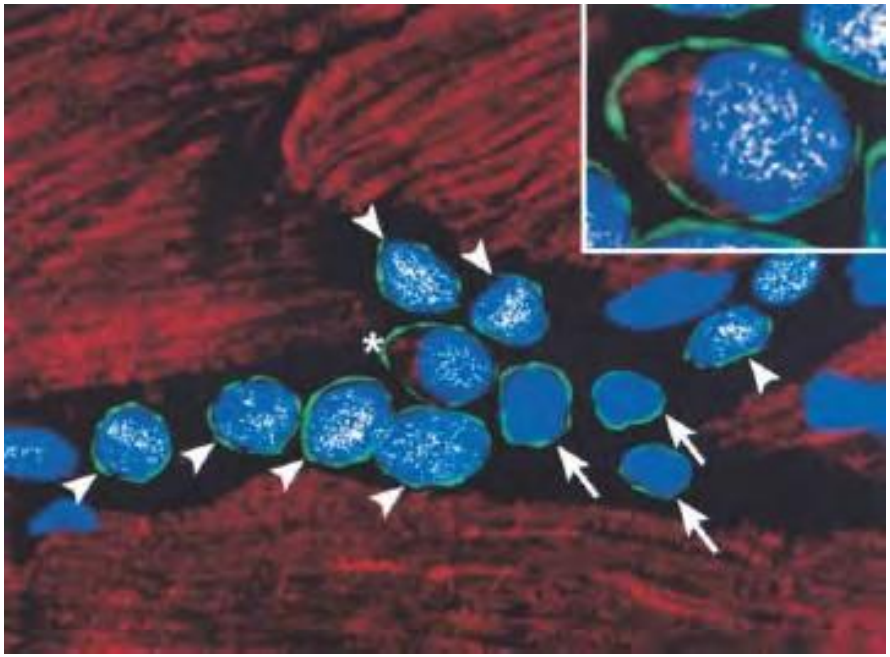

Adult cardiac stem cells are multipotent and support myocardial regeneration.
Beltrami AP, Barlucchi L, Torella D, Baker M, Limana F, Chimenti S, Kasahara H, Rota M, Musso E, Urbanek K, Leri A, Kajstura J, Nadal-Ginard B, Anversa P.

Life and Death of Cardiac Stem Cells

A Paradigm Shift in Cardiac Biology

Piero Anversa, MD; Jan Kajstura, PhD; Annarosa Leri, MD; Roberto Bolli, MD

Circulation March 21, 2006

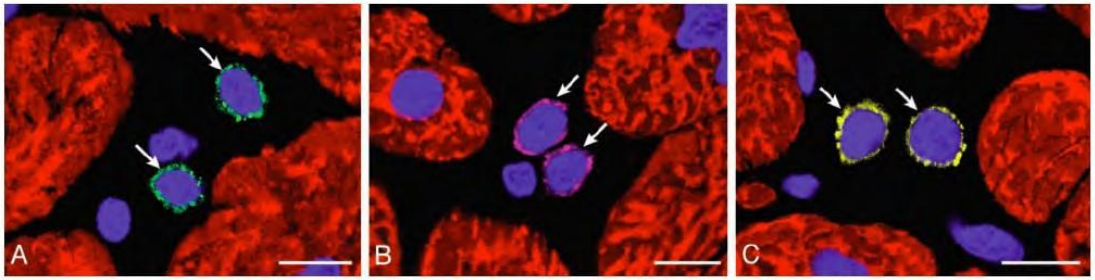

Fig. 1. Putative cardiac stem cells. Shown are detection of c-kit (*A*, green), MDR1 (*B*, purple), and Sca-1-reactive protein (*C*, yellow) in primitive cells (arrows) of hypertrophied hearts. Nuclei are stained by propidium iodide (PI; blue) and myocytes by cardiac myosin (red). (Bars = 10 μm.)

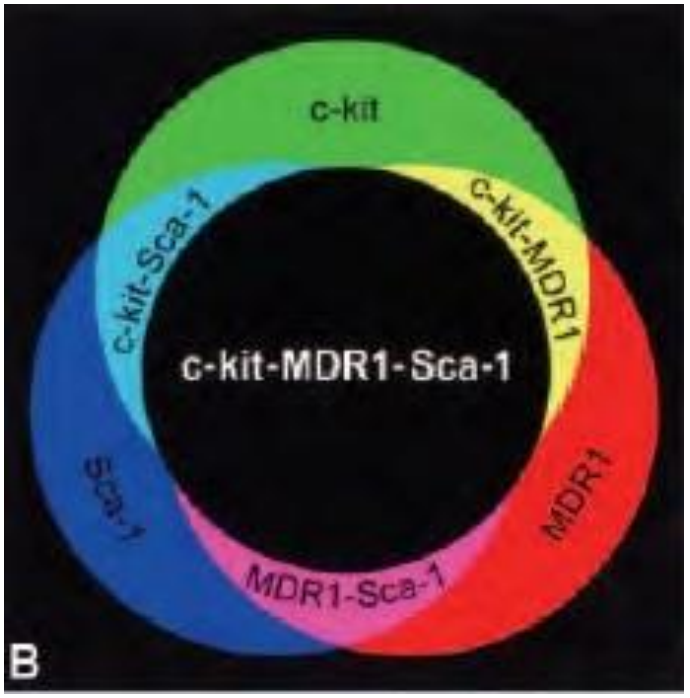

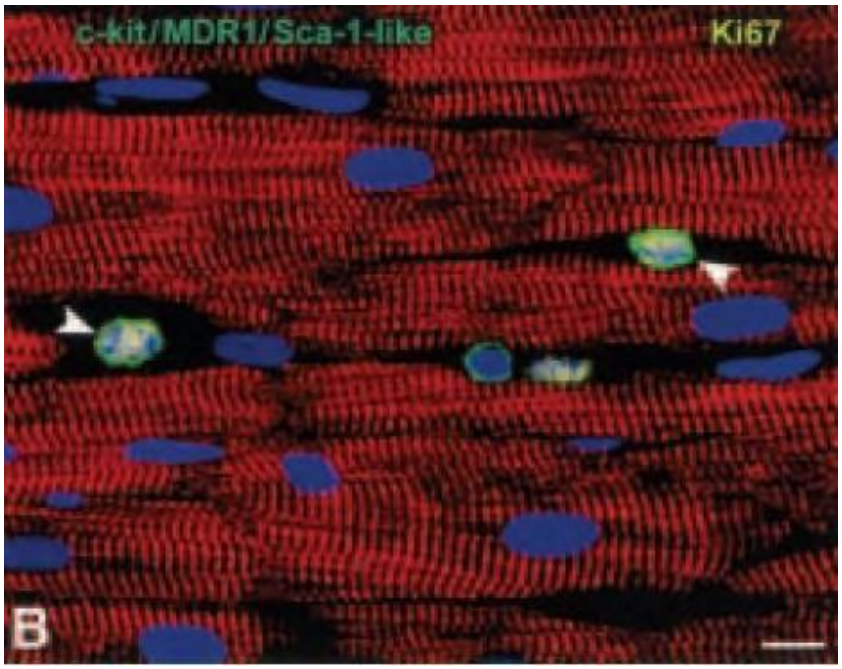

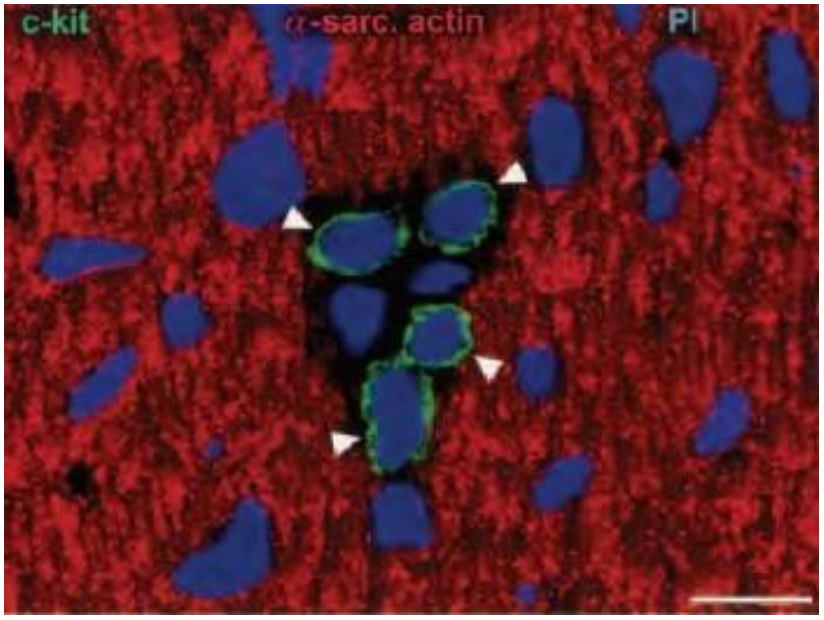

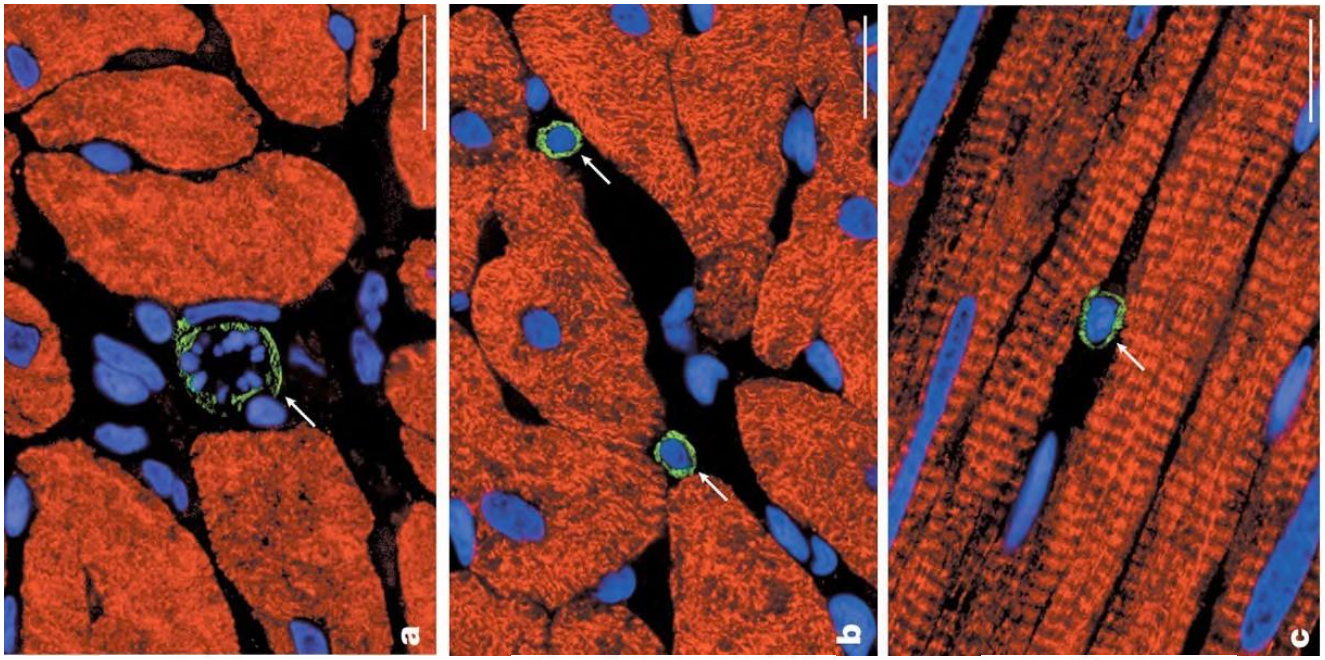

c-*kit*

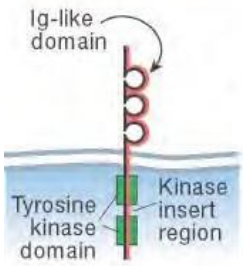

Distribution

- Melanocytes
- Mast cells
- Germ cells
- Stem cells

Functions

- Proliferation
- Migration
- Differentiation
- Secretion

P-glycoprotein or MRD1

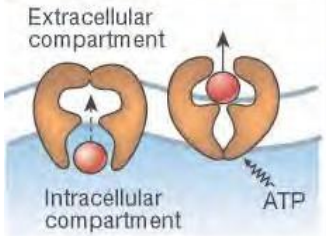

Distribution

- Hepatocytes–cholangiocytes
- Brush border cells
- Renal tubular cells
- Endothelial cells (brain)
- Cancer cells
- Stem cells

Functions

- Transmembrane efflux pump
- Inhibition of apoptosis

Sca-1

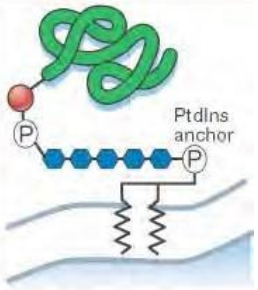

Distribution

- Vessel wall
- Kidney cortical tubules
- Thymus, spleen
- T lymphocytes
- Stem cells

Functions

- Cell adhesion
- Cell signalling
- T-cell activation

Cardiac stem cells delivered intravascularly traverse the vessel barrier, regenerate infarcted myocardium, and improve cardiac function

Buddhadeb Dawn*, Adam B. Stein*, Konrad Urbanek†, Marcello Rota†, Brian Whang†, Raffaella Rastaldo†, Daniele Torella†, Xian-Liang Tang*, Arash Rezazadeh*, Jan Kajstura†, Annarosa Leri†, Greg Hunt*, Jai Varma*, Sumanth D. Prabhu*, Piero Anversa†, and Roberto Bolli*‡

GFP-labeled CSCs delivered to the coronary arteries 4 hr after ischemia-reperfusion

Ventricular function monitored by echocardiography

Myocardial regeneration by histology

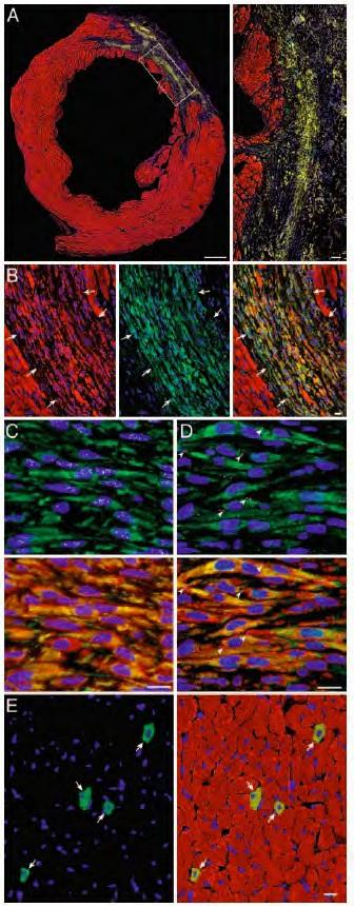

3766–3771 | PNAS | March 8, 2005 | vol. 102 | no. 10

Resident cardiac stem cells

c-Kit+ cells (Anversa)
Sca-1 cells (Schneider)
Side population cells (Liao)
Islet-1 cells (Chien)
Cardiosphere-forming cells (Messina/Marban)
SSea-4+ cells (Taylor)

One of the least regenerative organ in the body has multiple non-overlapping populations of cardiomyocyte progenitors??

Cardiac stem cells in patients with ischaemic cardiomyopathy (SCIPIO): initial results of a randomised phase 1 trial

Roberto Bolli, Atul R Chugh, Domenico D'Amario, John H Loughran, Marcus F Stoddard, Sohail Ikram, Garth M Beache, Stephen G Wagner, Annarosa Leri, Toru Hosoda, Fumihiro Sanada, Julius B Elmore, Polina Goichberg, Donato Cappetta, Naresh K Solankhi, Ibrahim Fahsah, D Gregg Rokosh, Mark S Slaughter, Jan Kajstura, Piero Anversa

Summary

Background c-kit-positive, lineage-negative cardiac stem cells (CSCs) improve post-infarction left ventricular (LV) dysfunction when administered to animals. We undertook a phase 1 trial (Stem Cell Infusion in Patients with Ischemic cardiOmyopathy [SCIPIO]) of autologous CSCs for the treatment of heart failure resulting from ischaemic heart disease.

Methods In stage A of the SCIPIO trial, patients with post-infarction LV dysfunction (ejection fraction [EF] ≤40%) before coronary artery bypass grafting were consecutively enrolled in the treatment and control groups. In stage B, patients were randomly assigned to the treatment or control group in a 2:3 ratio by use of a computer-generated block randomisation scheme. 1 million autologous CSCs were administered by intracoronary infusion at a mean of 113 days (SE 4) after surgery; controls were not given any treatment. Although the study was open label, the echocardiographic analyses were masked to group assignment. The primary endpoint was short-term safety of CSCs and the secondary endpoint was efficacy. A per-protocol analysis was used. This study is registered with ClinicalTrials.gov, number NCT00474461.

Findings This study is still in progress. 16 patients were assigned to the treatment group and seven to the control group; no CSC-related adverse effects were reported. In 14 CSC-treated patients who were analysed, LVEF increased from 30·3% (SE 1·9) before CSC infusion to 38·5% (2·8) at 4 months after infusion (p=0·001). By contrast, in seven control patients, during the corresponding time interval, LVEF did not change (30·1% [2·4] at 4 months after CABG *vs* 30·2% [2·5] at 8 months after CABG). Importantly, the salubrious effects of CSCs were even more pronounced at 1 year in eight patients (eg, LVEF increased by 12·3 ejection fraction units [2·1] *vs* baseline, p=0·0007). In the seven treated patients in whom cardiac MRI could be done, infarct size decreased from 32·6 g (6·3) by 7·8 g (1·7; 24%) at 4 months (p=0·004) and 9·8 g (3·5; 30%) at 1 year (p=0·04).

Interpretation These initial results in patients are very encouraging. They suggest that intracoronary infusion of autologous CSCs is effective in improving LV systolic function and reducing infarct size in patients with heart failure after myocardial infarction, and warrant further, larger, phase 2 studies.

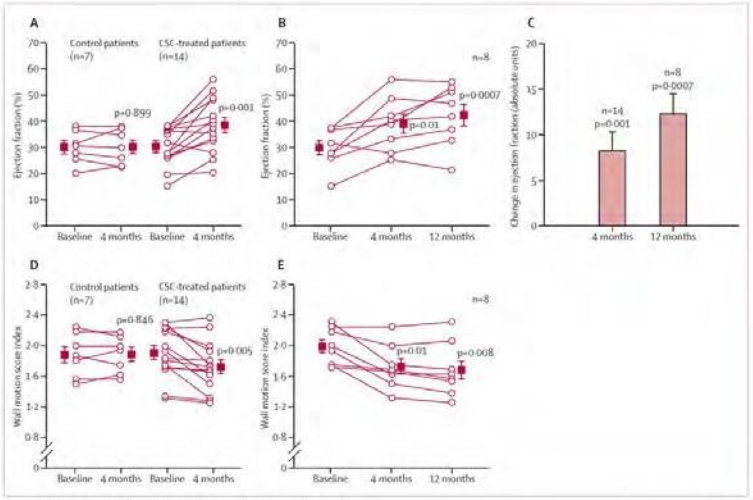

Figure 4: **Echocardiographic analysis of CSC-treated patients and controls**
(A) Left ventricular ejection fraction (measured by use of three-dimensional echocardiography) at 4 months after baseline in control and CSC-treated patients. (B) Ejection fraction at 4 months and 12 months after baseline in the CSC-treated patients who had 1 year of follow-up. (C) Change in ejection fraction from baseline at 4 months and 12 months in CSC-treated patients. (D) Wall motion score index at 4 months after baseline in control and CSC-treated patients. (E) Wall motion score index at 4 months and 12 months after baseline in the CSC-treated patients who had 1 year of follow-up. Boxes represent the mean values and error bars represent SE. p values are reported for difference between baseline and 4 months and between baseline and 12 months. CSC=cardiac stem cell.

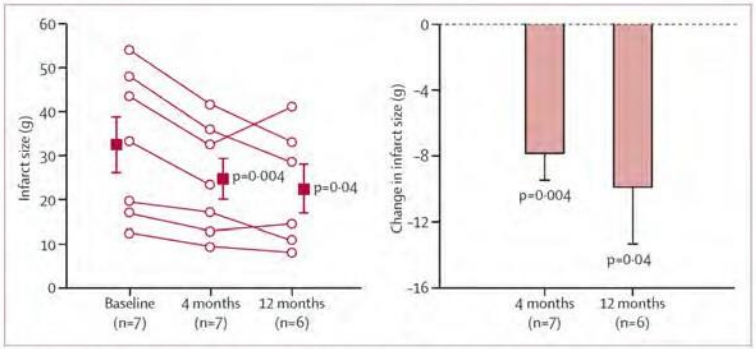

Figure 5: **Infarct size and change in infarct size at 4 months and 12 months after baseline in patients administered cardiac stem cells**
p values are reported for difference between baseline and 4 months and between baseline and 12 months. Boxes and bars represent the mean values and error bars represent the SE.

Cardiospheres

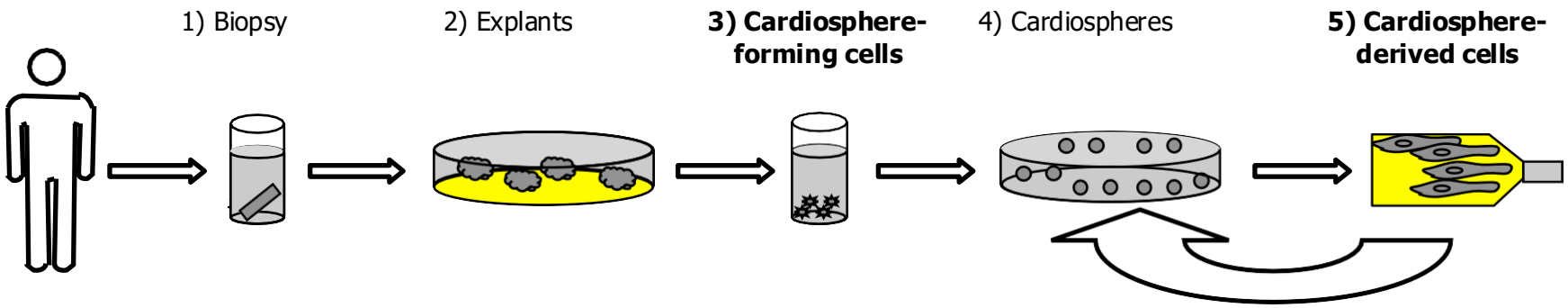

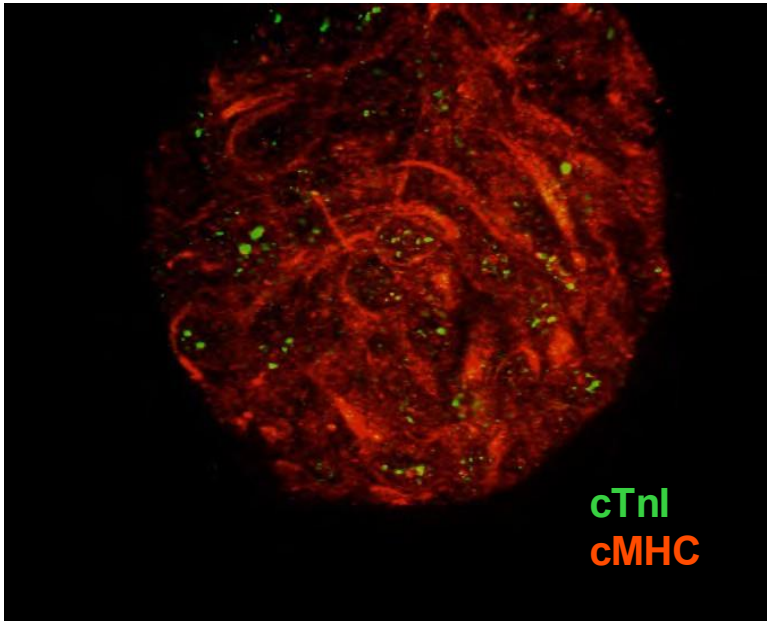

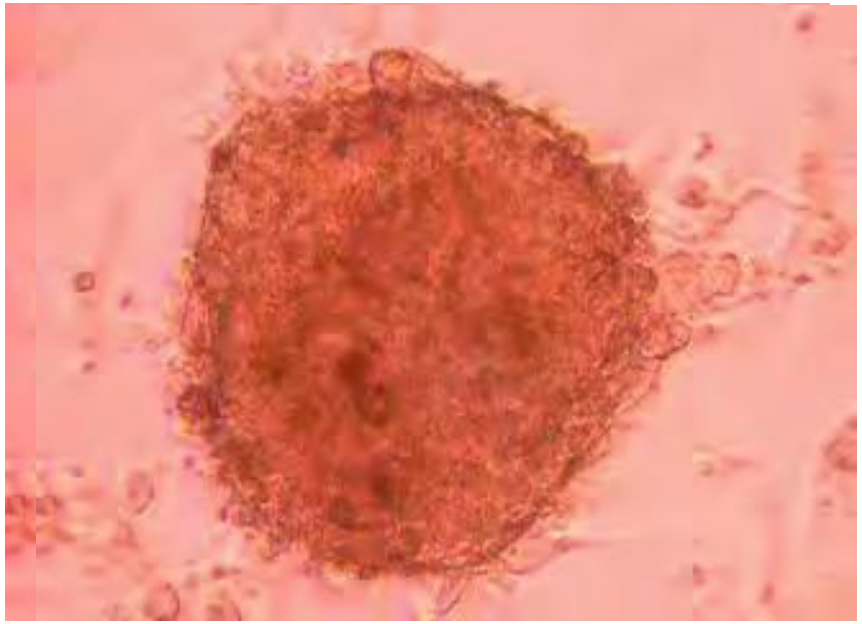

Isolation and Expansion of Adult Cardiac Stem Cells From Human and Murine Heart

Elisa Messina, Luciana De Angelis, Giacomo Frati, Stefania Morrone, Stefano Chimenti, Fabio Fiordaliso, Monica Salio, Massimo Battaglia, Michael V.G. Latronico, Marcello Coletta, Elisabetta Vivarelli, Luigi Frati, Giulio Cossu, Alessandro Giacomello

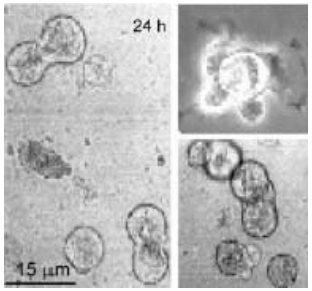

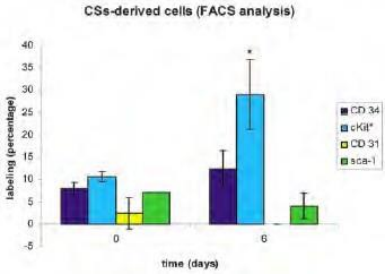

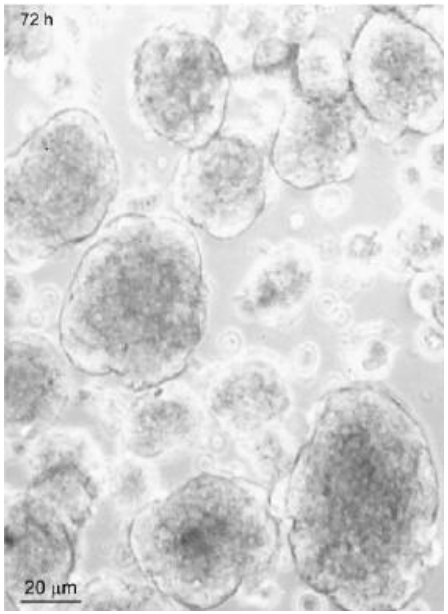

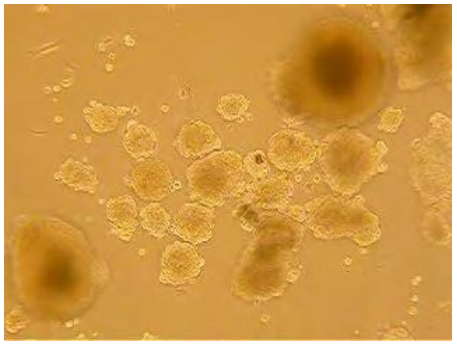

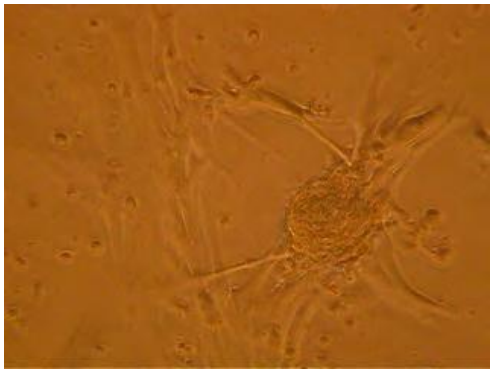

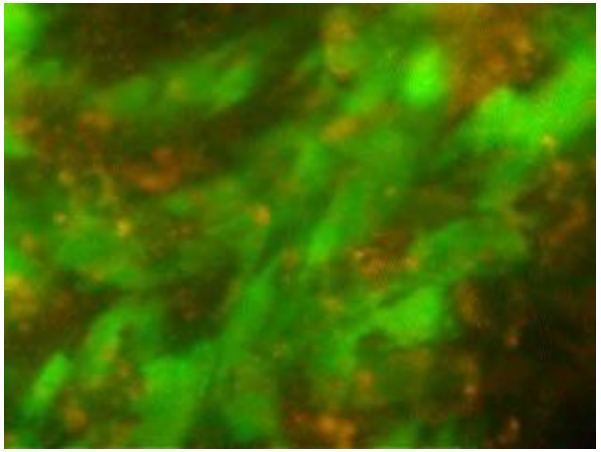

Mild enzymatic digestion
EDTA and mild trypsinization
Low serum, serum substitute B27, EGF, bFGF, cardiotrophin-1, **thrombin** (7-fold increase in the number of spheres)

PNAS | October 7, 2008 | vol. 105 | no. 40 | 15529–15534

Notch1 regulates the fate of cardiac progenitor cells

Alessandro Boni*†, Konrad Urbanek*†, Angelo Nascimbene*†, Toru Hosoda†, Hanqiao Zheng†, Francesca Delucchi†, Katsuya Amano†, Arantxa Gonzalez†, Serena Vitale†, Caroline Ojaimi‡, Roberto Rizzi†, Roberto Bolli§, Katherine E. Yutzey¶, Marcello Rota†, Jan Kajstura†, Piero Anversa†, and Annarosa Leri†‖

†Departments of Anesthesia and Medicine and Division of Cardiology, Brigham and Women's Hospital, Harvard Medical School, Boston, MA 02115; ‡Department of Physiology, New York Medical College, Valhalla, NY 10595; §Institute of Molecular Cardiology, University of Louisville, Louisville, KY 40292; and ¶Divison of Molecular Cardiovascular Biology, Children's Medical Center, Cincinnati, OH 45229

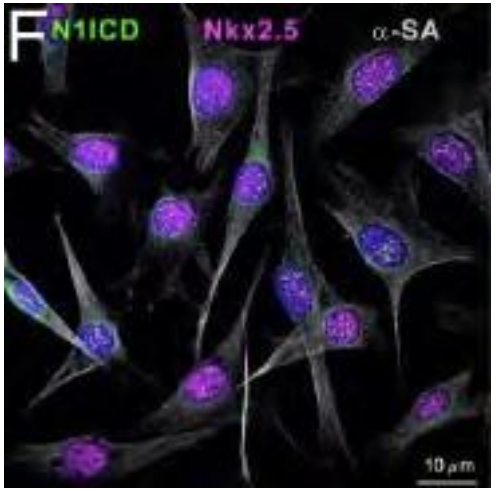

- Cardiac progenitor cells (CPCs) in the niches express Notch1 receptor, and the supporting cells exhibit the Notch ligand Jagged1.
- N1ICD and RBP-Jk form a protein complex, which in turn binds to the Nkx2.5 promoter initiating transcription and myocyte differentiation.

- Notch1 favors the early specification of CPCs to the myocyte phenotype but maintains the newly formed cells in a highly proliferative state.